University of Kerbala
College of Science
Department of Physics

Investigation on Characterization of Helium Atmospheric Pressure Plasma Jet

A Thesis
Submitted to the Council of College of Science, University of Kerbala in Partial Fulfillment of the Requirements for the Degree of Master in Science of Physics

By

Mustafa Musa Shaker

B.Sc. 2017

Supervised by

Prof. Dr. Fadhil Khaddam Fuliful

Prof. Dr. Rajaa K. Mohammad

2023 A.D   **1445 A.H**
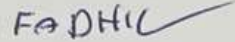
بـسم الله الـرحمن الـرحيـم

(قَالَ الَّذِي عِنْدَهُ عِلْمٌ مِنَ الْكِتَابِ أَنَا آتِيكَ بِهِ قَبْلَ أَنْ يَرْتَدَّ إِلَيْكَ طَرْفُكَ فَلَمَّا رَآهُ مُسْتَقِرًّا عِنْدَهُ قَالَ هَذَا مِنْ فَضْلِ رَبِّي لِيَبْلُوَنِي أَأَشْكُرُ أَمْ أَكْفُرُ وَمَنْ شَكَرَ فَإِنَّمَا يَشْكُرُ لِنَفْسِهِ وَمَنْ كَفَرَ فَإِنَّ رَبِّي غَنِيٌّ كَرِيمٌ)

صدق الله العليّ العظيم

سورة النمل آية (40)

Supervisors Certificate

We certify that the preparation of this thesis, entitled "**Investigation on Characterization of Helium Atmospheric Pressure Plasma Jet**" was made under our supervision by "Mustafa Musa Shaker" at the Department of Physics, College of Science, University of Kerbala in partial fulfillment of the requirements for the degree of Master in Science of Physics.

Signature: FA DHIL

Name: Dr. Fadhil Khaddam Fuliful

Title: Professor

Department of Physics, College of Science

Date: / / 2023

Signature:

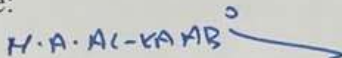Name: Dr. Rajaa K. Mohammad

Title: Professor

Department of Physics, College of Science

Date: / / 2023

In view of the available recommendations, I forward this thesis for debate by the examining committee.

Signature:

H·A·AL-KAAB

Name: Dr. Mohammed A.H. Al-Kaabi.

Title: Assistant Professor

Head of Physics Department, College of Science

Date: / / 2023

Examination Committee Certification

We certify that we have read this thesis entitled **"Investigation on Characterization of Helium Atmospheric Pressure Plasma Jet"** as the examining committee, examined the student "Mustafa Musa Shaker" on its contents, and that in our opinion, it is adequate for the partial fulfillment of the requirements for the Degree of Master in Science of Physics.

Signature:

Name: Dr. Abdalhussain A. Khadayar

Title: Professor

Address: Department of Physics

College of Education /University of Al-Qadisiyah

Date: / / 2023

(Chairman)

Signature:

Name: Dr. Nagham M. Shiltagh

Title: Assist. Professor

Address: Department of Physics

College of Science/University of Kerbala

Date: 7 / 11 / 2023

(Member)

Signature: Duaa A Uamran

Name: Dr. Duaa A. Uamran

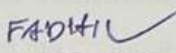Title: Assist. Professor

Address: Department of Physics.

College of Science/University of Kerbala

Date: / / 2023

(Member)

Signature: FADHIL

Name: Dr. Fadhil Khaddam Fuliful

Title: Professor

Address: Department of Physics.

College of Science/University of Kerbala

Date: / / 2023

(Supervisor)

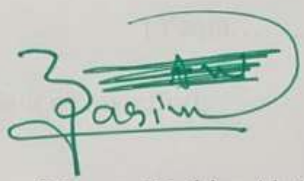Signature:

Name: Dr. Rajaa K. Mohammad

Title: Professor

Address: Department of Physics.

College of Science/University of Kerbala

Date: / / 2023

(Supervisor)

Signature:

Name: Dr. Jasem Hanoon Hashim Al-Awadi

Title: Professor

Dean of the College of Science/ University of Kerbala

Date 21 / 11 / 2023

Dedication

To…...The conqueror of what is closed and the seal of what preceded, the supporter of the truth with the truth, the guide to the straight path, the master of creation and the beloved of truth, our Prophet Muhammad, the Chosen One, upon him and his family and companions, the best prayers and peace.

To...... Those whom God commanded to be obeyed....... my dear parents Love, appreciation, and gratitude.

To...... The owner of divine sciences and mystical pearls, the reference that speaks the truth, the martyr of God, Sayyid Mohammad Mohammad Sadeq al-Sadr, and his two sons (their secrets are sanctified), and his children, the secret of the al-Sadr family, Sayyid Mortada al-Sadr, and the leader of the Husseini reform, Sayyid Muqtada al-Sadr (may God bless them).

To...... Who supported me and visited me step by step on this path, the symbol of purity, loyalty, love, and serenity, my dear wife.

To...... God made them a helper for me that will not be repeated...... My beloved brothers out of respect.

To...... The morning breeze and the fragrance of its fragrant symbol, the hope for a clear future is the fruit of the heart.

(Yaqin……...Mohammad)

I dedicate the fruit of my effort.

Mustafa...

Acknowledgments

Praise be to God who made praise the key to his remembrance and a reason for more of his bounty and a proof of his bounty and greatness.

I extend my sincere thanks to the dear Professor Dr. (Fadhil Khaddam Fuliful) and Professor Dr. (Rajaa K. Mohammad), for the assistance and effort they provided me in completing this thesis.

I extend my thanks and gratitude to all my dear teachers over the academic stages and to Professor Dr. (Abdel Sattar Karim Hashem Janabi), and all helped me in any way, even with a word.

I also extend my thanks and gratitude to my mujahideen brothers in the Peace Brigades for their standing and support for me throughout the school stage.

Mustafa...

Abstract

Characteristics of atmospheric pressure helium plasma jet (APHPJs) is significant because of their use in different application such as medical, biomedical, agriculture, and industry. In this work, a developed dielectric barrier discharge (DBD) system was used to study the properties of (APHPJs) in the advanced plasma laboratory at the University of Kerbala, College of Science, Department of Physics. The device components are a high voltage (0-20)kV alternating current generator, Pyrex tubes of different thicknesses (0.1, 0.2, 0.5, 1) mm, two electrodes which are made of aluminum with a thickness of 1 mm placed around the Pyrex, and the working gas for electrical discharge is helium (He). Plasma temperature and plasma plume length play a major role in various cold plasma applications, therefore the effects of tube thickness and distance between the electrodes on electrical characteristics (plume length and plasma temperature) of generated plasma are investigated. A simple electronic thermo-sensor of the type (UTS) is used to estimate the temperature of the plasma and the plasma plume measured by standard metric. The plasma temperature and the length of the flame are estimated for different gas flow rates (1-6) L/min and a range of applied voltage (8-14) kV.

The optical emission spectroscopy (OES) method is used to record and analyze the spectrum of helium plasma jet for a range of applied voltage (8-14) kV and flow rate of helium gas (1-6) L/min. Electron temperature (T_e) and electron density (n_e) are calculated using the Boltzmann plot method and considered in the database recorded in the NIST.

The results show that the plasma plume length is random variation due to the thickness of the Pyrex tube, then the optimization characteristic is obtained when the applied voltage is 8kV and the gas flow rate is (4L/min) in the case of 1mm thickness of Pyrex tube, the length of the plasma plume is 6cm and the plasma temperature is confined between (24-26) °C, which is close to room temperature.

When the distance between the electrodes is at a range (1-2.5) cm, the applied voltage is (8 kV) and the helium flow rate is 4L/min, the plasma is generated but its plume length decreases as the distance increases, as well as the plasma temperature, has the same behavior.

Spectra of Helium plasma jets at atmospheric pressure for voltage (1-14) kV and a rate of flow (1-6) L/min are recorded and analyzed, and the spectrum lines in the helium plasma jet appear in the UV-Vis-NIR regions. Six spectral lines of the reactive species radicals of the generated plasma were used to estimate the (T_e) and (n_e). The optimum working parameters to generate helium plasma with good properties are the rate of gas flow is 4L/min and the employed voltage of 8 kV. The optimum characteristic of generated plasma in this work is a plume length of 6 cm, plasma temperature is 26ºC, and high reactive species intensity of (O_2, N_2, OH, NO) are (357,875, 2476,403) respectively, and the temperature of the electron is less than 1eV(6102.22K), and the electron density is (1.57×10^{13} cm^{-3}). The generated (APHPJs) can be used in biomedical and medical applications due to the high intensity of reactive species, Also the values of electron temperature (T_e) and electron density (n_e) are in the range of artificial plasma.

List of Contents

List of Figures

List of Table

List of Symbols and Abbreviations

APPJ	Atmospheric pressure plasma jet.	
CAP	Cavities or capillaries.	
DBD	Dielectric barrier discharge.	
DC	Direct current.	**A**
F	Frequency.	**Hz**
HV	High voltage.	**kV**
I	Current.	**A**
LTE	Local thermal equilibrium.	
m_a	Atom mass.	**u**
n_a	Atom density.	
n_e	Electron densities.	**cm^{-3}**
NO	Nitrogen oxide.	
NTP	Non-thermal plasma.	
RF	Radio Frequency.	**Hz**
RNS	Reactive nitrogen species	
ROS	Reactive oxygen species	
T	Oscillation period.	
T_e	Electron temperature.	**^{0}K**
TF	Tissue factor.	
T_g	Gas temperature.	**^{0}K**
TP	Thermal plasma.	
UV	Ultraviolet.	
κ	Thermal conductivity of the gas.	

Chapter One

General Introduction

1.1 Introduction

Plasma is a word of Greek origin that means linguistically gelatinous matter. It originally means something formed according to a specific system. Matters usually exist in three states, which are solid, liquid, and gaseous states. In general, in all states of matter, the atoms and particles of matter are electrically neutral, meaning that the net charge is zero, and this characteristic is achieved even during the process of transforming matter from one state to another [1]. In the case of plasma, the property of the electrical equilibrium of the atoms and molecules of matter is disturbed, and the concept of plasma is usually associated with the ionization state of matter. Therefore, plasma the fourth state of matter, occupies 99% of the total matter of the universe, as the sun and stars are large masses of hot plasma, and some Planets form plasma for most of their matter, as Jupiter is a huge mass of plasma [2].

In 1857, when the first preliminary investigation into the electric discharge of gases was presented by the scientist Artist Siemens, ozone gas O_3 was produced from oxygen or air. A potential difference is applied between two electrodes in two coaxial tubes made of glass to initiate the space among the tubes where the electric current is forced to pass through the walls of the tubes to act as dielectric barriers this type of discharging is called a DBD dielectric barrier discharge [3].

In 1928 American physicist Irving Langmuir, a Nobel Prize winner, suggested that the electric discharge used to designate the part of the arc if the density of ions and electrons was high but they were substantially equal. The discharge carriers were described as electrons, ions, and reactive species [3,4].

Since 1930 there has been an increase in studies on barrier discharges and plasma jets which are used for various applications such as surface modification, environmental, biomedical, and medical in our lives. In 1968,

Menasha was the first to use plasma as a fogging and sterilization method, and for this purpose, using low-pressure and temperature plasma to sterilize contaminated surfaces. In 1970, plasma physics was applied to building microelectronic devices, and in the year 1990, studies increased significantly, also to generating discharge atmospheric pressure plasma, such as barriers discharge and plasma reactors in modification of surface materials, biomedical, and environmental applications [5,6].

Plasma was known as the 4th case and was considered an ion gas that exhibits collective behavior for containing free electrons and ions. The charge particles generate electric and magnetic fields. Lightning, aurora borealis, and the earth's ionosphere were good examples of natural plasma [7].

As seen in figure (1.1), the bonding strengths between the particles varied in the plasma. While the bonding force was strong in the solid state, it was less and less strong in the liquid and gas states [8,9].
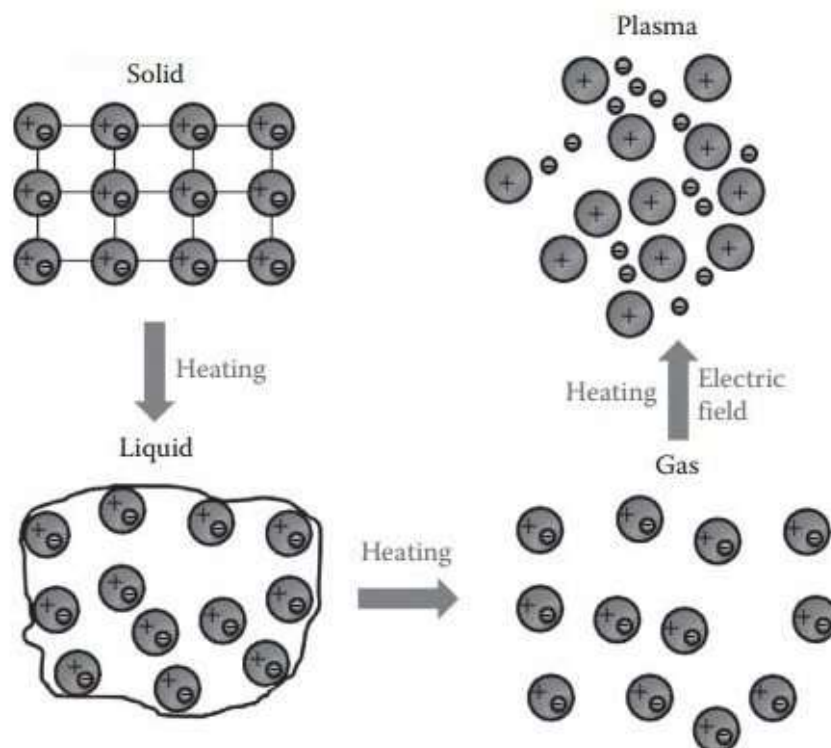
Figure (1.1): The bonding change in the matter states due to energy [9].

By providing energy, such as fusion potential energy, to displace the bonding energy between (molecules or atoms), it is possible to change the solid state into a liquid state. In another instance, the liquid becomes gaseous by adding energy, but for plasma, the formation must enough energy is required to separate the electron from an atom. This process is known as the Ionization energy, and the transformation to a plasma state occurs from one type of species(gas) to more than two species [10].

Under a variety of pressure and temperature conditions, plasma could be produced; the plasma was formatted under conditions such as atmospheric pressure. and room temperature. Many sources of energy like chemical, thermal, and radiological energy, are used to make electrical discharges to obtain plasma, laser, and electromagnetic waves, and additionally, the bonding energy between atoms or molecules in the gas state is destroyed by an applied voltage. Then ions and electrons were separated into groups, so the plasma is active and safe for an environment that combines photons and charged particles [11].

The plasma contains many types such as natural atoms and ionic, (positive and negative ions) electron and reactive species, as well as non-ionized radiation (visible light and ultraviolet). The plasma is electrically conductive because of its electrons, ions, and reactive species, which also interact internally and react to electromagnetic fields [11,12].

1.2 Plasma Concept

Plasma science has long been a subject of increasing interest. For many applications, plasma, which describes the ionized state of matter, has grown in importance [13]. The voltage variations between the electrodes can produce plasma through a series of microdischarges that are dispersed erratically in time and space [14]. Plasm is defined as " a quasi-neutral gas of charged and neutral particles which presents collective behavior," even though there is always a

small amount of ionization in any gas. The term "quasi-neutrality" refers to the property that the positive and negative space charges would balance within the plasma, causing the plasma to be regarded as being electrically neutral in most cases. Electrostatic forces produced by the space charge would act to restore charge neutrality if the local concentrations of charge developed. Long-range Coulomb forces that interact distant regions with one another are what produce the collective behavior of plasma. To distinguish a plasma state from a neutral gas and other ionized gases, these countenances are crucial [15]. One of the characteristics of plasma is its chemical activity; inside the plasma, radicals and other highly reactive species are formed. Plasma can be created in a laboratory. Typically, this is done inside a vacuum vessel at low pressure. Modern plasma sources have become quite friendly and "bio-cooperative," with temperatures ranging from 5000 to 70000K and consisting entirely of plasma. [16,17].

1.3 Elastic and Inelastic Collisions

The most significant group in the plasma disturbance state is the collision of elastic and inelastic materials. In an elastic collision, neither the internal energy of the approaching particles nor their structural makeup is altered by the contact. The elastic impact and kinetic energy transition may lead to electromagnetic radiation conducting, diffusing, and being absorbed. However, in inelastic contact, the kinetic energy is transformed into internal energy, because excitation, dissociation, and ionization may occur [18].

1.4 Collective Behavior

In all gases, the collision between particles (molecules) is the main element that determines the movement of these gases. For example, vibrational motion can be transmitted as energy in the atmosphere by collisions between atoms or molecules, such as the transmission of sound in the air. In the case of plasma, the situation is different, as the plasma consists of electric charges, in

addition, to neutral particles, as charges generate electric fields. When they move, they generate electric currents. magnetic fields, and these magnetic fields in turn affect the particles themselves and distant particles. The movement of a part of the plasma in a specific area affects the plasma particles in distant areas through the effects of electrical and magnetic, so the collision-free plasma is considered important to calculate the electromagnetic forces. From here, the collective behavior of the plasma can be defined as the following [19]:

The movement of the plasma does not depend only on the local state, but also on the state of the plasma in distant regions as well. The dynamics of the body in the plasma are controlled by the self-fields arising from the movement of other particles and the body is surrounded by an electric field and is affected by the rest of the charred bodies according to Coulomb's law with its inverse dependence on the square of the path separating it from other particles, in addition to the magnetic field accompanying the charged particle, which it results in a force that affects the rest of the charged particles, and this is what makes Coulomb's law the basic law in calculating. The basic properties of plasma and the effect of group behavior are very clear in collision-less plasma [20].

1.5 Plasma classification

Plasma can be classified due to the value of temperatures of ions, electrons, and neutrals, and it is possible to divide the plasma into mainly two categories [21].

1- Equilibrium plasma (High-temperature plasma)
2- Non-equilibrium plasma (Low-temperature plasma)

As in figure (1.2).
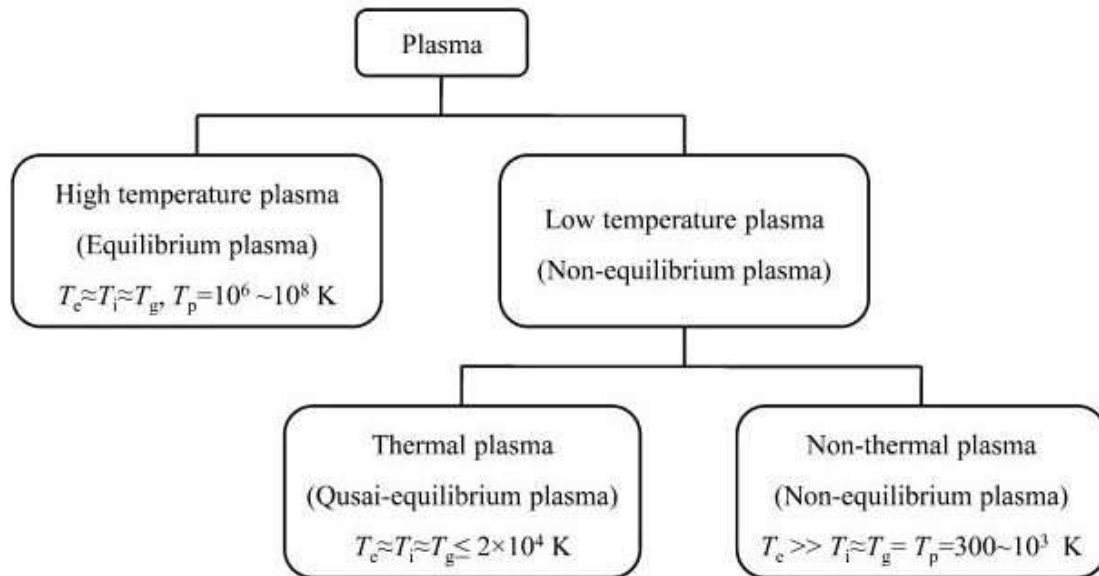
Figure (1.2): Plasma classification [21].

1.5.1 Equilibrium plasma (High-temperature plasma)

The temperature of the electron T_e in this type of plasma was the same as the neutral T_n and ion T_i respective surface temperatures, it can be said that were identical, (i.e., $T_e \approx Ti \approx T_n = 10^6 - 10^8$ k). Because there were huge collisions between the components of plasma, it is very dense the temperature was high, degree of ionization was high and close to 1, for example, plasma in the sun, stars, the interstellar, and the solar wind [22,23].

1.5.2 Non-equilibrium plasma (Low-temperature plasma)

The temperature in this type of plasma was described as much lower in comparison with high-temperature plasma, the degree of ionization was 0.1 approximately, and low density. It can be classified into two types [23,24]:

1- Thermal plasma.
2- Non-thermal plasma (cold plasma).

1.5.2.1 Thermal Plasma (Plasma in a semi-equilibrium)

This type of plasma was characterized as a gradient between cold plasma and hot plasma and has temperature relative equally of the electron T_i the ion T_i and the neutral T_n. (i.e., $T_e \approx T_i \approx T_n \leq 2 \times 10^4$ K). it is used in coatings, chemical, and physical vapor deposition [24].

1.5.2.2 Non-thermal plasma (cold plasma)

Plasma could be generated when applying high voltage with two electrodes about a tube filled with a noble gas. Reactive species, charged particles, photons ,visible light, electromagnetic field, and UV radiation are created with this type of plasma as illustrated in figure (1.3). The formed reactive species has a temperature close to room temperature $30 - 60$ °C [25].

The temperature of the electron T_e in this type of plasma was much higher than the temperature of the ion T_i and the neutral T_n (i.e., $T_e \gg T_i = T_n = 300…..10^3$ K). Due to collision, the conservation of momentum for electrons and heavy ions is not valid, in addition, the ionization degree was slight, the other properties of cold plasma are weak ionization, which is about 1% with a low density of free electrons. Cold plasma is frequently classified as a nonequilibrium plasma state as a result of the low temperature of ions (Te>>Ti), and the applications of cold plasmas manufactured in the laboratory have expanded in all different areas of life [26].

There were many applications of cold plasma such as environmental engineering, aviation engineering, biomedicine, and analytical chemistry. Charged particles, reactive types, ultraviolet radiation, and visible light all exist in cold plasma, as shown in figure (1.3), also used in the treatment of bacteria and fungi and the results show a good effect on microbial [26-27].
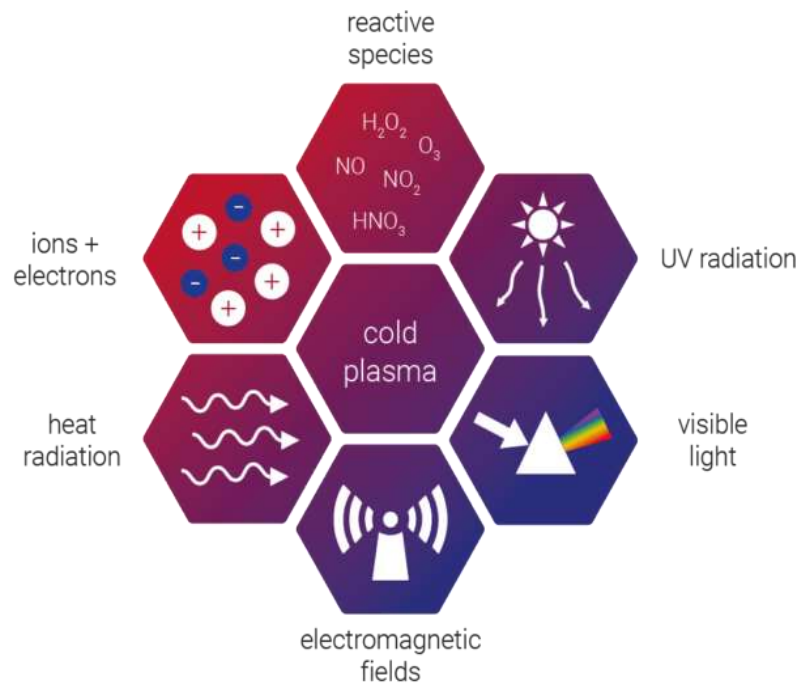
Figure (1-3) Components of Cold plasma [25,27].

The degree of ionization in cold plasma was weak and about 1%. the electron density was not as high as it is in hot plasma (i.e., $n_e=10^{10}$ m^{-3}). In cold plasma, the collisions of electrons-electrons lead to thermodynamic equilibrium. Distinguished Free electrons were achieved by their high kinetic energy. The electron cannot transfer its high kinetic energy to ions and neutral particles despite having a temperature that is significantly greater than theirs [28].

1.6 Plasma Ionization

Ionization energy, which is defined as the energy required to change one atom into an ion, is typically equal to the energy of the outer electron attaching to the atom. The energy source for ionization can be heat, light, or radiation. The thermal energy of the gas particles determines the ionization ratio. Saha equation was a suitable method for calculating the degree of designation. There are three different sorts of atoms (ionized gas, reactive species, positive and negative ions, and electrons). The ionization degree of gases is calculated due to the relationship [29].

$n_i / n_n \approx 2.4 \times 10^{21}\, T^{3/2}/ni* \exp{(-\,vi\,KT)}$ …………   (1-1)

$n_i =$ ionized atoms $(no.of\ atoms/\ m3)$, $n_n =$ neutral atoms $(no.of\ atoms/m3)$

T=temp (K) vi= ionized energy of gas (eV)   K= Boltzmann constant .

$$\alpha_i = \frac{N_i}{N_n + N_i}$$ ……………...   (1-2)

where N_i: is the number density of ions, and N_n: is the number density of neutrals.

The effects of magnetic and electric fields in the plasma depend on the degree of ionization, when is close to or equal to (1eV), the plasma is hot, while when the degree of ionization is between $(10^{-4}$–$10^{-6})$ the plasma is cold [23, 24].

1.7 Plasma diagnostics

It was necessary for plasma, to know the temperature of electron T_e and the density of electron n_e, which are considered as the basic parameters of the plasma diagnostic. The plasma parameters were important in the interaction between plasma and external turbulence, such as the effects of magnetic and electric fields on plasma. The dynamics of plasma and its response to external electromagnetic fields depend on the electron density and electron temperature [30].

The densities of both electrons and ions are equal, and plasma is nearly neutral gas. The electron density in cold plasma was less than that in thermal plasma, the type of plasma was determined according to the degree of ionization, so it is one of the basic parameters of plasma diagnostics [31].

The temperature of the electron determines the kinetic energy, so if the temperature is high, the kinetic energy is high, and vice versa. The ionization level of the plasma is determined by the electron temperature. When the electron temperature decreases, the electrons and ions recombine and become neutral, thus the plasma becomes a gaseous state [32].

Plasma diagnostic methods can be divided into two parts [33]:

    A- Internal diagnostic methods:

        1- Electrical sensors.

        2- Magnetic sensors.

    B- External diagnostic methods:

        1- Visual diagnosis.

        2- Spectroscopic diagnosis.

        3- Microwave diagnosis.

1.7.1 Plasma diagnosis using Optical Emission Spectroscopy (OES)

This technique is used to determine the gas composition, gas temperature, rotational and vibrational temperatures of electronically excited states, the reduced electric field, the electron density, and electron temperature. Optical emission spectroscopy (OES) is the main diagnostic technique for determining different essential plasma parameters. OES is a diagnostic technique that detects spontaneous emission signals from electronically excited species generated in plasmas [33]. The emission signal collected by an optical fiber is directed to a monochromator grade, where it is decomposed into an emission spectrum. Consequently, the spectrum is registered. The optical emission spectra are used to monitor gas phase composition and can be calibrated in absolute units using emission reference signals or a collisional radiative model. Moreover, the spectra can be analyzed in terms of line intensities for temperatures and reduced electric field determination, and line broadening for electron density and temperature estimations [34].

However, efficient detection is needed when rapid analysis is important and only a small fraction of the surface is being processed. A lens projects the emission from a particular area of the plasma chamber onto the entry slit of a

spectrometer. It is possible to get the necessary spatial resolution. UV-grade fused silica lenses should be utilized [33,34].

Figure (1-4) Device Optical Emission Spectroscopy [34].

1.8 Plasma Production

Plasma production takes place in many ways, one of the well-known methods can be achieved, it can be produced by applying electricity to the inert gas using two electrodes. This procedure may cause disturbance within the system. Plasma could be generated when electrons are separated from molecules or atoms under the appropriate pressure. The atom or molecule, that gives the electron, will become positive ions. These generated ions and electrons are affected by the magnetic and electric fields in terms of motion. Scientists consider this behavior as the main difference between the ionized gas and plasma state. In addition, in the lab, many types of plasma could be produced, for example, glow discharges, arcs fluorescent lamps, neon signs electrical sparks thermonuclear, and fusion experiments homely [35].

1.9 Aims of the Work

This work aims to investigate the characterization of the atmospheric pressure helium plasma jets:

1- Calculate the temperature and flame length of the plasma jet at different geometrical parameters such as Pyrex tube thickness and distance between electrodes, the electrical potential, and the gas flow.

2. Recorded and analyzed the spectra of helium plasma jets under different conditions (applied voltage and gas flow rate) to show the formation of reactive species and determined their intensity.

3- Investigation of plasma diagnostics by using the Boltzmann method to estimate the electron temperature and electron density.

Chapter Two

Theoretical Part

2.1 Introduction

Discharge phenomena can be defined as the transition of electrons and ions through the medium of gas. Plasma could be generated in many ways, such as vacuumed plasma, and DBD plasma. The ion-electron pair and flow current could be formed when the atoms and molecules of the gas break down electrically by using a very high voltage applied across the electrodes. The breakdown point could be characterized when the gas transition between poor and high electrical areas is achieved. In addition, the breakdown potential may be characterized when the transition occurs as a function of the difference between two electrodes [36].

The gas density and identity, electrode type, separation of inter-electrodes, and preexisting ionization degree are crucial parameters for determining voltage breakdown. The created ions and electrons are the result of the electrical discharge, the breakdown of gas may be developed in the area between electrodes dictating that the charged particles accelerated toward the cathode and anode. Separation charges could be observed as a result of collision processing therefore, the suitable voltage is important to achieve self-sustaining, which is usually lower than the breakdown voltage [37].

2.2 Plasma jet production in the laboratory

To create plasma in a laboratory, heating the gas at a pressure that is lower than that of the surrounding atmosphere until the gas's molecules have developed enough kinetic energy to start the ionization process, separate their electrons, form an electron-ion pair through an inelastic collision, and reach the material's fourth state [38].

There are several ways to create plasma, but the most popular method involves discharging in neutral gases. To do this, neutral gases are passed

between two electrodes while a high voltage difference is created between them under a specific amount of pressure, causing an electrical discharge to take place between the two electrodes (anode and cathode).

There are five ways in which an electric field can produce plasma [39]:

 1. DC Discharge.   2. Pulsed AC Discharge.

 3. Microwave Discharge.   4. Radiofrequency discharge.

 5. Laser-induced plasma.

2.3 Gas discharge

Electrical discharge brought on by gas moving through an electric field results in the creation of cold plasma. When an electric current passes through a gas, the gas molecules and atoms become ionized. This occurs when an applied voltage is employed between two electrodes, which causes the feeding gas to collapse between the electrodes, increasing the rate at which ionization processes occur. The electric field created by the accelerating electrons during the ionization process close to the cathode electrode causes them to jolt the gas atoms, which leads process of ionization or excitation [40]. The ionization of gas is adequate to produce light as an energy release. A luminous plasma is a discharge that is shining. The term "glow gas" is interchangeable with "cold plasma." Michael Faraday (1835–1831), a scientist, used the glow discharge to investigate the electric discharge in gases. Electrode configuration, their spacing, the energy source, the gas pressure, and the type of gas are used to categorize the gas-electric discharge, which is a phenomenon that happens naturally through lightning [41].

Two categories of apparent electrical discharge exist [42].

1- Glow discharge.   2- ARC discharge.

2.3.1 Glow Discharge

A type of luminous plasma known as a glowing discharge is one in which repeated collisions create a thin film with a significant amount of visible light. A significant number of positive and negative charges, as well as a variety of neutral types, make up a partially ionized gas [43]. As shown in Figure (2-1), the shape of electrodes is flat with space between them, and a low potential difference is considered, also the current in this process is low. These results show that glowing discharge, which is produced in a cell that contains inert materials at a low pressure of fewer than 10 millibars is investigated [44].

The identification of the discharge gas's atoms and the formation of both positive ions and electrons, also known as (gas breakdown). The glow discharge happens as the positive ions are propelled toward the negative electrode. The applied field accelerates the ions and electrons, giving them more kinetic energy that allows them to agitate atoms. These impacts result in the glow discharge's distinctive light being produced. Ionization encounters result in the production of new ions, electrons, and pairs, different types of lamps, discharge tubes for advertisements, generation gas by laser sector, and materials processing technology are just a few industrial applications that use the glow-discharge method [45].
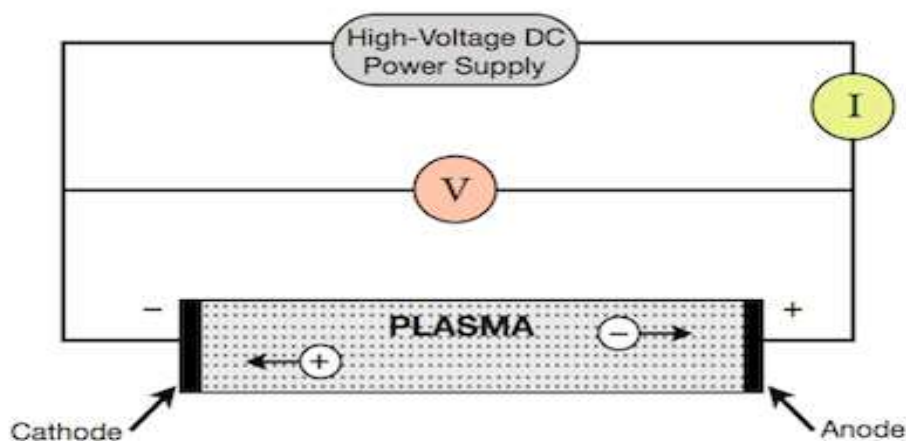
Figure (2.1): Glow discharge for low pressure [45].

2.3.2 ARC Discharge

Electrodes heat up sufficiently and release thermal electrons when they absorb high energy of the current. The gas in the electrical insulator breaking down causes a rise in temperature in the electrode material, resulting in a continuous discharge that causes an electric current to flow in an insulator medium like the air, which leads to the electric spark (arc). This result occurs when the is a drop because of the breakdown so that the electrons produce a thermal field that is released from the hot cathode as a result. This thermal field is used practically in the welding and plasma-cutting process, as depicted in figure (2.2) [46,47].
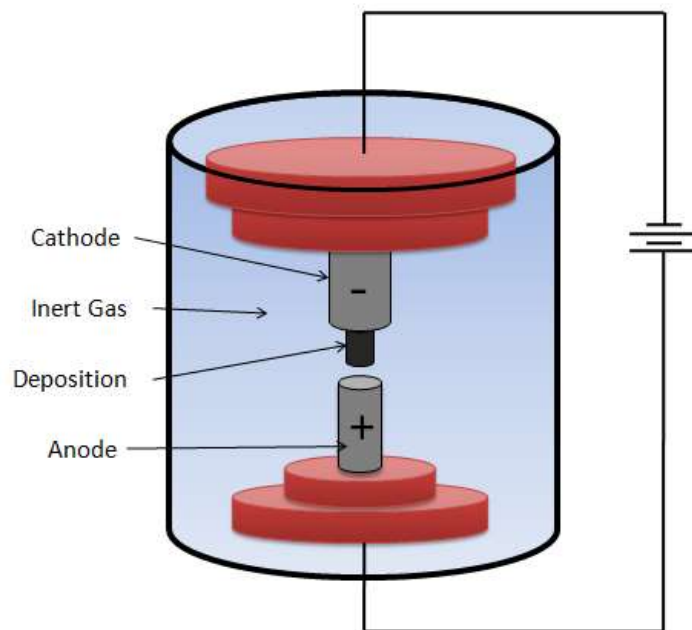
Figure (2.2): ARC discharge schematic [46,47].

2.4 Production of non-thermal plasma at atmospheric pressure

Non-thermal plasma at atmospheric pressure, which necessitates the provision of a vacuum-sealed system and is therefore very expensive, has recently decreased due to the plasma produced by the glowing discharge method at low pressure, which has proven to be extremely beneficial in laboratory

scientific research as well as its use in industry [48]. It contains only a small number of energetic particles. The generation of cold plasma at atmospheric pressure was therefore the new direction. These devices are easy to make, inexpensive, and full of active particles that function at standard atmospheric pressure. They can be developed in one way as a result of these characteristics, and various kinds have been employed in this process. Talk about the most significant gas discharges that operated at normal atmospheric pressure, including their elements, energy sources, electrode configurations, and uses [47,49].

2.4.1 Corona Discharge

Corona discharge is the first design successfully for the generation of non-thermal plasma under the atmospheric atmosphere When using electrodes with pointed ends, it manifests. because it results from the collapse of the gas gap in the vicinity of a powerful, sharply irregular electric field. When at least one of the electrodes is much smaller than the others, irregular electric field distributions develop. A gas discharge can be created by a high electric field with a pointed tip that is close to the electrode. which depends on the electrode spacing and whether it is fed by AC or DC. The orientation of the electrode determines the corona discharge classification, and the corona voltage can be either positive or negative [50].

According to figure (2.3), the corona is an irregular discharge phenomenon that occurs around the cathode (sharp end) and moves toward the anode which is flat but does not exist in the high field area. Corona discharge is used to gather impurities from water filtration, ozone generators, deposition processes, and many industrial bad gases [51].
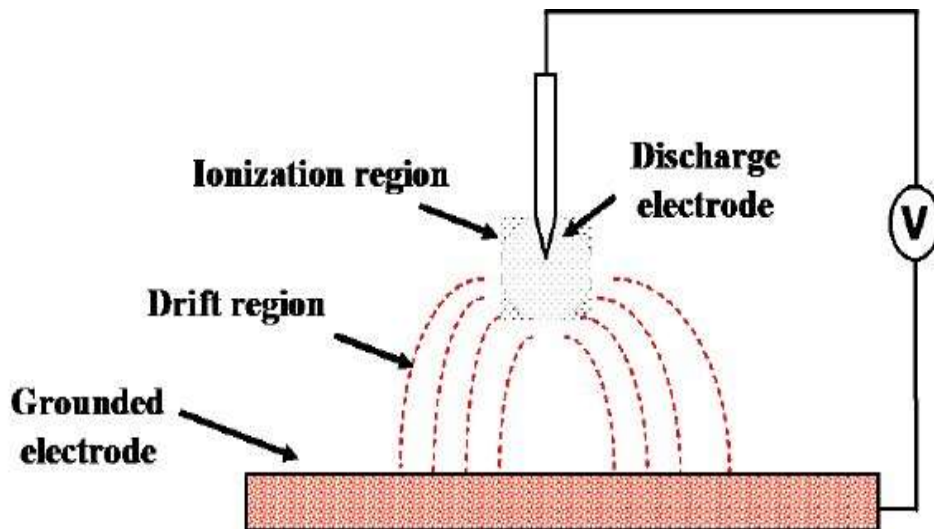
Figure (2.3): Corona discharge schematic [51].

2.4.2 Radio Frequency Discharge

High-frequency RF discharge occurs at (1−100) MHz.It is produced when the gas passes through an oscillating electromagnetic field. RF discharge has the benefit that it can be used at low pressures of less than 1 bar, and occasionally normal atmospheric pressure. It is possible to keep the electrodes in the discharge tube's exterior. This characteristic stops the electrode from deteriorating and causing metallic fumes to contaminate the plasma. Either capacitance or induction drives plasma [52]. While one electrode is grounded, another receives electricity from an alternating current voltage source via a capacitor. As shown in figure (2.4), the capacitor is charged at a high rate of ionic current, which results in a decrease in voltage and points the plasma into the negative half cycle, (2.4). Microelectronics, aerospace, and the manufacture of semiconductors all frequently use this variety [52, 53].
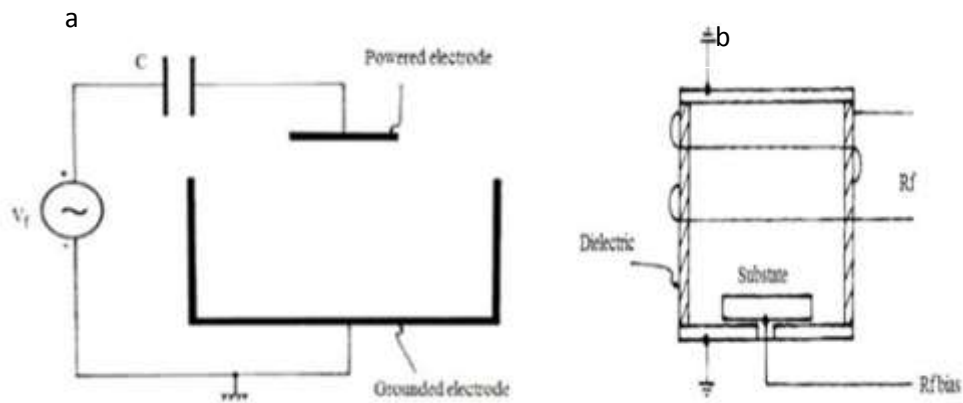
Figure (2.4): RF discharge: a. System with a capacitively coupled discharge b. inductively coupled discharge system [53].

2.4.3 Microwave Discharge

High-frequency electromagnetic radiation (300 MHz to 3 GHz) shown in figure (2.5), is one of the popular sources used to create electrical discharge in gases. This type of discharge can produce non-thermal plasma with high density when the fraction of ionized gas is higher compared with other gas ionization from (1mpa) to standard atmospheric pressure in a wide range of atmospheric pressures, high temperatures of 100,000 °C. Wide range, high effectiveness, and no need for electrodes are present in applications such as the production of lasers, light sources, plasma chemistry, and analytical chemistry [54,55].
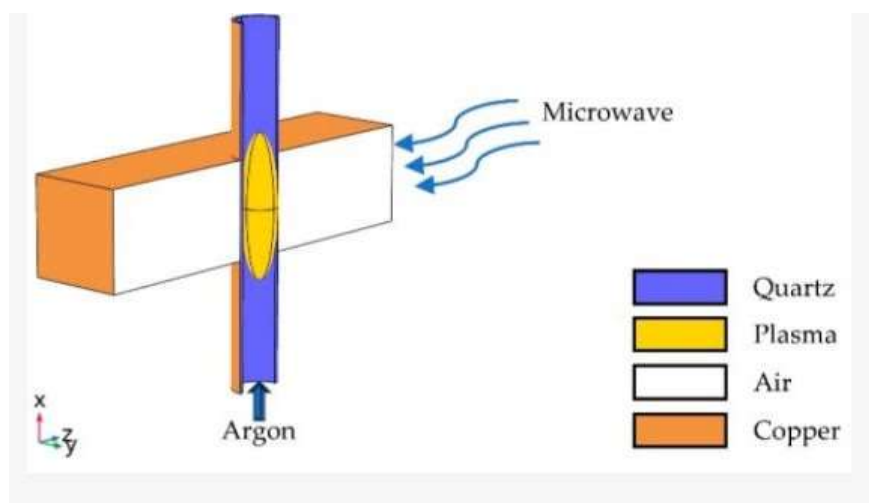
Figure (2.5): Microwave discharge view [55].

2.4.4 Dielectric Barrier Discharge (DBD)

Discharge through an electric barrier, also known as "silent discharge,". It uses a frequency range (50 Hz) to radio frequency MHz). The components of the system are two metal electrodes separated by a small gap of a few (mm) or a few (cm). The electrodes are covered in the tube which is made of quartz, Pyrex, or ceramic. These guarantees lead to the generation of cold plasma (arc transmission). creation of plasma is caused by the ionization of the gas atoms as the gas travels between the two poles [56].

An AC voltage source is frequently employed in an ionized gas, the system operates in various atmospheric pressure ranges. The significant difference between the classic discharge and this type of discharge is that the electrodes of the first one are in contact directly with the discharge gas, which causes scraping or erosion during the discharge process, in barrier discharge, the discharge, gas, and electrode are isolated from one another using a method called the barrier. the corrosion of wires is prevented by the electrically insulating barrier [57]. DC voltage is not used in the bulk head discharge, because capacitive coupling of the dielectric, which necessitates an AC voltage to operate the displacement current. The bulkhead discharge configuration is shown in figure (2.6). An insulating layer covering one of the electrodes, see (figure 2.6 a), and figure (2.6 b) further describes this phenomenon. The insulating layer separating the two wires can be seen in figure (2.6c) [58].

This kind is utilized in numerous industrial and laboratory uses, including chemical vapor plasma deposition, plasma medicine, flat plasma display panels, and surface modification of polymers [59].
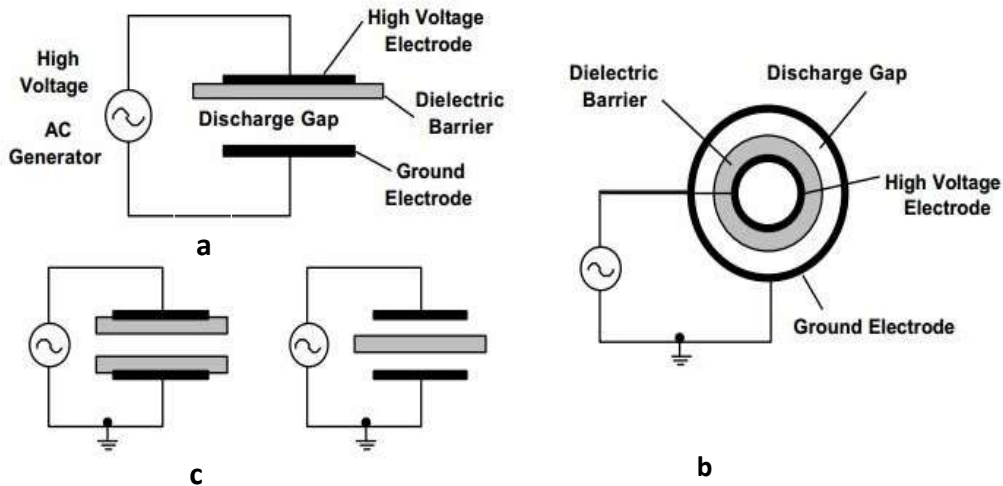
Figure (2.6): Configurations of DBD electrodes [59].

2.4.5 Atmospheric pressure plasma jets (APPJs)

It is a promising method for producing plasma, (APPJs) are capable of producing various reactive species and cold plasma at room temperature. An electrode is wrapped around or placed inside a tube made of quartz, Pyrex, or porcelain. To increase the reactive species, noble gas such as Ar, He, or N_2 is fed to the insulation tube and in some cases, a very tiny amount of oxygen can be added. For a few kilovolts, a variable-frequency sinusoidal or pulsed voltage is administered. (several hundreds of hertz to gigahertz) [60]. As it works at standard atmospheric pressure, this procedure occurs without using a vacuum chamber, allowing for the low-cost production of plasma. In modern times, the use of plasma discharges is growing. Surface modification, etching, and nano-deposition are examples of material manufacturing and biomedical uses. The destruction of cancer cells, wound healing, sterilization, and decontamination are some of the medical applications [61]. In endoscopic uses, such as the treatment of colorectal, dental, and pancreatic cancer, the delivery of cold plasma through a flexible tube can be very helpful. Attention has been paid to the creation of plasma sources for in vivo therapy in recent years through in-depth research on this subject, APPJ has been intriguing because it offers a medium

for conducting reactive plasma types, such as ion radicals, and UV radiation at normal temperatures and atmospheric pressure. The target is located a few centimeters from the tube end and the ionization occurs in the air. An energy source created from scratch that could be used for biomedicine and other medical applications was used in the design, construction, and operation of the plasma jet machine [62].

2.5 Configurations of Atmospheric Pressure Plasma Jets

Cold plasma jets in air pressure are divided into four categories: ("single electrode (SE)", "dielectric free electrode (DFE)", "Dielectric Barrier Discharge (DBD)", and "DBD-like jets") [63].

2.5.1 Dielectric Free Electrode Jets

The first APP-Js (Atmospheric pressure plasma jets) was the Dielectric-Free Electrode (DFE) Jet, which is generated by a radio frequency power source. It comprises an outer electrode that is grounded and an inner electrode that is wired to a power source. To avoid a high temperature, a noble gas containing reactive gases like oxygen is introduced into the annular area between the poles [64]. Depending on the radio frequency energy and its strength, the plasma jet's temperature ranges from 50 to 300 degrees Celsius. (between 50 and 500 watts), which is supplied to the plasma jet as depicted in figure (2.7). Due to its comparatively high temperature, the plasma jet is not appropriate for use in biological applications or medical, but it's used to treat materials because the materials are not sensitive to heat [65].
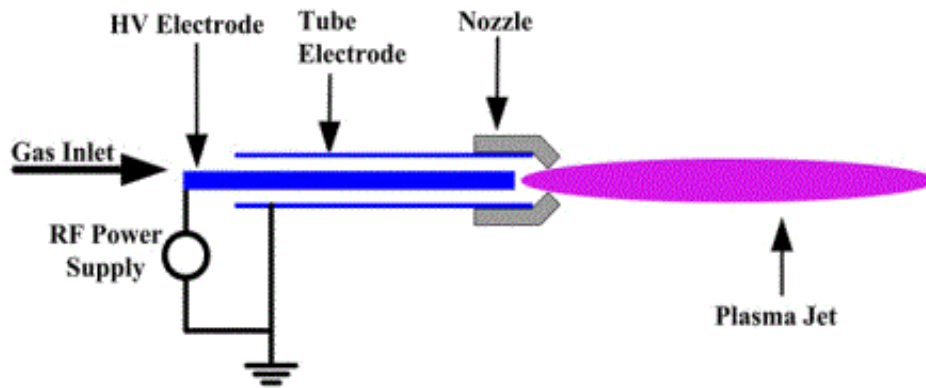
Figure (2.7): Dielectric-free electrode (DFE) jet [65].

2.5.2 Single Electrode Jets

AC or DC or Radio Frequency RF generator, as shown in figure (2.8) a and b, is used to generate single electrode (SE) jets. The system consists of an electrode connected to the power supply and an insulating tube and uses one or more noble gases to fuel it. The plasma flame is developed using a single electrode having a hollow shape, and the electrode is connected to the power source (see figure. 2.8c). Plasma for use in biomedical medical applications. The plasma jet can be touched without causing any harm in biomedical applications, which is why this form of jet is used, especially in dentistry [65,66].
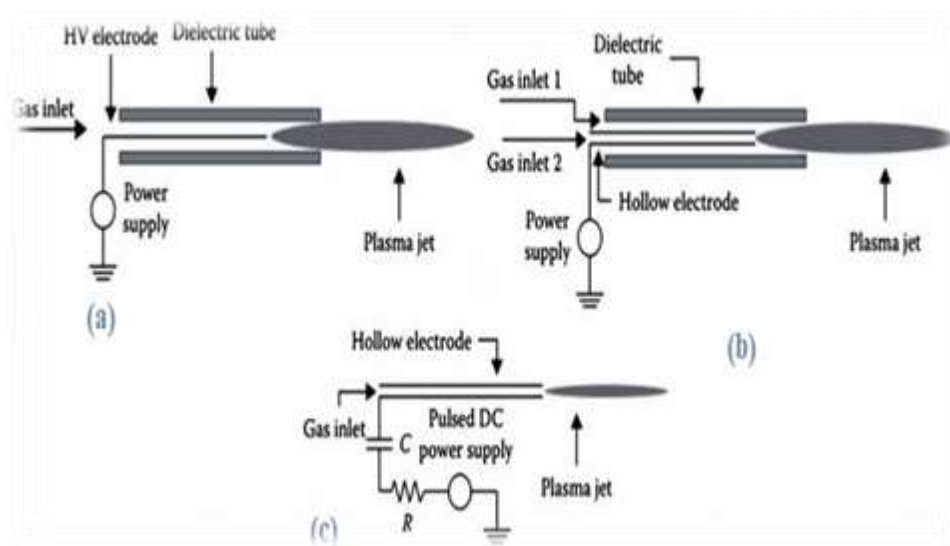
Figure (2.8): Single Electrode jet [66].

2.5.3 Dielectric Barrier Discharge-Like Jets

The plasma plume is in contact with the sample, in this type of plasma configuration the electrical discharge occurs between the electrode which is connected to high voltage, and the treated object, as shown in figure (2.9). (DBD-like), typically using two types of gas and between various mixing causes, may be used. One of the reactive gas kinds used for this function operates using a variety of sources, including an alternating current source, a direct current source, or a radio frequency source, and if necessary, an insulating tube and a ring electrode. When treating large-scale cells and tissues, this particular form of plasma flame is suitable for employment in medical applications. The possibility of bending these gadgets necessitates careful use [65,66].
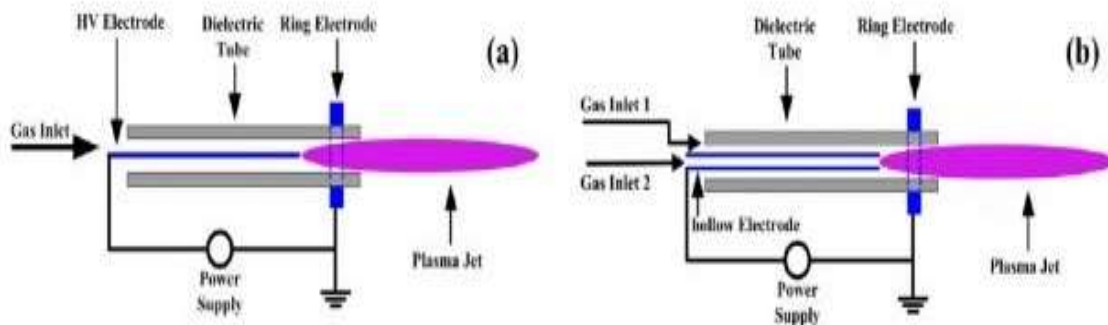
Figure (2.9): Dielectric Barrier Discharge-Like Jets (DBD-like jets) [66].

2.5.4 Dielectric Barrier Discharge Jets

Creating an electromagnetic field Barrier discharge jet powered by a high-voltage AC or continuous power supply, as shown in figure (2.9). While the (DBD) jets in Figure (2.10) are produced by DC high-voltage or AC high-voltage. The DBD jet is comprised of an insulating tube with double metal ring electrodes covering the outer of the Pyrex tube, and these electrodes are connected to electricity, see figure (2.10 a). Figure (2.10 b) illustrates the shielding tube being filled with noble gases. One toroidal electrode is in the flow while the other electrode is in the object. The jet in figure (2.10c) is made up of

two electrodes, exterior insulating, and an inner tube. (pin and ring). In this variety, the electric field is stronger along the plasma column. The plasma stream in figure (2.10 d) is made up of two insulating tubes connected by an electrode, which attenuates the electrical discharge inside each tube as well. Due to the low energy density in reactive species, DBD jets have the benefit of maintaining the cold plasma jet's temperature near that of ambient air. Additionally, there is no chance of the plasma-treated material curving. These two characteristics are crucial for many uses, particularly in the biomedical field [65,67].
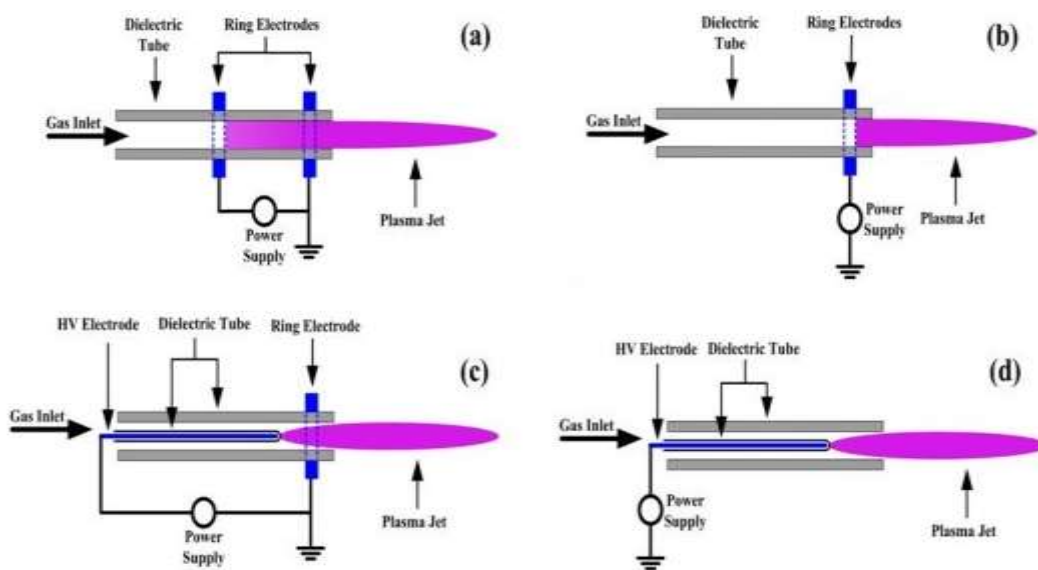
Figure (2.10): Dielectric Barrier Discharge Jets (DBD jet) [67].

2.6 Non-Thermal Plasma Jet Application

A normal atmospheric pressure plasma jet has several key benefits, including the ability to produce a natural, similar, and constant jet of plasma to a normal atmospheric pressure jet, and that ionized gas causes the plasma to flow through a small nozzle, allowing it to hit the target more precisely. It can handle hard surfaces by applying pressure to thin surfaces that are undamaged or have a high temperature of more than 300ºC [68].

The plasma jet can be used for a variety of purposes to these characteristics. In the handling of materials, it is frequently employed. Additionally, it is employed in the deposition of silicon dioxide thin layers using chemical vapor and plasma deposits. Because the plasma treatment has no side effects, it can shield the patient from discomfort. Because it will clearly distinguish between the exposed area to the plasma and the area that was not exposed cold plasma therapy has some control over the treatment area and has positive effects [69].

Due to the plasma's high degree of precision, the plasma therapy procedure is carried out by shedding the plasma directly on the cancerous cells without harming the healthy cells nearby [70]. Another significant use of the plasma jet is to sterilize dental equipment, surgical equipment, and hospital textile floors. It can also be used to remove radionuclides from surfaces and equipment, disinfect large industrial parts more efficiently than solvents, and remove radionuclides from surfaces and equipment [71].

2.7 Reactive Species

The collision between the accelerated charge particles with molecules or atom gas could produce reactive plasma species (reactive oxygen and nitrogen species (RONS)) by ionization, exiting, or dissociating the molecule's gas. Reactive oxygen species (ROS) are meaning highly reactive and oxygen-carrying, molecules consisting of a superoxide anion (O_2^{-0}) a hydroxide radical (OH), a single oxygen($1O_2$), and hydrogen peroxide(H_2O_2) [72].

Many parameters could affect and control the density of reactive species, for instance, frequency, and the applied voltage. Noble gases, such as (He, Ne, Ar, Kr, or Xe), might be utilized as a working gas. In addition, Air, Oxygen, and Nitrogen could be presented with a very small amount for increasing the reactive species density [73]. RONS are suggested to treat the medical subject directly for two reasons: first of all, they have a significant effect

on the organism, and second, they have a lifetime of up to several milliseconds. The chemical reaction inside the generated plasma could produce reactive oxygen species (ROS) when it has the O_2 or H_2O. It can produce the reactive nitrogen species when it has an apocopate nitrogen molecule. Oxygen, hydroxyl radical, and ozone are the constant of ROS, while the RNS constant of N2, NO, and NO2. The reactive species are easily produced in ambient air, and water with enough lifetime to destroy the bacterial cell [74]

2.8 The temperature and density of electrons by using Optical Emission Spectroscopy (OES)

Spectroscopic measurement can be done by the Boltzmann plot method which is a straightforward, and well-known utilized procedure, especially to deduce the electron temperature of plasma, the relative intensity of more than two-line spectra possessing a relatively huge energy difference [75]. The Boltzmann plot method is practically employed when the excitation level reaches the Local Thermal Equilibrium (LTE) [76]. Gas type always determines the ionization process. Hydrogen molecules require energy for dissociation of approximately (3,500 K), while the ionization of pure argon gas starts at (8,000 K). Argon and Hydrogen require ionization energies at (15.8, and 13.6 eV) respectively. Electron temperature T_e is a significant parameter to describe the properties of an APPJ, and T_e is estimated from the Boltzmann plot method using the equation (1) [77].

I is the relative intensity of the emitted line, λ is the wavelength, g_u is the statistical weight for the upper level and can be calculated from the total angular momentum for quantum number *J* by ($g_u = 2J + 1$), A_{kl} is the transition probability, that meaning is the probability per second that an atom in upper-level state emits in a random direction, and is de-excited to a low-level state.

K_B is the Boltzmann constant 1.38×10^{-23} J/K, T_e is the temperature in Kelvin, C is a constant, and E_u is the energy of the upper level. To calculate the Te, a graph is plotted for different values of (ln $\lambda I / g_u A_{kl}$) versus the energies E_u for the upper level giving a straight line with a slope of (-1/Te). All the parameters (λ, A_{kl}, g_u, and E_U) are obtained from the (National Institute of Standards, and Technology (NIST)), atomic spectra database levels form [78].

The electron density ne is calculated from the spectral lines emitted by the plasma jet using the Saha-Boltzmann relation (2-2) [79].

$$n_e = 6.04 \times 10^{21} \frac{I^a \lambda^a g^i A^i}{I^i \lambda^i g^a A^a} T^{\frac{3}{2}} \times \exp\left[\frac{E^a - E_{ion} - E^i}{k_B T_e}\right] \ldots\ldots (2\text{-}1)$$

I and a are indices that indicate the singly charged ion and the neutral particle. E $_{ion}$ is the ionization energy [80].

$$ln\left(\frac{\lambda I}{A g_u}\right) = -\frac{E_u}{K_B T_e} + C \ldots\ldots (2\text{-}2)$$

Where, λ: wavelength, I: Relative Intensity, A: Transition Probability,
gu: Statistical Weight, Eu: Energy of the Upper Level, KB: Boltzmann constant,
C: Constant, Te: electron temperature.

2.9 Literature Reviews

Characteristics of atmospheric pressure plasma jets (APPJs) are significant because of their use in various applications such as biomedical, medical, agriculture, and industry

U. Urabe *et al.,* 2010 estimated reactive species intensity in a plasma jet by using spectroscopic methods, plasma jet was created when double electrodes were connected to a voltage pulse with a helium gas flow. The results show the radial reactive species distributed in a uniform shape of the negative phase, while the phase in the positive case seemed to as a hollow shape. The length of the plasma jet was investigated with the same conditions for the processing of material in a conductive substrate put in front of the plasma jet [81].

Nie *et al.,* 2012 constructed a dielectric barrier discharge plasma as a coaxial type to produce a stable cold plasma at atmospheric pressure by improving the electric field between the electrodes. The results show that the unstable discharge stage occurs with increasing the employed voltage. The temperature of the electron and the electron density were evaluated and their values ranged from, (8.0 - 8. 9) eV and (4.6-6.4) $\times$ 10^{11} cm^{-3} respectively. The plasma jets with low temperature (~ 300 K), were slightly steady in the normal direction, the plasma with this characteristic was a useful tool for the treatment of heat-sensitive materials [82].

J. Raud *et al.,* 2013 investigated atmospheric pressure argon DBD plasma jet characteristics, the working parameters are 6 kHz in case of negative and positive half-cycles of voltage were considered. The results show that the argon plasma jet propagated in air differs from that found by the helium plasma jet, because Ar-air mixing was negligible or low [83].

Chen *et al.,* 2014 generated a plasma jet with atmospheric pressure by using an array system. Different working parameters such as applied voltage, power supply, frequency, and gas flow rate were examined to explain their effects on plasma properties. The results illustrate that these parameters affect the length and shape of the plasma jet, the maximum jet length obtained at an applied voltage (8.5 kV), frequency (20 kHz), and rate of gas flow was 20 L/min [84].

Cheng *et al.,* 2014 studied the influence of power supply on the characteristics of plasma jets with atmospheric pressure, to investigate the ionization process that occurs in the generated plasma. The results show that the properties of helium plasma jets were studied by both microsecond-pulse and nanosecond-pulse generators. Initially, the electrical discharge happened in a small region near the high-voltage electrode, in case of increasing the applied voltage the helium plasma jet is stable. The discharge current was larger in using a nanosecond pulse than that of using the microsecond pulse because the consumption energy was less in the latter case. Both Jet length and spectral line intensity of reactive species were stronger in the nanosecond-pulse excitation case, also rise time of the employed voltage led to an important role in the generation of plasma jets [85].

W. Yan *et al.,*2015 used a dual-power electrode (DPE) system to generate a helium plasma jet with atmospheric pressure and investigated its characteristics. A comparison between two configurations, the DPE and the single-ring electrode was achieved to estimate the influence of a needle electrode on the electrical discharge. In using needle electrodes, the generated helium plasma jet had a higher distribution velocity. Also, the effects of the needle-to-ring discharge distance and needle radius on the generation of a plasma jet are studied. The simulation results illustrated that the needle electrode has a significant effect on the characteristics of the plasma jet [86].

Rizan *et al.*, 2017 analyzed the electrical properties of generated plasma by estimating the voltage, current, and force through the electrical discharge process. It was clear that the total energy consumed in the case of the inner needle electrode was slightly less than that on the outer electrode, because of the polarization charges that happened on the inner needle electrode. The characteristics of discharge were further investigated using optical emission spectroscopy OES, measured during the OES measurements, its process was performed by aligning the optical quartz lens and the fibers of the spectrometer in two positions of the plasma discharge. The intensity of OH was higher than the intensity of N in the plasma aperture [87].

Bo. Zhang *et al.*, 2018 constructed an array system to generate a helium plasma jet by using a linear field. The electrode structure was a toroidal excited by alternating current. The dependence of helium plasma jet properties (electrical and diagnostics) on the employed voltage and rate of gas flow was checked visually. The generated plasma with the linear-field jet was relatively large-scale, with better uniformity and longer flame in comparison with the cross-field. The results can be obtained at a gas flow rate of 4 L/min and a peak applied voltage of 7 kV [88].

Nima *et al.,* 2019 studied a helium plasma jet with atmospheric pressure at various gas flow rates using optical emission spectroscopy (OES). The spectrum of plasma was estimated in the case of direct interaction with de-ionized (DI) water and without. The temperature of electron and electron density was determined by using the Boltzmann plot and the Stark broadening of wavelength (486.1 nm) for atomic hydrogen, the examined parameters were checked with various rates of gas flow. The peak of hydroxyl concentrations contacts with DI water directly, in addition, to contact the upstream of the plasma jet, according to the spectra collected by OES. The relative hydroxyl intensities were determined by adjusting the flow rate of gas [89].

Jõgi *et al.,* 2020 studied the operational performance of cold atmospheric plasma jets (CAPJ) in two configurations to compare their properties of them. The first was a needle-to-cylinder electrode configuration and the second was a single high-voltage cylinder electrode encircling the Pyrex tube. The plasma was generated by a sinusoidal kHz frequency AC power supply, and the working gas was argon that passed through a Pyrex tube, the inner diameter was 0.5 mm. The results illustrated the mechanism of electrical discharge for these two designs. Both CAPJs have a lower waveform of the applied voltage, and as the voltage amplitude increased, the number of ionized waves increased [90].

M. Hofmans *et al.,* 2020 characterized the He plasma jet driven by a pulse of positive employed voltage. The comparison of numerical and experimental results shows excellent agreement between them. It focuses on the pulse width of pulsed employed voltage, the distribution of the mixed gas, the length and speed of the flame jet, and the voltage droop in the discharge region. Also, a comparison to simulations reveals that the jet length can be controlled by the pulse width and magnitude. The employed voltage reaches the critical value in the discharge front during long pulses (1000 ns). The critical value is reached 90–130 ns after the pulse falls. The gas mixture determines the magnitude of this critical value [91].

A. Asghar and Galaly 2021 constructed oxygen/argon (O_2/Ar) atmospheric pressure plasma jets (APPJs) with a rate of flow ranging from 0.2 to 4 slm for alternating current. Investigations of characteristics were achieved on the voltage-current relation of the APPJ discharge, at various working parameters such as gas flow rate, plasma plume length and width, discharge plasma power, distribution of plasma temperature, and optical emission spectra. As the argon flow rate decreased, the plasma temperature noticeably dropped. The optical emission spectra of a plasma jet were examined [92].

H. Sakakita *et al.,* 2021 measured the electrical characteristics of an atmospheric-pressure helium plasma jet at low temperatures. The results show that the employed voltage and actual plasma current are nearly in phase. The production energy by the plasma is used to heat neutral particles in collisions. The estimate of charged particles at the inner surface of the dielectric quartz tube was done by integrating the plasma current. The polarity of the discharge particle was bipolar due to exposure of the plasma to ambient air without the target plate [93].

Yuanyuan *et al.,* 2021 developed the estimation of OH and O densities in helium–humid air plasma jets with atmospheric pressure, under different working parameters by considering numerical simulation in two-dimensional. The results show when the gas flow velocity decreased, the density of reactive species increased. The O atom had higher density throughout the channel of the jet at a low velocity of gas flow before the plasma jet reached the substrate surface, but the high velocity of flow made the O density shift to the jet head, increasing the speed of gas flow had a little effect on the O density distribution in case of the plasma jet passed along the substrate surface. The OH radical is distributed in a region near the tube nozzle and unaffected by the velocity of gas flow. Changing the relative permittivity of the substrate lead to an increase in the densities and the axial extension lengths of O and OH radical [94].

Ayat *et al.,* 2022 used argon gas to create non-thermal (cold) plasma with working parameters microwave frequency up to 2.4GHz, flow rates (1, 2, 3, 4) L/min) and voltages (150 V). The electrical properties were investigated and optical characteristics were using the technology of optical emission spectrometry (OES). The Boltzmann diagram method and Stark broadening were used to estimate the electron temperature (T_e) and electron density (ne) respectively. With higher gas flow rates, the electron temperature decreases from 0.991 to 1.273 eV, and the electron density increases from (2.173 to 3.664) x

10^{17} cm^{-3}. In addition, the plasma plume length increases from 1.1 to 3.5 cm when the plasma temperature decreases [95].

Olivera *et al.,* 2022 investigated the atmospheric pressure plasma jets (APPJs) that were generated with liquid samples. A pin electrode configuration connected to DC-applied voltage and a frequency of 330 kHz produced a helium plasma jet that was in contact with a distilled water sample. Plasma diagnostics was necessary as one step that will estimate electron temperature and electron density which make the plasma become suitable for applications in different areas. An electrical characterization of produced plasma was found by using two methods. The first one is based on the current measurement and voltage signals directly, and the second uses Lissajous figures. The results show that both of these methods determined the consumed power successfully when the discharge is in contact with water, at this condition the dissipation power consumed must be taken into account [96].

Shiuan and Zhang 2023 constructed an atmospheric pressure plasma jet (APPJ) that works by mixing oxygen with the inlet gas of nitrogen. A mathematical model that determines the fluid dynamics to simulate the nitrogen APPJ properties such as heat transfer, mass transfer, diffusion, and chemical reactions. The results show that, if the oxygen impurity increased, the plasma temperature dropped, also the excited and neutral species were affected by oxygen impurity. Because the most important reactant in APPJ treatment is an excited state species, this work could be used as a database for the modification of a nitrogen source APPJ [97].

Radhika and Kar 2023 designed and constructed a configuration of a cross-field electrode system to generate atmospheric pressure plasma jets, and the influence of an additional floating electrode on the properties of a cross-field plasma jet was studied. The results show that the floating electrode was used in

the jet spread path, the required power was less for making the plasma jet pass the nozzle. This threshold power and the maximum flame length depend on the electrode widths. Using a floating electrode led to an increase in the intensity of reactive oxygen and nitrogen species (RONS), also the relative production of ions increased [98].

Chapter Three

Experimental Part

3.1 Introduction

In this chapter, we describe in detail the cold plasma system used in this work, information about the components used in its construction, and information about the electrical equipment and accessories that were employed to monitor the system's voltage and current. Measurements of electron density, electron temperature, and plasma temperature were performed using thermal and optical instruments.

3.2 Components of the APPJ System

The cold plasma system at atmospheric pressure, which was worked on in the laboratory of the College of Science, Department of Physics, University of Kerbala, is shown in figure (3-1).

Figure (3-1): Photograph of APPJ plasma jet system:
1. Earth wire, 2. Helium gas,3. Power supply, 4. Pyrex tube, 5. Electrodes,
6. OES sensor, 7. High voltage prob., 8. Helium flow meter.
9. OES device, 10. Oxygen flow meter, 11. Oscilloscope, 12. Laptop.

The atmospheric pressure plasma jet system was constructed at room temperature with different Pyrex tube thicknesses (1, 0.5, 0.2, 0.1) mm. Electrical properties, electron temperature, and electron density are calculated. Finally, the optimum working parameters of the plasma jet were determined.

3.2.1 AC power supply

Applying an atmospheric pressure differential to helium gas in the lab will produce artificial plasma. This energy is sufficient to ionize the gas and excite its atoms. A high-voltage AC power supply device is utilized, as shown in figure (3.2). With variable frequencies ranging from 0 to 120 kHz, this device offers high voltages of 0 to 20 kV, to create the plasma jet. Initially, the AC power source is connected to the electrodes of the cold atmospheric plasma jet system.

Figure (3.2): a homemade AC power source with high voltage.

3.2.2 Pyrex tube

This work employs a dielectric barrier discharge (DBD) type atmospheric pressure plasma device. Pyrex tubes are used for bulkhead discharge, and with different thicknesses (1, 0.5, 0.2, 0.1) mm as shown in figure (3.3). The effects of tube thickness on the electrical properties of the generated plasma are investigated, such as column length of plasma and plasma temperature, which play a major role in various cold plasma applications.
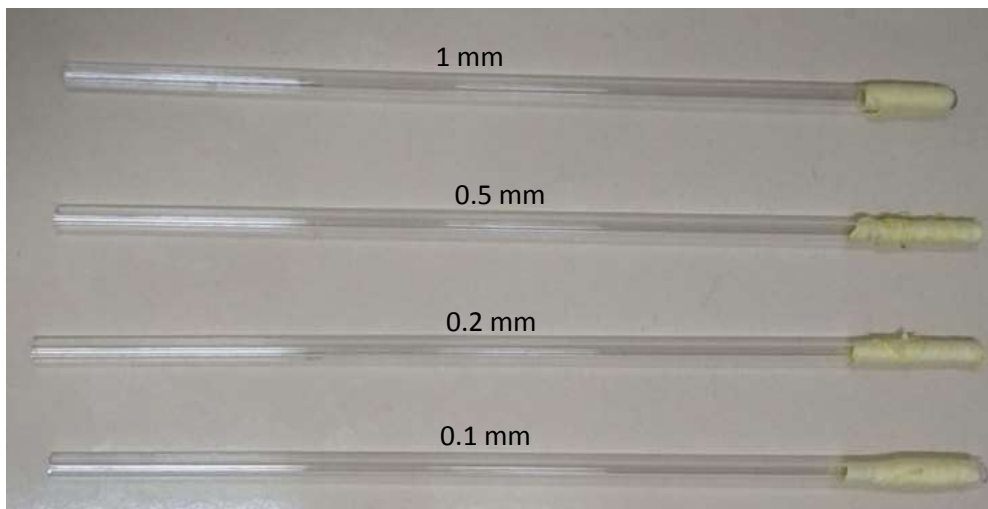

Figure (3.3): Photograph of the Pyrex tubes with different thicknesses [99].

3.2.3 Discharge electrodes

Double- electrodes are used to build the DBD plasma which is made of aluminum covering the outer Pyrex tube. The electrodes have 0.1 mm thickness and 10 mm width. The distance between the electrodes was 10 mm and the distance between the ground electrode and the nozzle of the Pyrex tube was 3mm. The upper electrode was connected to a power source and the lower electrode was earthed (as shown in figure (3.4)).
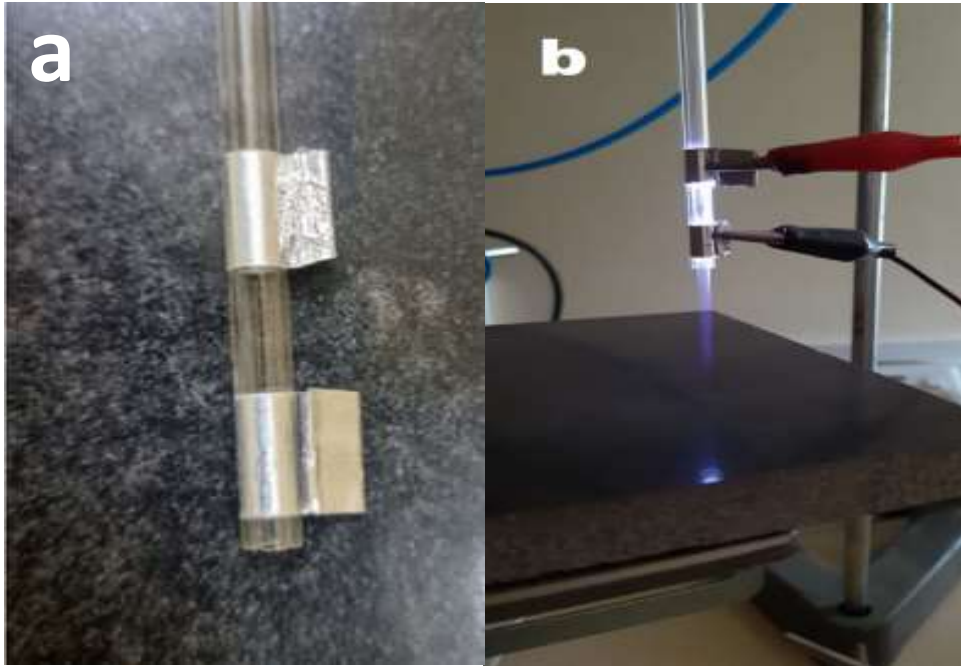
Figure (3.4): An image of a DBD plasma jet. (a) Electrode configurations. (b) Photograph of a Pyrex tube and connected electrodes with the power supply to generate a plasma jet.

3.2.4 Gas Flow Controller

Commercial-grade helium gas (99.999% purity) is fed through a flexible plastic tube and into the top of the Pyrex tube. The flow meter is connected to the Pyrex tube by a tight lock and is employed to regulate the flow of helium gas through the flexible plastic tube at a rate of (1-6) L/min see figure (3.5).

Figure (3.5): flow meter.

3.3 Measurement of plasma jet Parameter

3.3.1 Measurement of the Electrical Characteristics

The waveform of the applied voltage between the electrodes of the system was measured using a high-voltage probe, the high-voltage probe and the probe are linked to a digital oscilloscope (Max 28 kV AC 40 kV DC cat III) is used to estimate the electrical wavefront of the generated plasma, it has a division ratio (1000:1) and bandwidth of 75 MHz, as shown in figure (3.6). The connection way is summarized as, the downstream electrode connected to the ground lead, and the upper electrode of the Pyrex tube is connected to the tip part of the high-voltage probe.
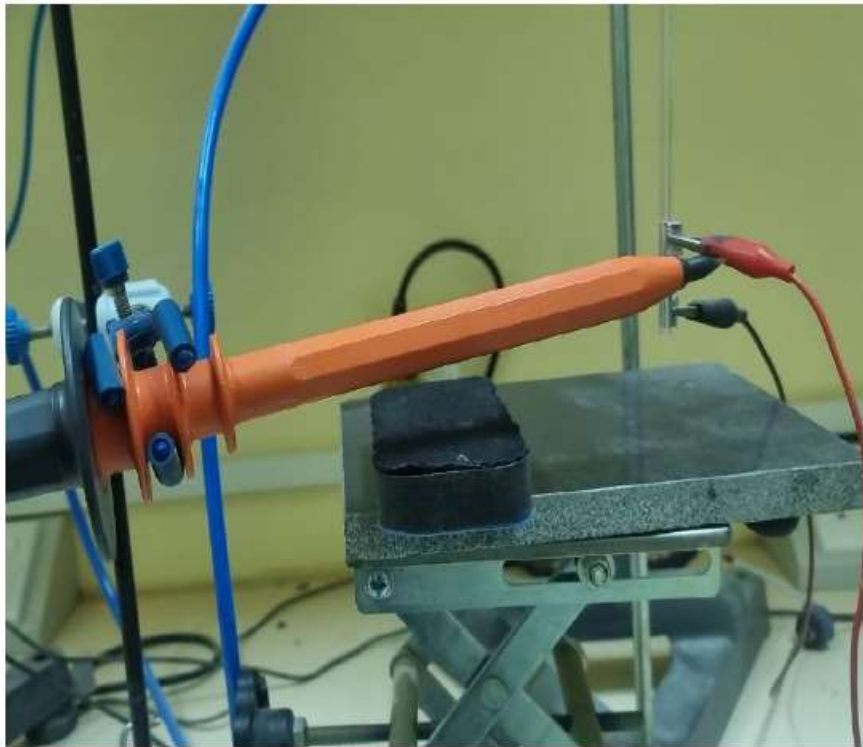

Figure (3.6): Photograph of high voltage probe.

To determine the bandwidth of the voltage waveform, the input channel of the oscilloscope (Hantek, China) is connected to the voltage probe. The oscilloscope has three input channels, as shown in figure (3.7), and a bandwidth of 20 MHz.

The wavefront can be shown by connecting the apparatus to a laptop computer. In addition.

Figure (3.7): Photograph of oscilloscope device.

When the secondary coil of the other oscilloscope, which is used to detect the current in the wire at a high frequency, is connected to its input, the waveform of the discharged current is measured. The secondary coil will be encircled by the wire. A coil inside the circuit will experience an alternating magnetic field that the voltage transformer will counteract. An iron core is encircled by the coil. As shown in figure (3.8), the other coil's magnetic field will disperse in the oscilloscope.
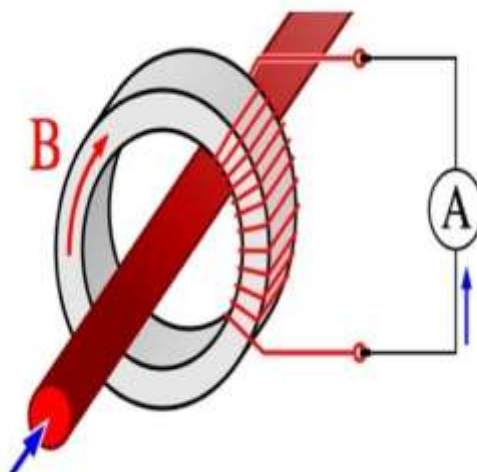

Figure (3.8): Schematic and photograph of a coil current.

3.3.2 Plasma jet length measurement

The distance between the lower edge of the Pyrex tube and the plasma jet's end is referred to as the plasma jet length (see figure 3.9). In other words, the plasma jet's visible length in the surrounding air. At various gas flow rates and voltages, A metric ruler was used to determine the plasma jet's length starting from the bottom of the Pyrex tube.
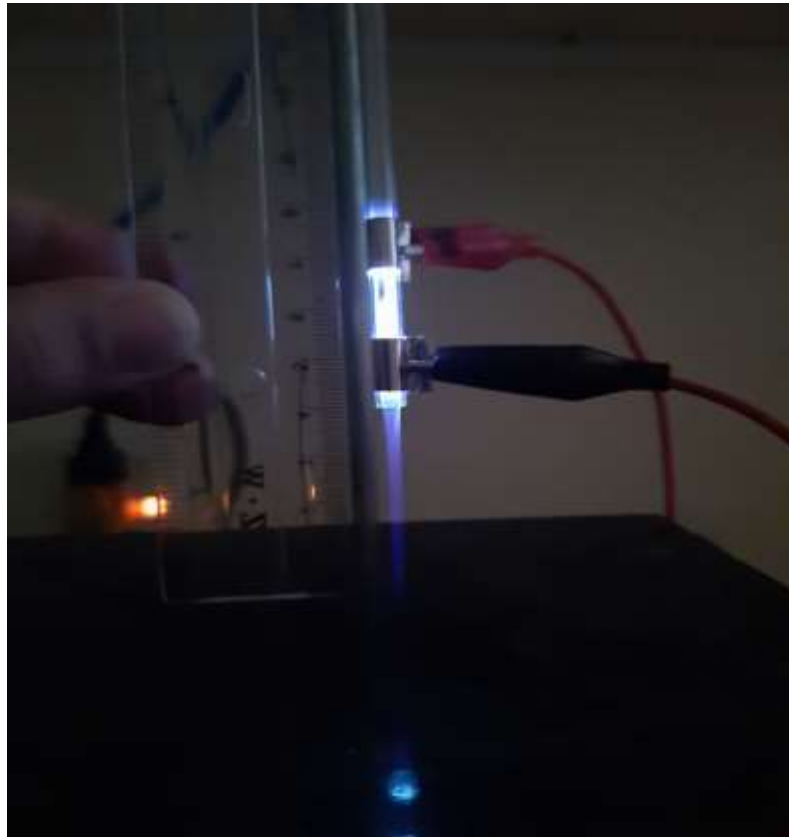
Figure (3.9): Plasma jet length measurement.

3.3.3 Plasma jet temperature measurement

One crucial factor that affects the type of applications for the plasma jet is its temperature, as was already mentioned. A laboratory mercury thermometer (see figure (3.10)) or a straightforward electronic thermocouple sensor of the UTS type (see figure (3.11)), where the temperature-sensitive part is located at various distances from the end of the tube nozzle at various gas flow rates, can be used to measure the temperature. It was determined that the plasma

temperature along the column was in the (26-46) °C range, which is for many biological applications.

Figure (3.10): Photograph of the mercury thermometer.

Figure (3.11): Photograph of a simple electronic thermocouple sensor of the UTS type.

3.3.4 Measurement of the Optical Properties

An ultraviolet-visible near-infrared (UV-Vis-NIR) spectrometer with a wavelength range of 150 nm to 1000 nm was used to measure the emission spectra of the plasma jet, as shown in figure (3.12). To capture the spectral emission, a fiber-optic cable was attached to the spectrometer. The radiation emitted from the plasma jet was collected using a lens to prevent scattering of the plasma radiation. A spectrometer connected to a laptop captured information about the spectral emission lines and their lengths, which were then plotted.
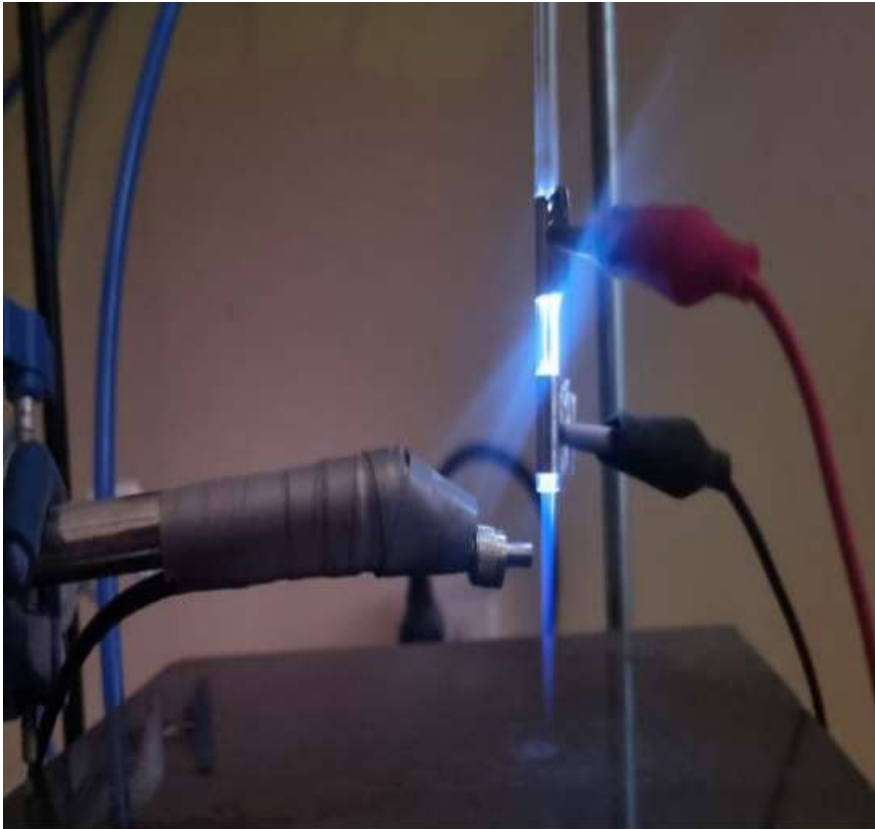
Figure (3-12): An optical fiber cable with a collimator.

Optical emission spectroscopy (OES) contains the collection, spectral dispersion, and detection of light. OES is based on the excitation of particles (atoms, molecules, ions) and measurement of radiation (light) that is emitted while the particle returns to the lower levels, The Wavelength of emitted radiation is specific for each particle, and qualitative analysis of elements. However, efficient detection is needed when rapid analysis is important and only a small fraction of the surface is being processed. A lens projects the emission from a particular area of the plasma chamber onto the entry slit of a spectrometer. It is possible to get the necessary spatial resolution. UV-grade fused silica lenses should be utilized since emission from 200–1000 nm is frequently captured. Moving the collection lenses or, in research reactors only, shifting the plasma reactor itself might be used to scan the imaged volume laterally [70]. In this experiment, the convex lens with a (10 mm) and radius (2.5 cm) focal lens was used.

Chapter Four

Results and Discussion

4.1 Introduction

This chapter describes and discusses the findings of cold plasma jet systems, including their electrical, thermal, and optical properties. Information on how electrical qualities affect the voltage and frequency needed to make a system function is provided in this chapter. Along with taking into account the gas flow rate, which was investigated in terms of how it affected the plasma jet's length and temperature, it also examined how raising the voltage and frequency affected the plasma jet's length and temperature. It was calculated that the plasma jet's electron temperature T_e and electronic density n_e.

4.2 Electrical Characteristics

The plasma jet is generated at a frequency of 60 kHz, with an applied voltage of (8 kV), and a flow rate of (4 L/min). The electrical waveforms shown in figure (4.1) were obtained by measuring the high-voltage with a probe connected to the input of the first oscilloscope, measuring the current with a secondary coil connected to the input of the second oscilloscope, and then connecting the monitor to a computer: A pulse is produced by using helium plasma. a fluctuating sinusoid having values that rise and decrease in response to the applied voltage before reaching a peak. This happens as a result of the accumulation of negative charge on the Pyrex tube surrounding the negative electrode, and it is a crucial component of the DBD plasma system since it lowers the chance of arcing [100].
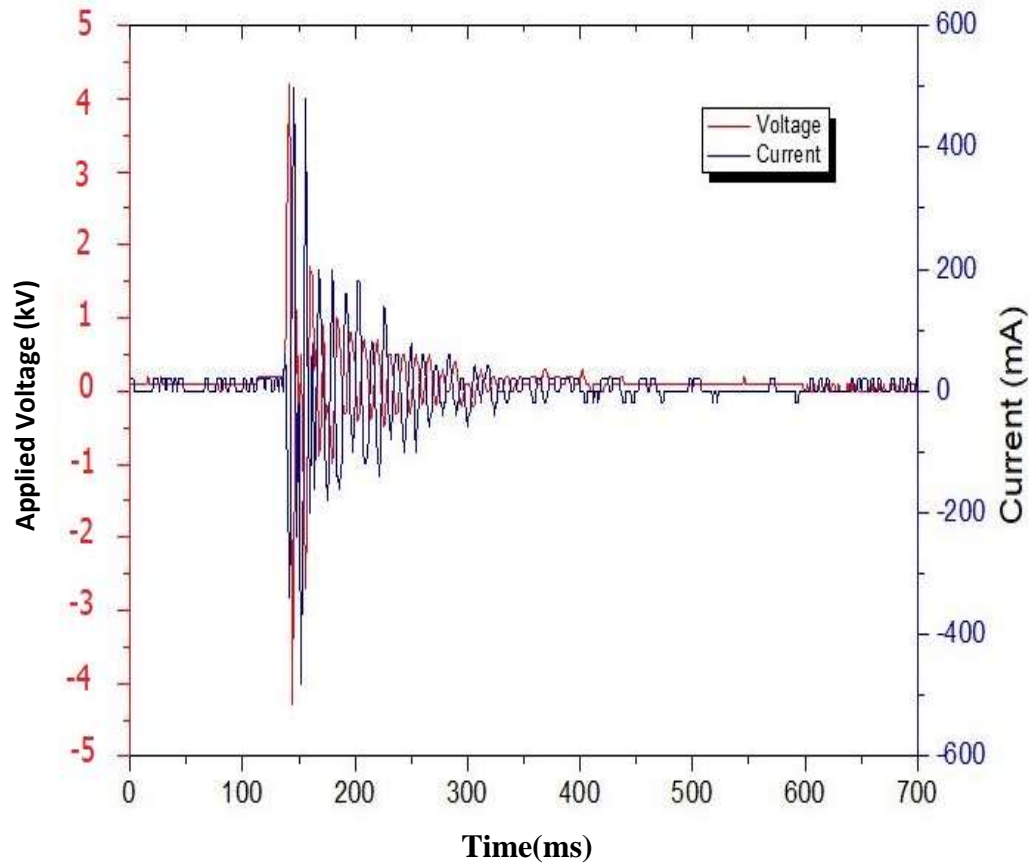
Figure (4.1): Waveforms of the Discharge Current and the Applied High Voltage.

4.3 Length and Temperature of the helium plasma jet.

Different Pyrex tubes were used to generate atmospheric pressure plasma jet to show the effects of tube thickness on plasma temperature and plasma plume length as shown in table 1.

Table 1. Plasma temperature and plasma plume length at different Pyrex tube thicknesses in case of 8kV applied voltage and gas flow rate (4L/min), the distance between the electrodes was (1cm)

Table (4-1): Effect of Pyrex tube thicknesses on plasma plume and plasma temperature.

Tube length (cm)	Inner diameter (mm)	Thickness (mm)	flame length (cm)	Temperature (°C)
21	2	0.1	7	40
21	2	0.2	6.5	35
17	2	0.5	8.5	32
16	2	1	6	26

Shows the plasma plume length randomly variation due to the thickness of the Pyrex tube because the drift velocity of ions is unstable in different thicknesses. The maximum jet length of 8.5cm has been observed at 0.5 mm thickness and the plasma temperature is 32 °C, The suitable results for use in biomedical and medical applications are obtained at 1 mm thickness because of plasma temperature is 26 °C. Figure (4.2) presents a plasma column of different Pyrex tube thicknesses when the applied voltage is 8kV and the gas flow rate is 4L/min, the plasma temperature strongly depends on the thickness of the Pyrex tube, with 1mm thickness has a low temperature of 26 °C than other tubes which is close to room temperature because of collisions between electrons and ions.
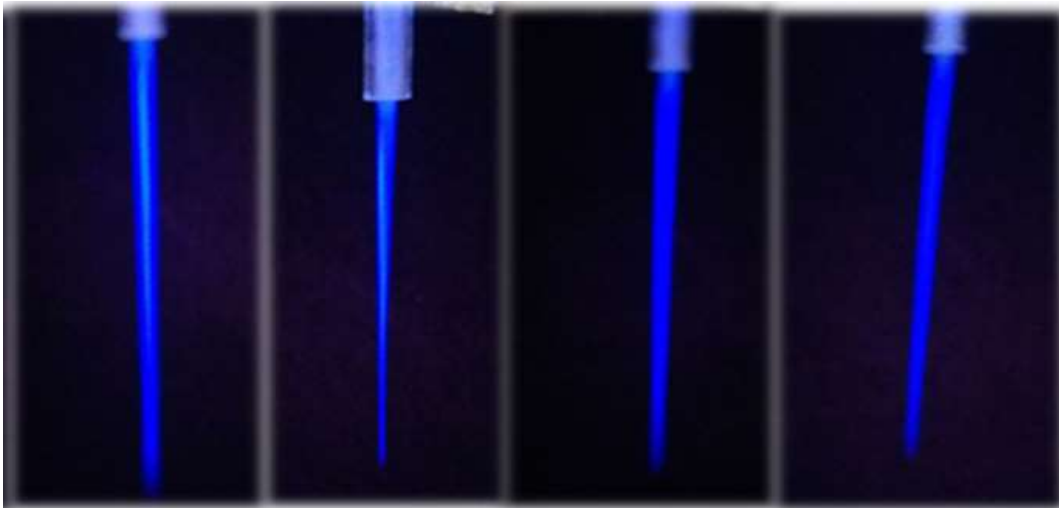

Figure (4-2): Plasma plume length at different of Pyrex tube thicknesses.

Figure (4.3) explains the behavior of plasma temperature with time, for more than one minute the increase in the plasma temperature becomes constant and can be recorded the temperature of the plasma. Figure (4.4) shows the plasma is generated at a range (1-2.5) cm distance between the electrodes but the plume length of the plasma jet decreases as the distance increases in constant applied voltage (8 kV) and helium flow rate (4L/min), this behavior occurs due the voltage drops [101].
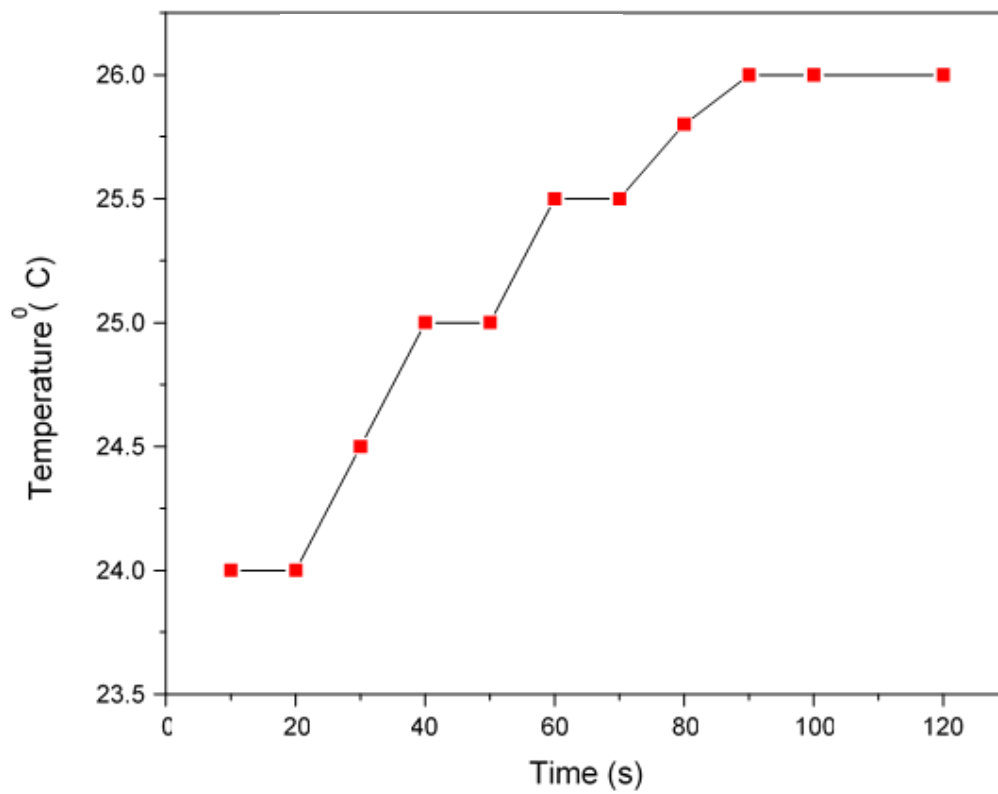
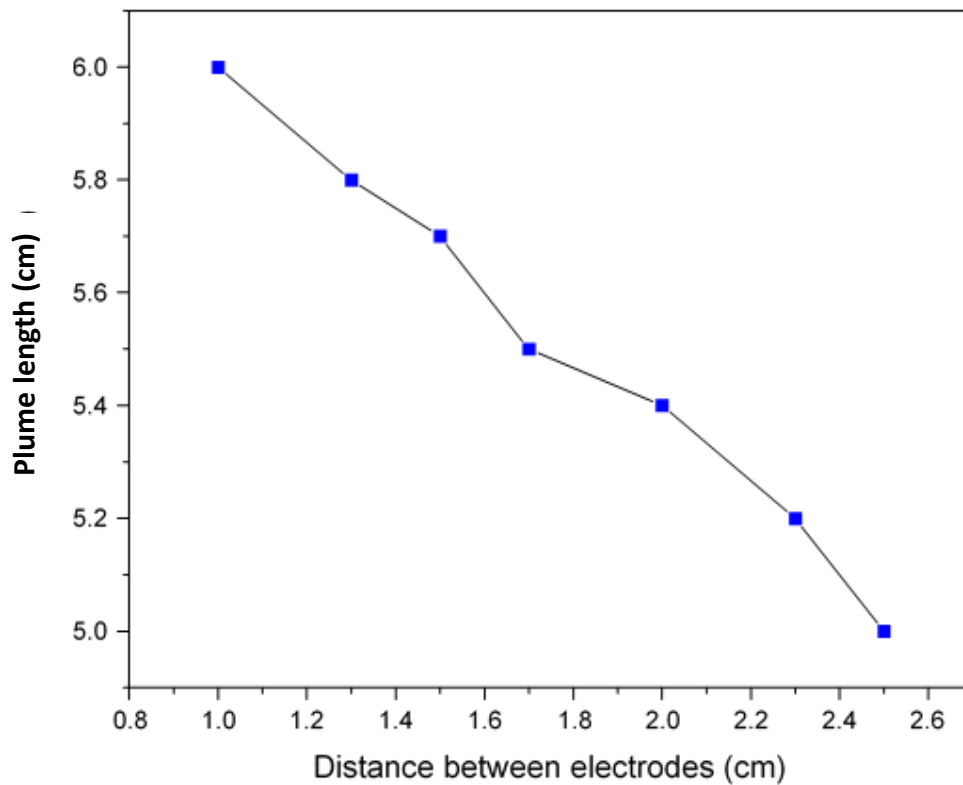Figure (4-3): Helium plasma temperature as a function of time.

Figure (4-4): Dependence of plasma plume length on the distance between electrodes.

Dependence of Plasma temperature on the distance between the electrodes in the plasma system illustrated in figure (4.5), the reduction of plasma temperature is clear when the distance between the electrodes increased at a constant applied voltage of 8 kV, at (1) cm the plasma temperature is 26°C. This value decreases slightly when the distance increases until reaches more than (2.5) cm the plasma is not generated [102].
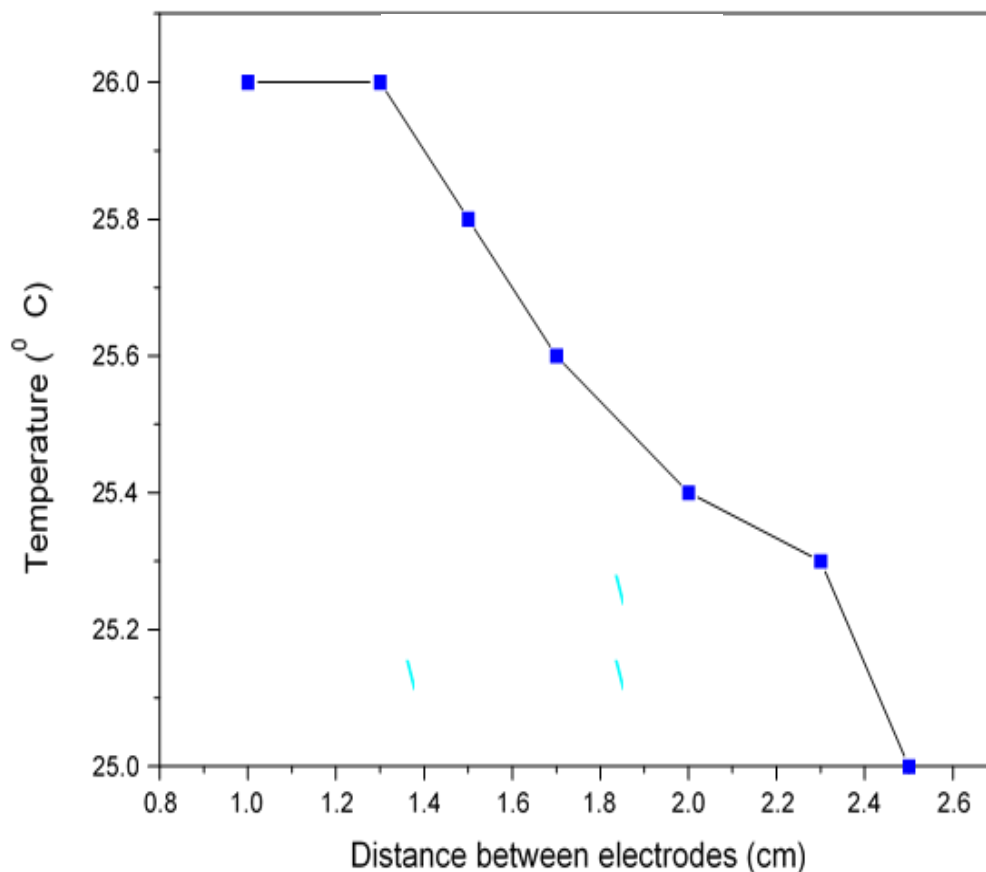

Figure (4-5): Influence of distance between electrodes on plasma temperature.

A tube with a length of (16 cm), an inner diameter of (2 mm), and a thickness of (1 mm) was taken. The flame length and the temperature of the plasma jet were calculated for several cases of helium gas flow (1-6) L/min and applied voltage (8-14) kV.

Table (4-2): Length plume and temperature of the plasma for applied voltage (8-14) kV and flow rate 1 l/min

Volt (kV)	Flame length (cm)	Temperature (^{0}C)
8	3.2	35
9	3.5	36
10	3.8	38
11	3.8	38
12	4	40
13	4.2	45.5
14	4.5	46

Table (4-3): Length plume and temperature of the plasma for applied voltage (8-14) kV and flow rate 2 l/min

Volt (kV)	Flame length (cm)	Temperature (^{0}C)
8	5.5	34
9	5.7	35
10	5.8	37
11	6	38
12	6.1	40
13	6.3	41
14	6.5	42

Table (4-4): Length plume and temperature of the plasma for applied voltage (8-14) kV and flow rate 3 l/min

Volt (kV)	flame length (cm)	Temperature (^{0}C)
8	5.6	29
9	5.7	30
10	5.8	30.5
11	6.1	30.5
12	6.3	31
13	6.4	31.5
14	6.7	32

Table (4-5): Length plume and temperature of the plasma for applied voltage

(8-14) kV and flow rate 4 l/min

Volt (kV)	flame length (cm)	Temperature (^{O}C)
8	6	26
9	5.8	27
10	5.5	27.5
11	5.2	27.8
12	5	28
13	4.8	28.5
14	4.5	29

Table (4-6): Length plume and temperature of the plasma for applied voltage

(8-14) kV and flow rate 5 l/min

Volt (kV)	flame length (cm)	Temperature (^{O}C)
8	2.3	26
9	2.5	26.5
10	2.8	27
11	3	27.5
12	3.2	28
13	3.4	28.5
14	3.6	29

Table (4-7): Length plume and temperature of the plasma for applied voltage

(8-14) kV and flow rate 6 l/min

Volt (kV)	flame length (cm)	Temperature (^{O}C)
8	2	26
9	2.3	26.5
10	2.4	27
11	2.5	27.5
12	2.7	28
13	2.8	28.5
14	3	29

Figure (4.6) illustrates the effect of gas flow rate on plasma temperature at range (8-14) kV of applied voltage, When the electrical voltage applied in the discharge Pyrex tube is high, the kinetic energy of electrons increases and the plasma temperature increases at a low gas flow rate (1L/min). But at high concentrations of helium plasma, the electrons have little time to exchange energy with their surroundings and the plasma temperature becomes low at a gas flow rate (3-6) L/min [103].
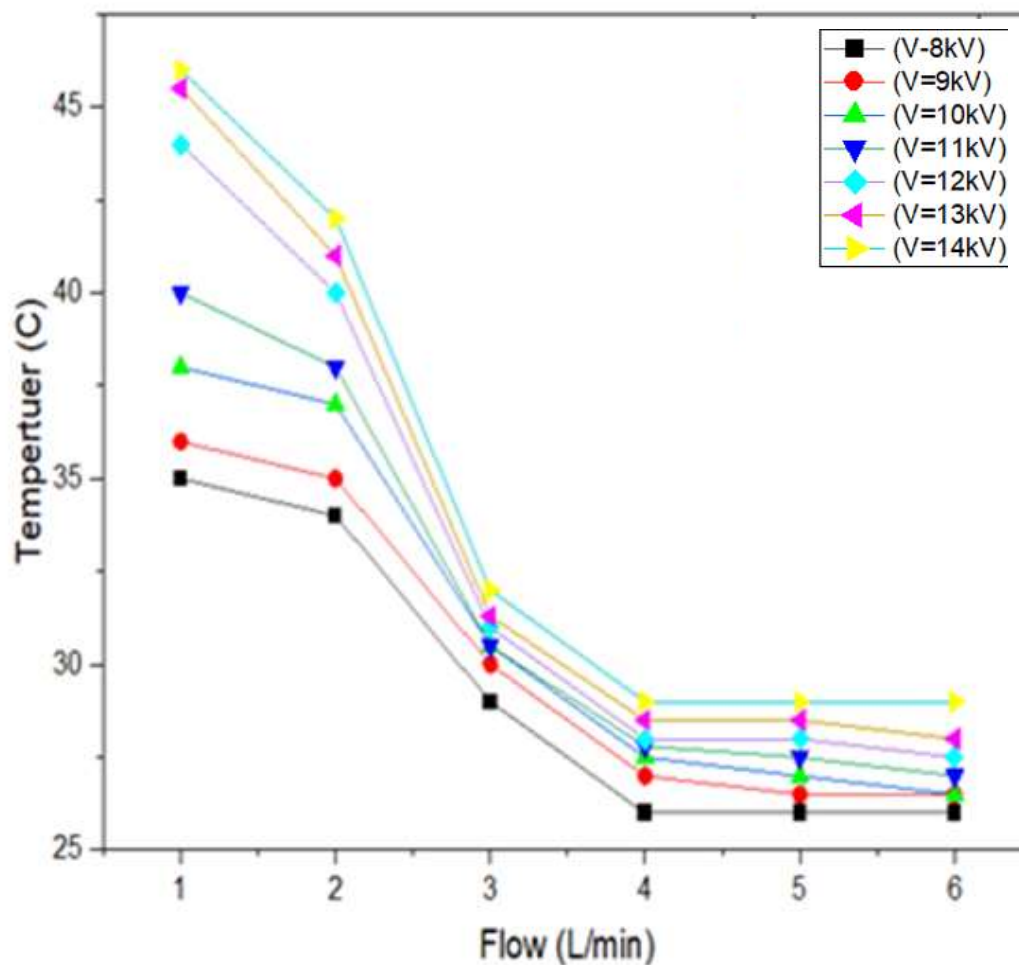

Figure (4-6): Effect of gas flow rate on plasma temperature.

The influence of the helium flow rate on the plasma plume length is illustrated in figure (4.7) at range (8-14)kV applied voltage on the electrodes, the plume length increased at (2-3) L/min, gas flow rate but at (4-6) L/min, gas flow rate,

the behaviors of plume length like randomly because of the electric discharge non-uniform which affects negatively on plume length [103].
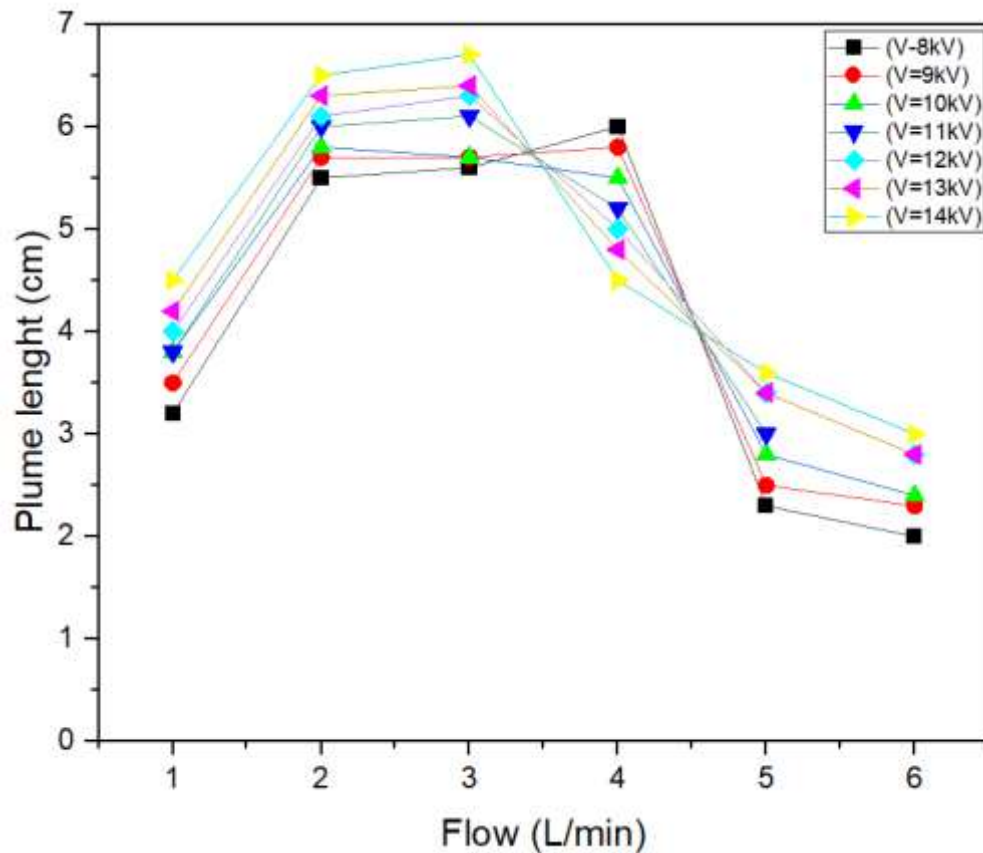

Figure (4-7): Effect of gas flow rate on plasma plume length.

In figure (4.8) the plasma temperatures become higher. When the discharge voltage is increased when the voltage reaches 14 kV, the plasma temperature is up to 45°C, and the electric discharge may be unstable and cause sparking, A higher voltage also damages the glass capillary tube and causes the discharge to. In figure (4.9) the length of the plasma flame becomes higher. When the discharge voltage is increased when the voltage reaches 14 kV, the length of the plasma flame reaches 6.7 cm, and at 4 l/min the flame length begins to decrease to 4.5 cm. This is due to the increase in gas jet flow and the electrical discharge may be unstable. Practically, the best length of the helium plasma jet is (6 cm) at (26 ^{0}C) at an applied voltage of (8 kV) and a frequency of (60 kHz) and 4 L/min as seen in figure (4.10).
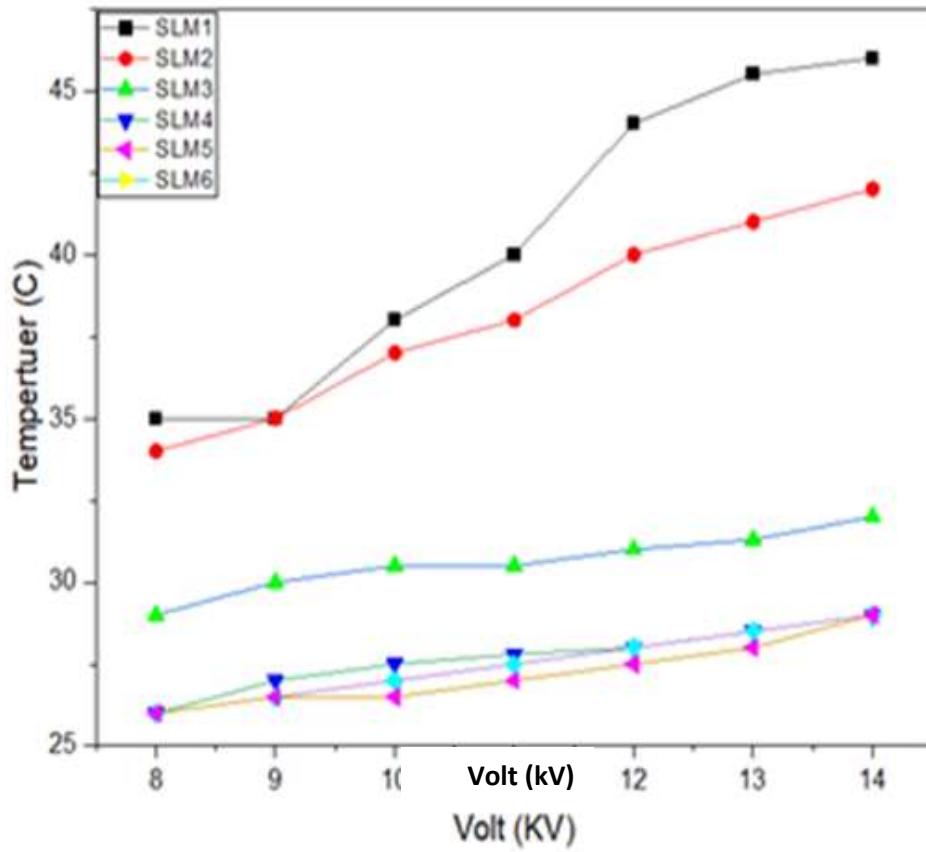
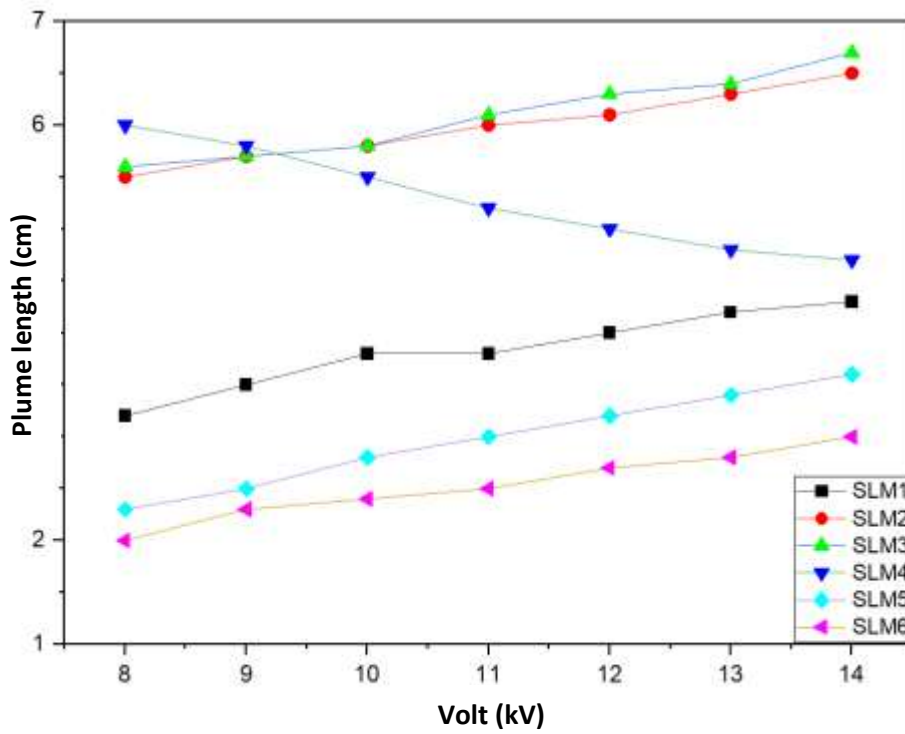Figure (4-8): Influence of applied voltage on plasma temperature.

Figure (4-9): Influence of applied voltage on plasma plume.

54
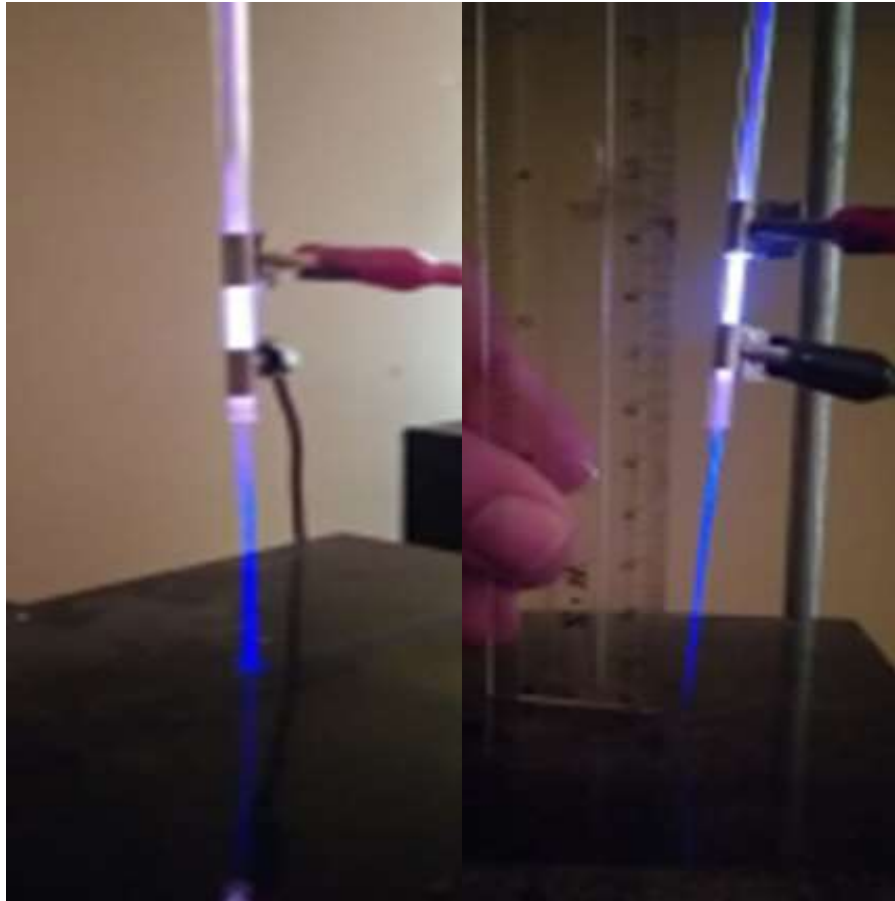
Figure (4.10): Plasma jet length.

Use a mercury thermometer as well as an electronic sensor (UTS) to measure the temperature of the helium jet of plasma, being one of the primary plasma factors and a significant property, temperature is crucial in choosing the right application. The thermometer shows the end of the plasma flow for a while until the system is calibrated thermally at a temperature of 22°C, as shown in figure (4.11) []104].
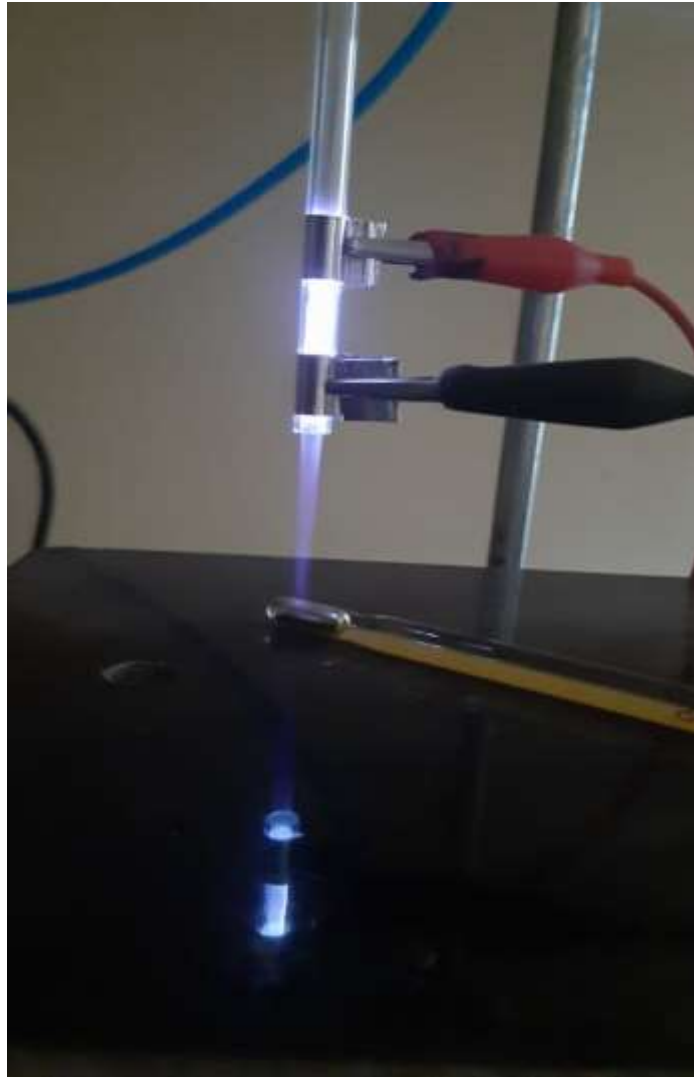
Figure (4.11): Plasma jet temperature measurement using a mercury thermometer.

4.4 Optical Emission Spectroscopy Diagnostics

Analyzing the spectral emission of the helium plasma jet by using the OES device is investigated, (OES) is a suitable method to optimize the reactive species that are employed in different applications such as medical, biomedical, agriculture, and industry by cold plasma. Frequency, jetting length, and the helium flow rate are the pest parameters that must be discussed to know its effects before use.

4.5 Optical Properties

To determine the plasma diagnostics, the optical emission spectroscopy method was suitable to achieve this function. The spectrometer is used to record the spectrum of the helium plasma jet, and the emitted wavelengths have been determined in the range of 200 to 1000 nm when a voltage (1-14) kV is applied for several gas flows (1-6) L/min. The peak intensity of reactive species is adjusted by the inlet aperture of the spectrometer via the optical fiber for the end of the flame. The intensity of reactive species is estimated by analysis of the intensities of the atomic and molecular emission lines obtained from a spectrometer. The Boltzmann scheme method is employed to determine electron temperature and electron density from the spectral data. In the spectra, ionized states of (NO) and hydroxyl radicals (OH) are observed along with the He lines, the spectrum with the highlighted lines (reactive species that are active for many applications) is shown in figure (4.12- 4.17) The presence of (OH, NO, He I, He II, N_2^+, O_2^+, etc.) is determined by the database of NIST, which confirms the suitability of our plasma column for many applications such as industrial and biological [105].
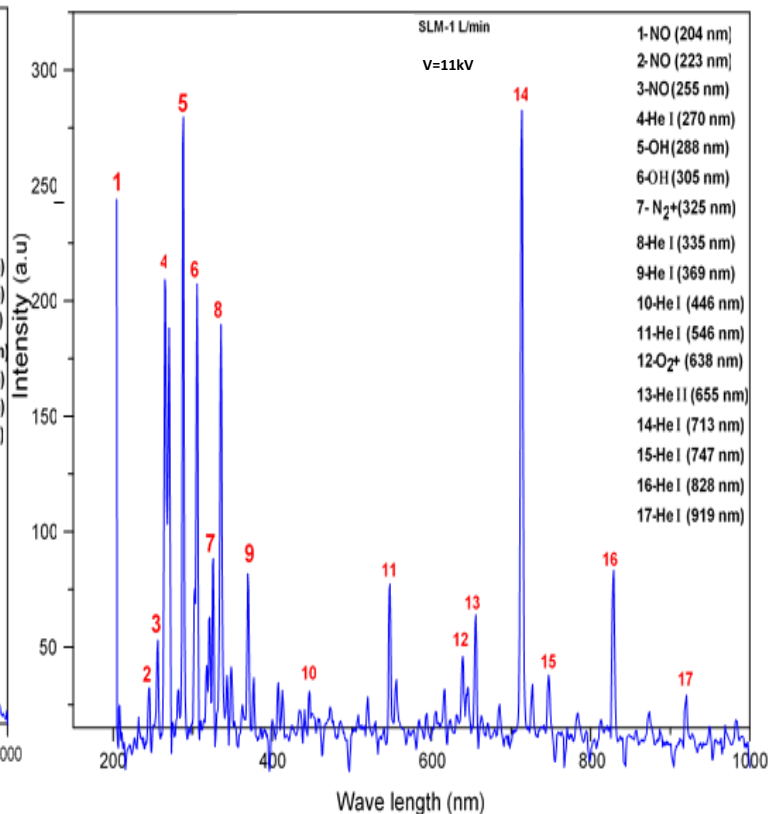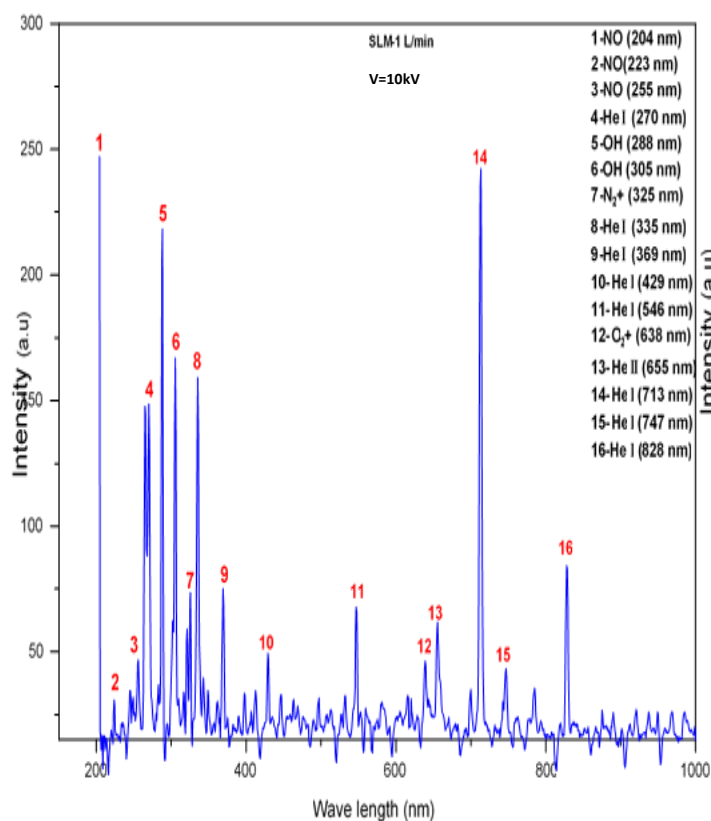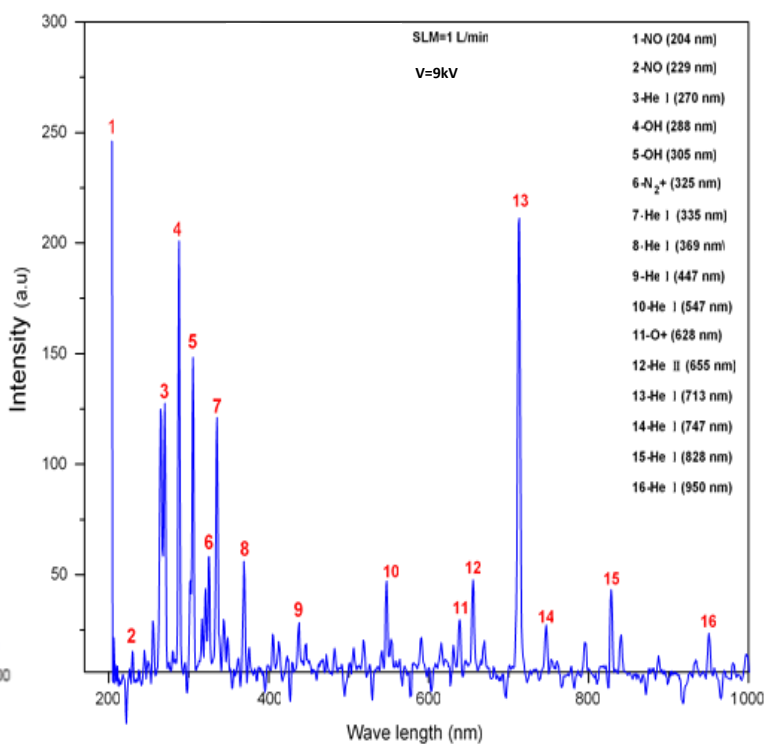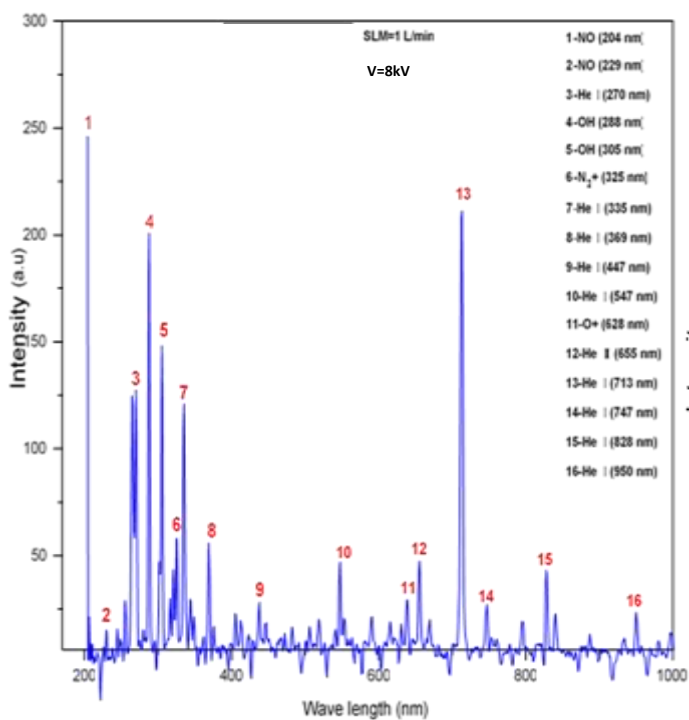
Figure (4-12): The spectrum of Helium plasma jets at atmospheric pressure for voltage (1-14) kV and a rate of flow 1L/min.
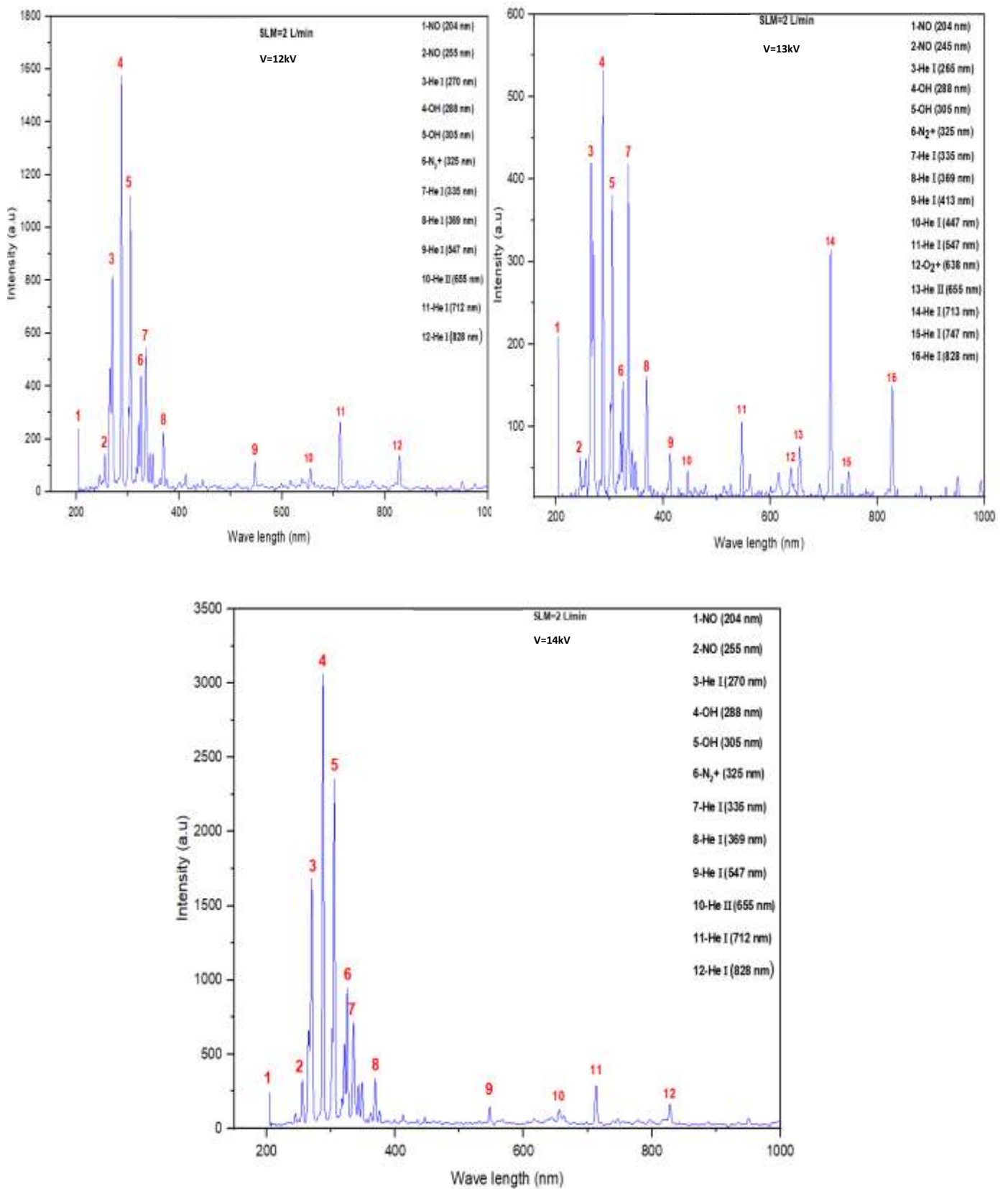
Figure (4-13): The spectrum of Helium plasma jets at atmospheric pressure for voltage

(1-14) kV and a rate of flow of 2L/min.
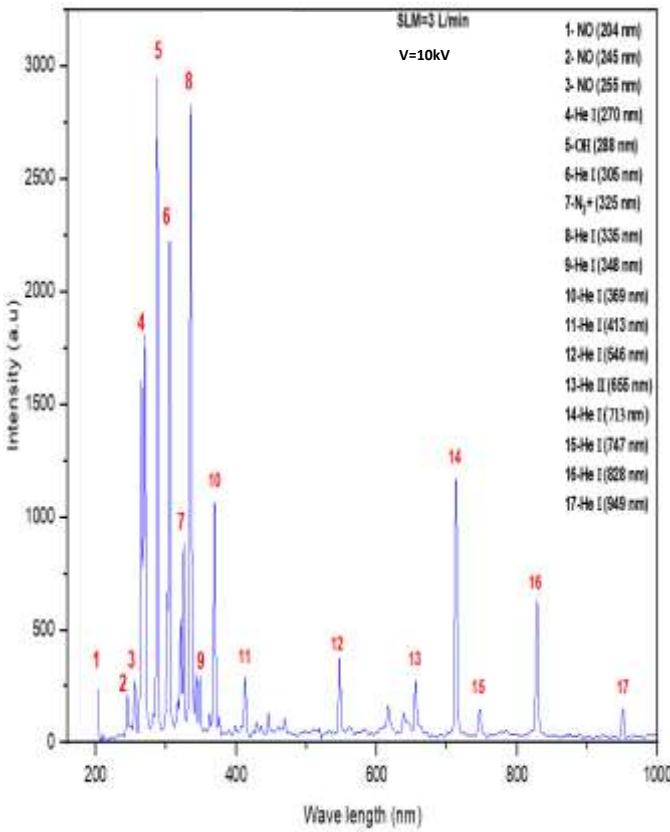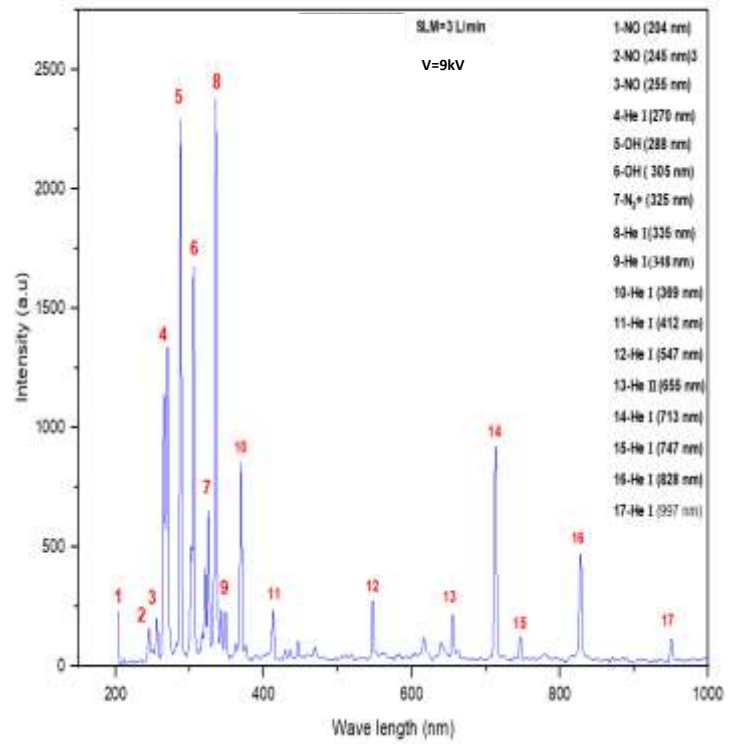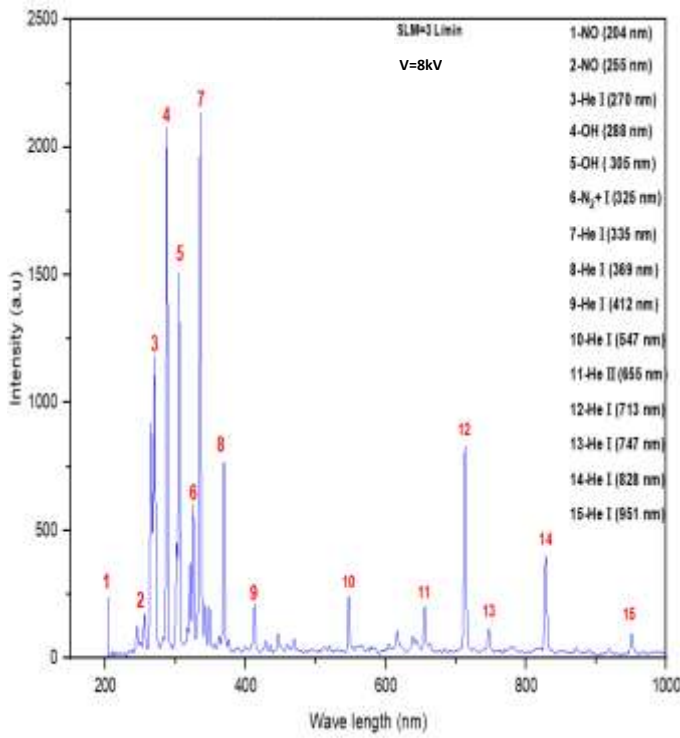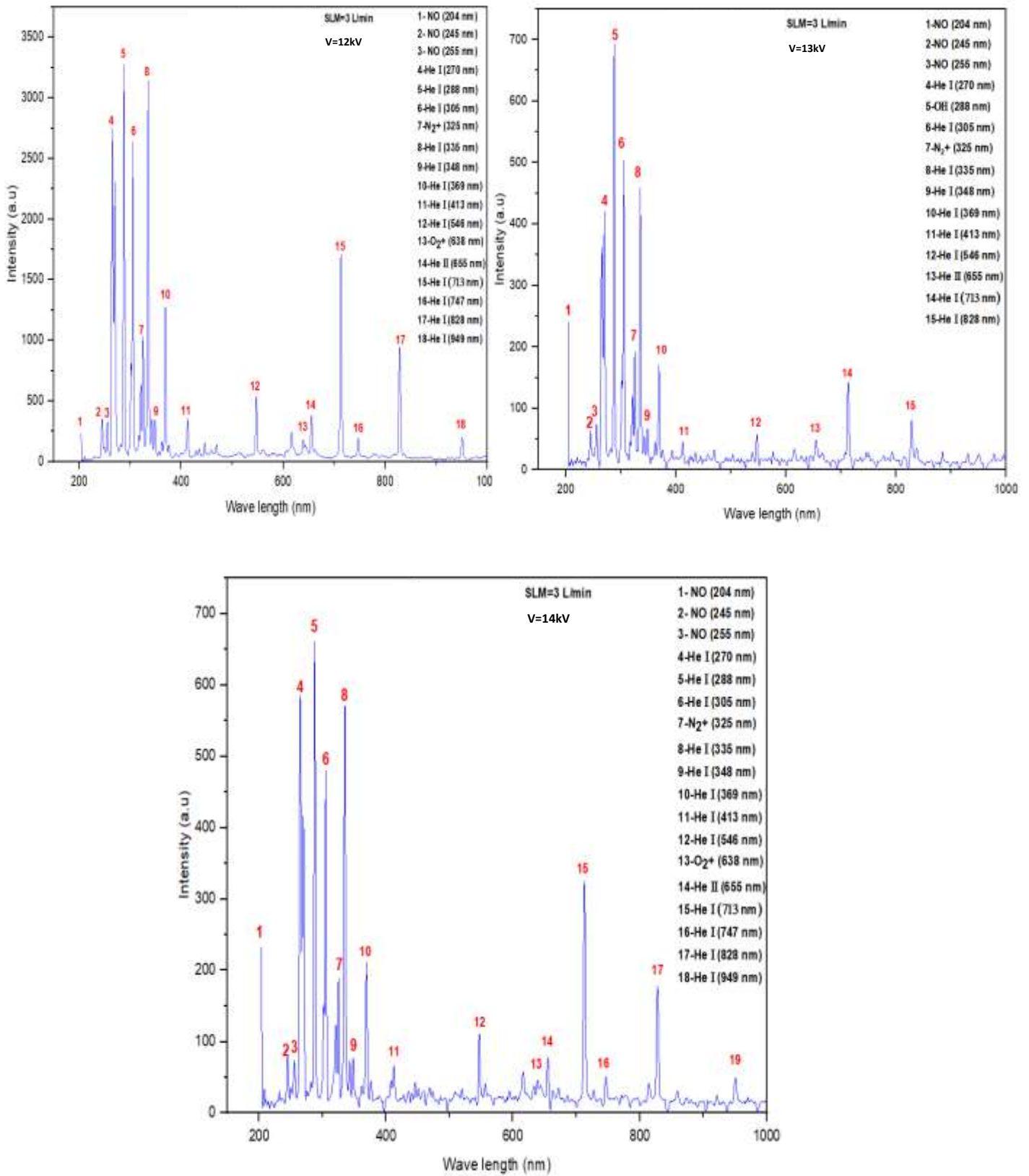
Figure (4-14): The spectrum of Helium plasma jets at atmospheric pressure for voltage (1-14) kV and a rate of flow of 3L/min.
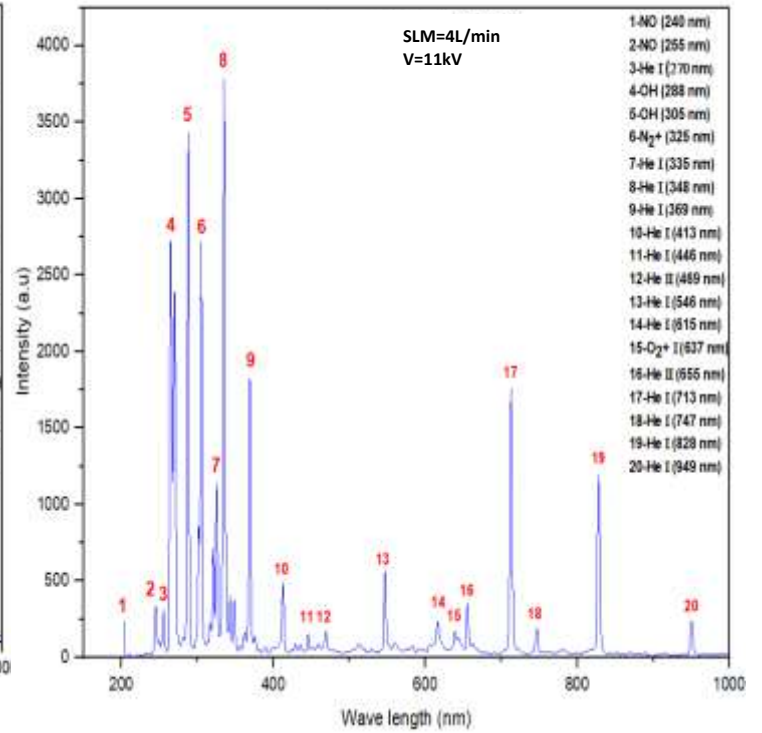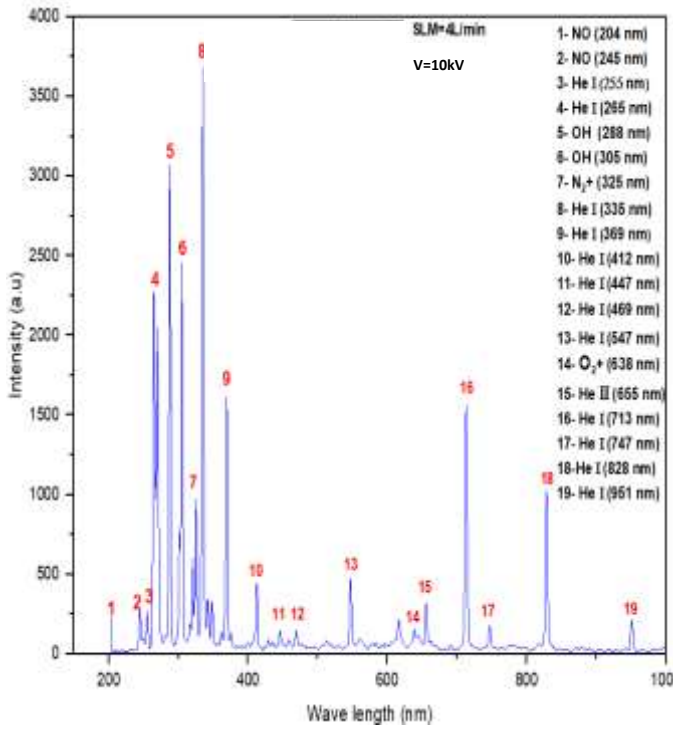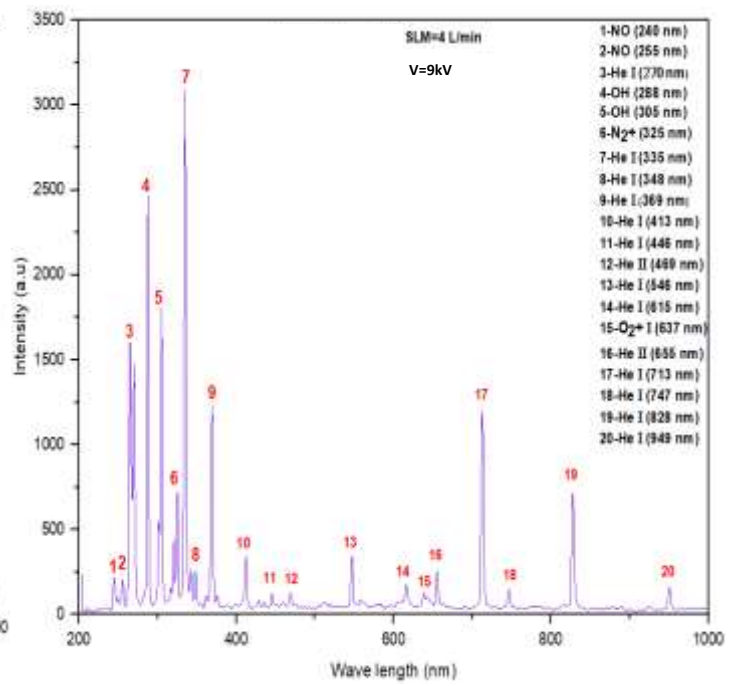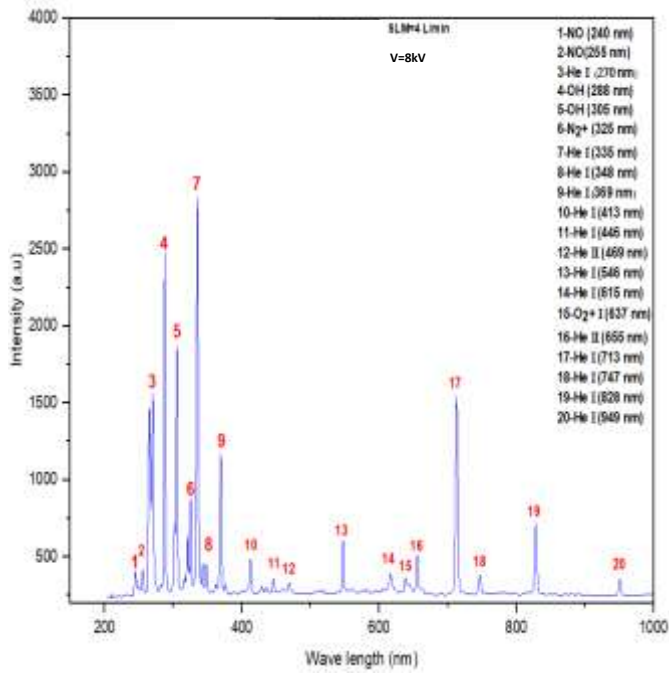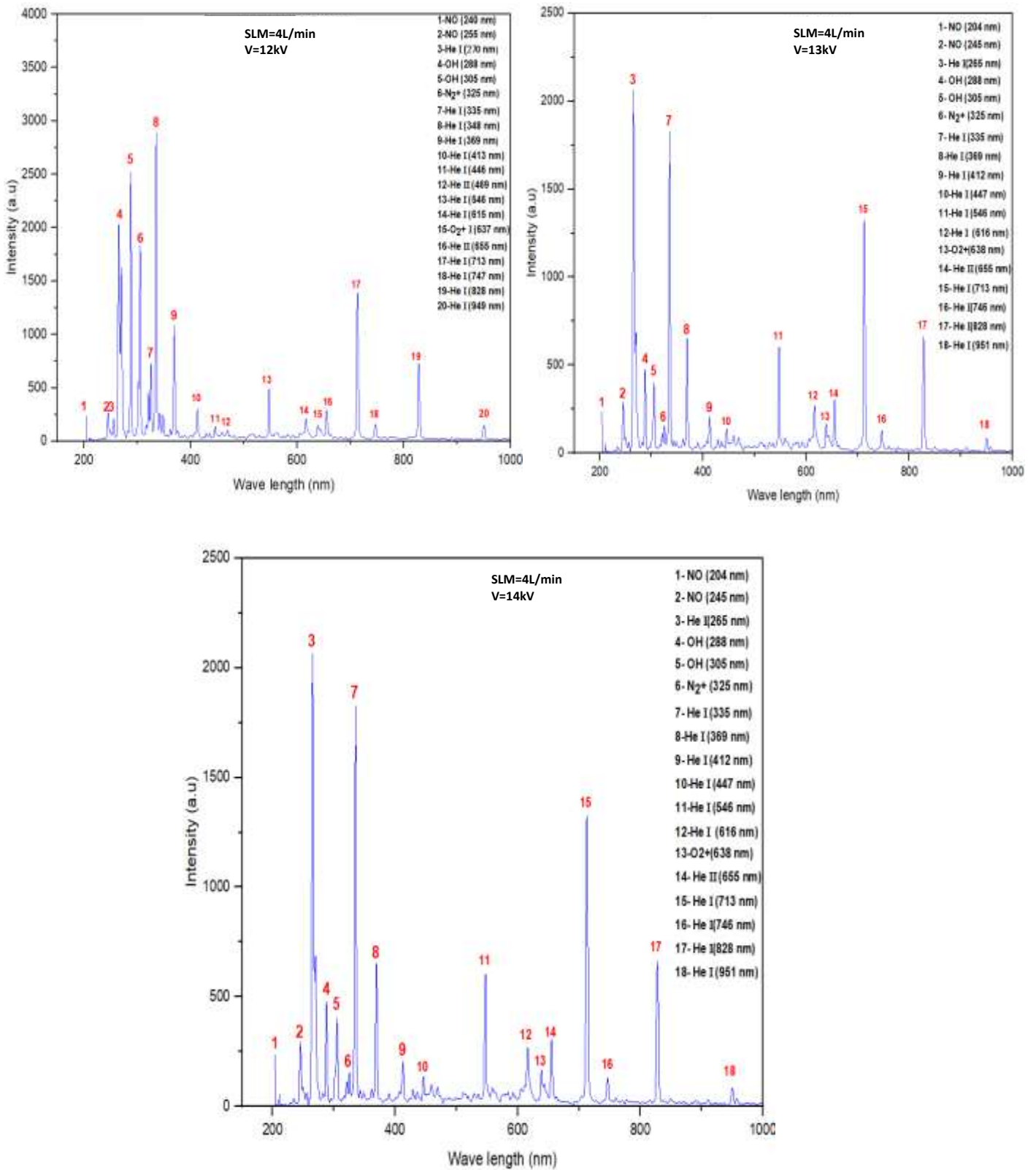
Figure (4-15): The spectrum of Helium plasma jets at atmospheric pressure for voltage

(1-14) kV and a rate of flow of 4L/min.
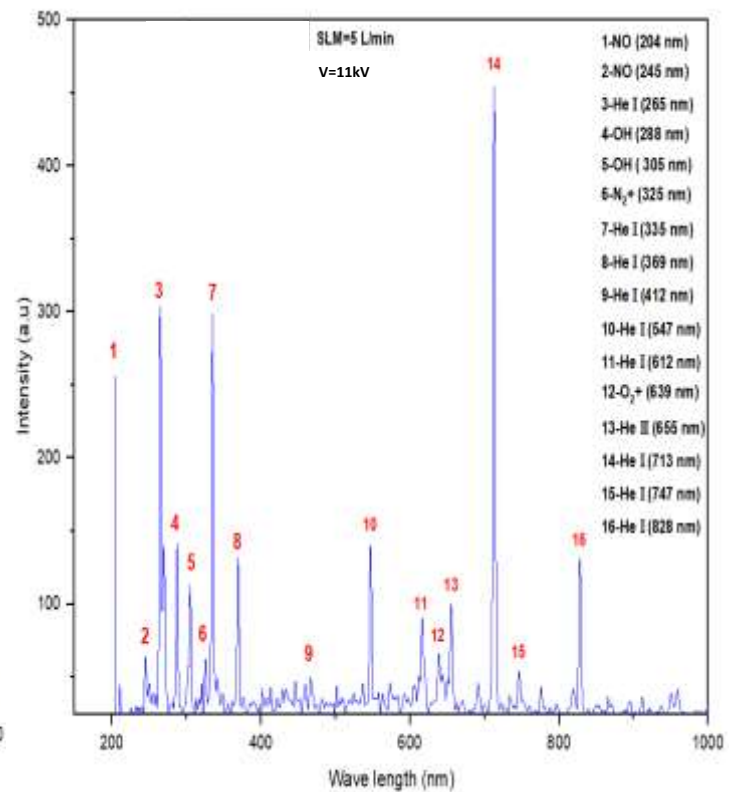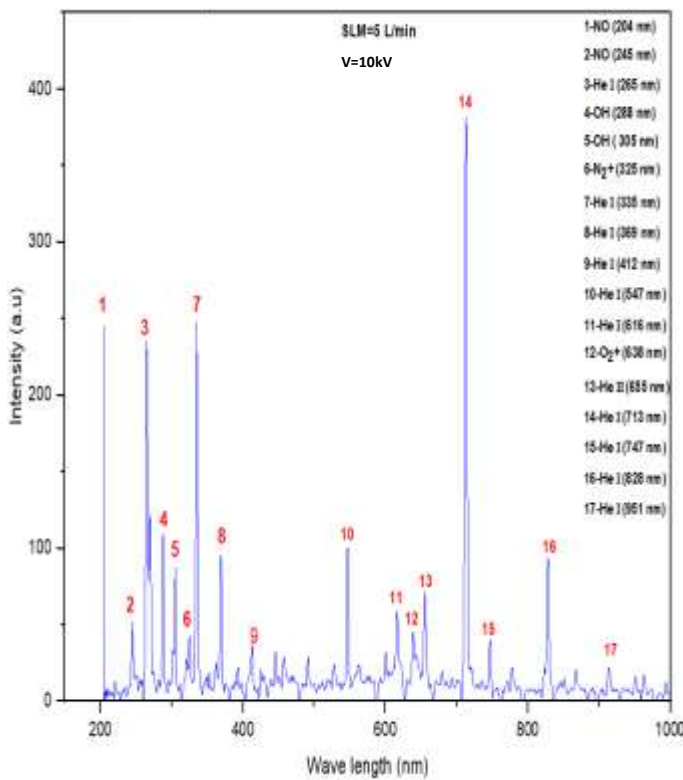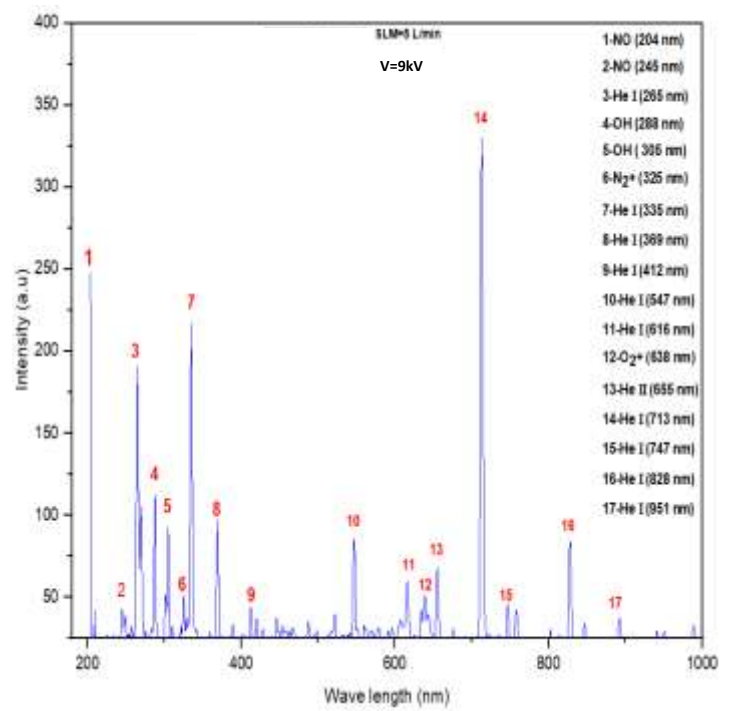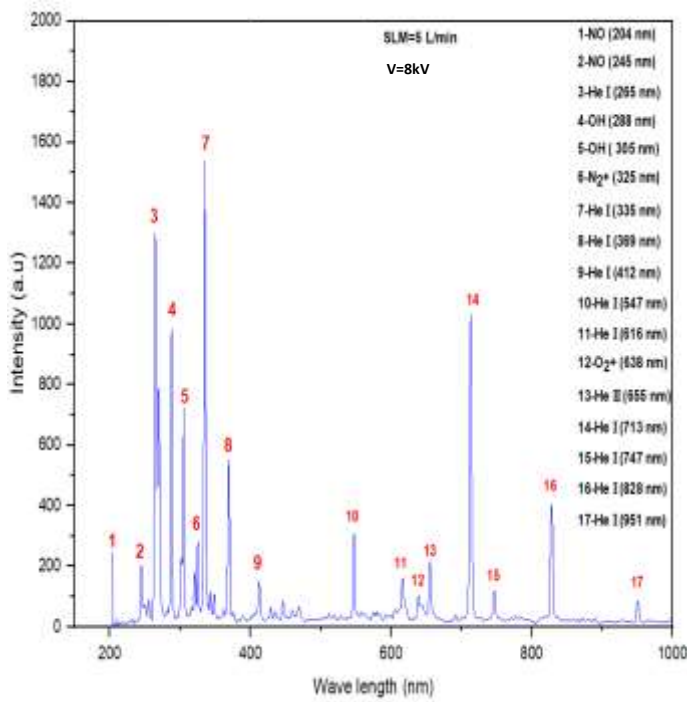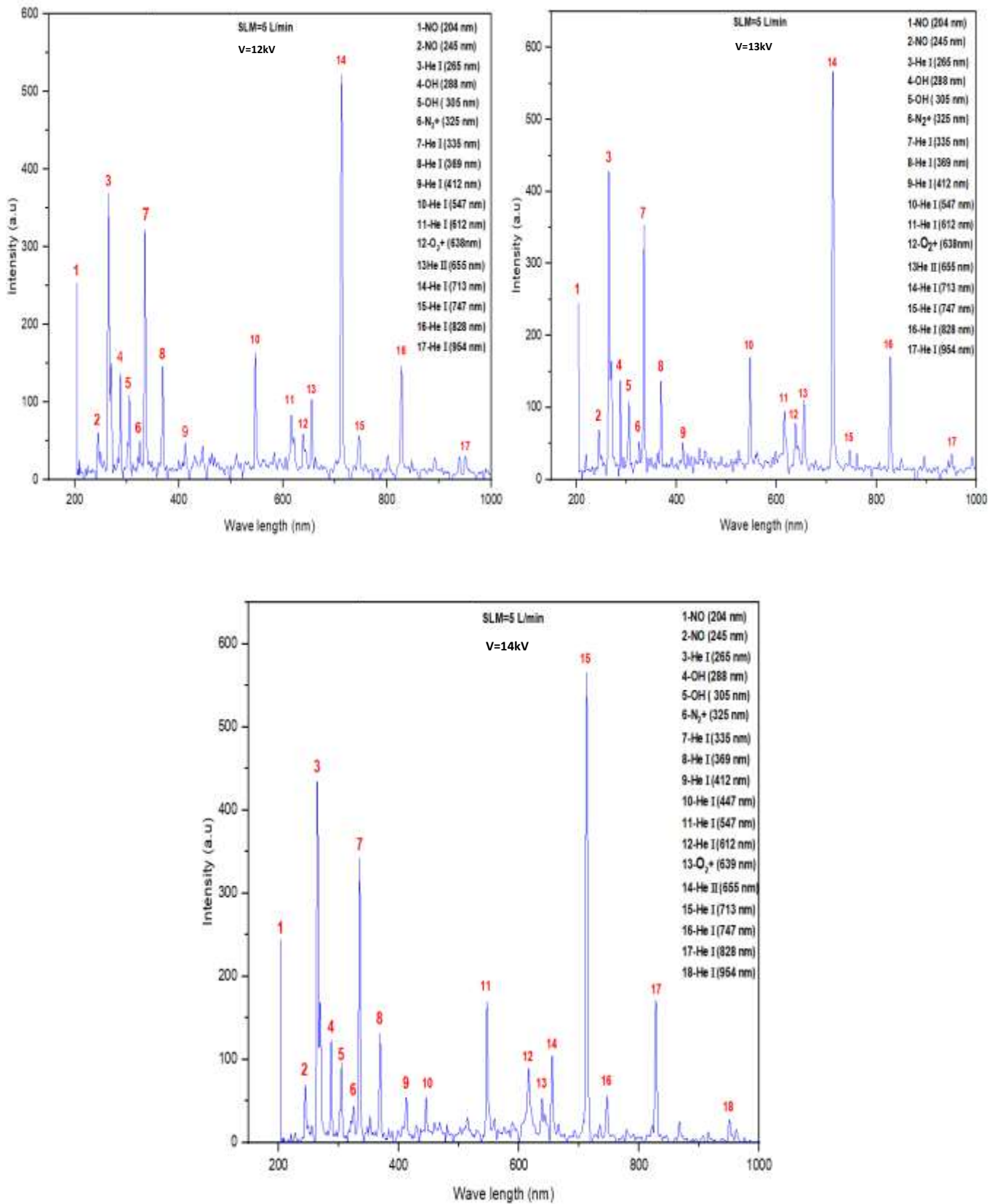
Figure (4-16): The spectrum of Helium plasma jets at atmospheric pressure for voltage (1-14) kV and a rate of flow of 5L/min.
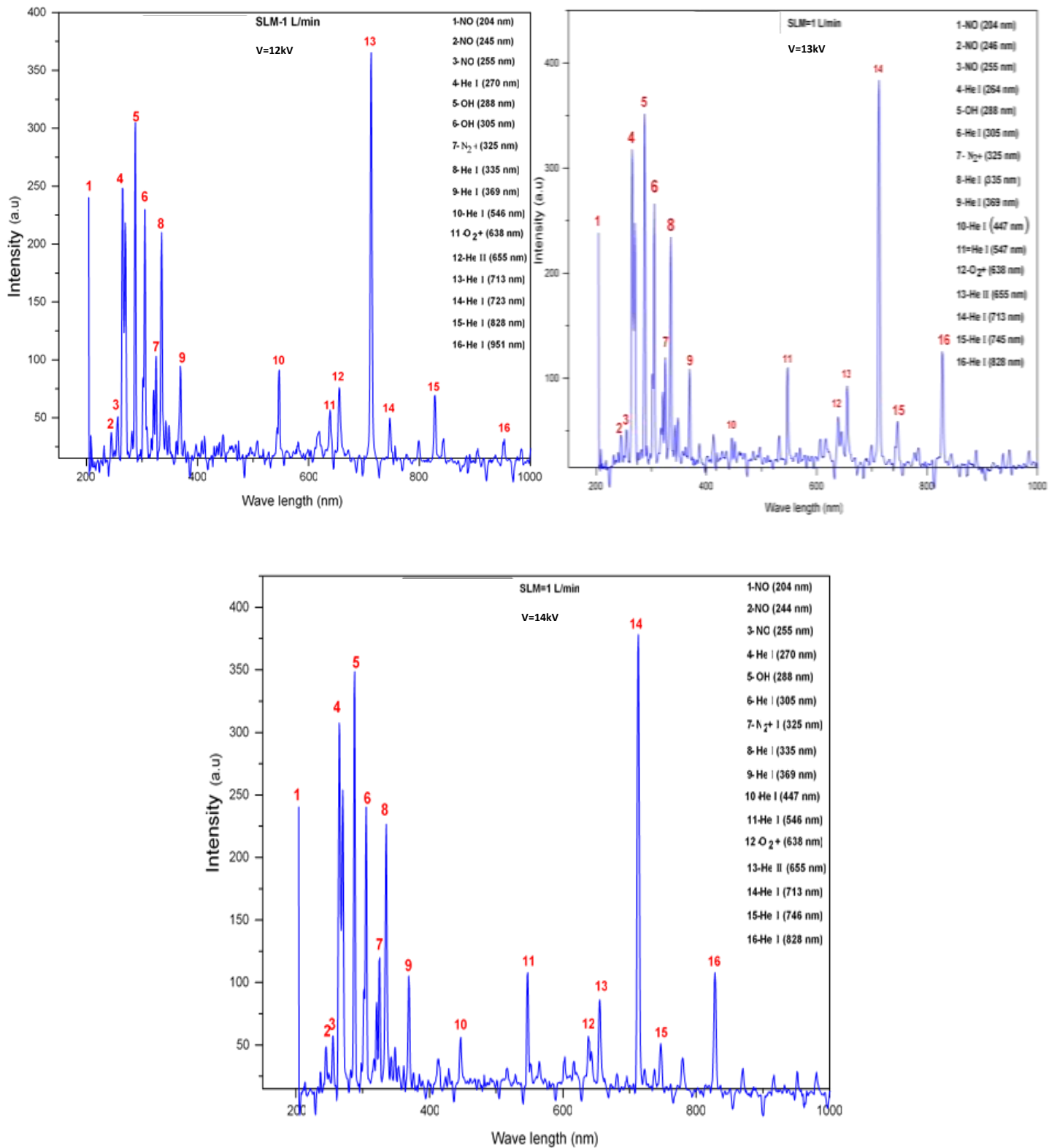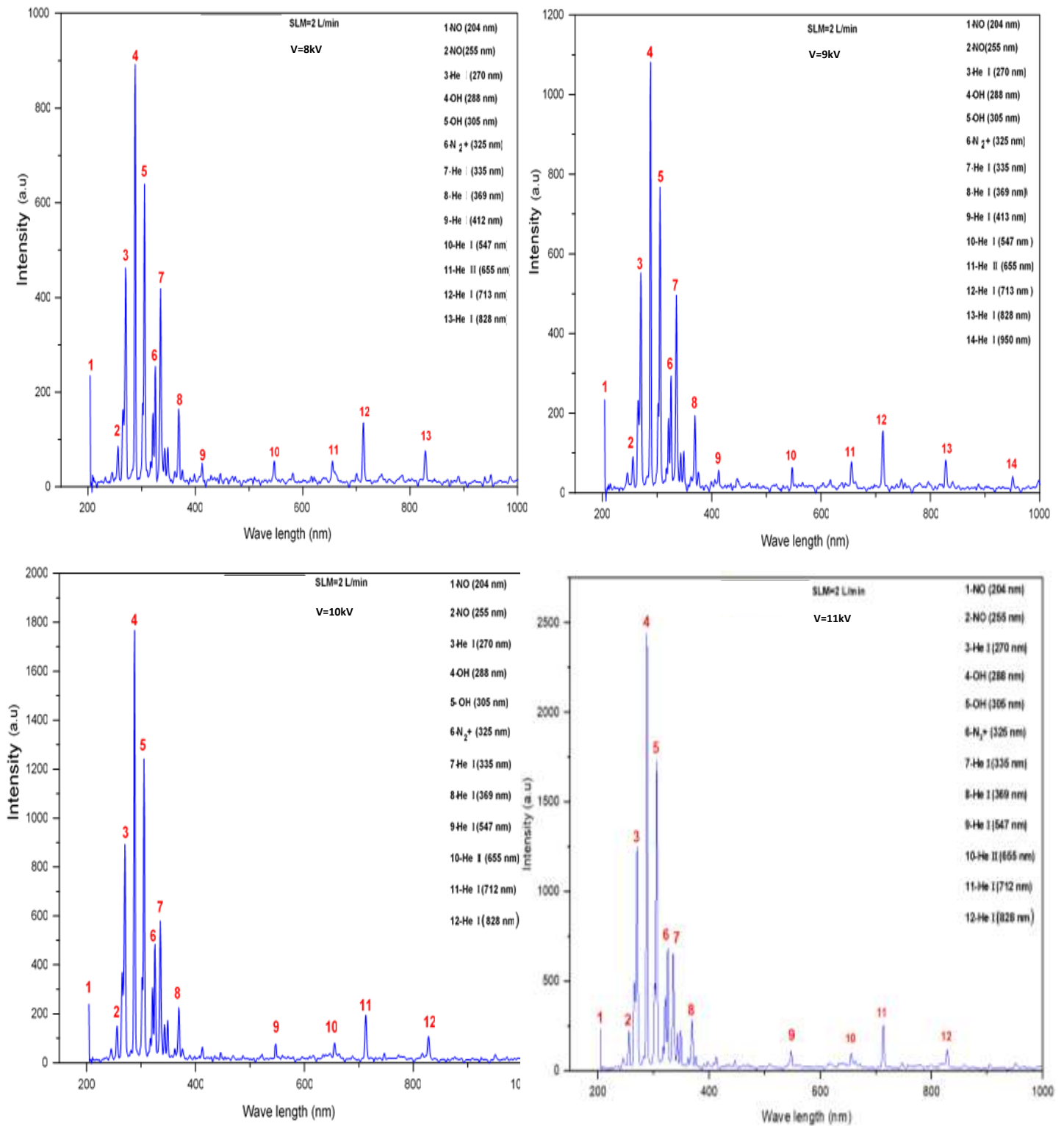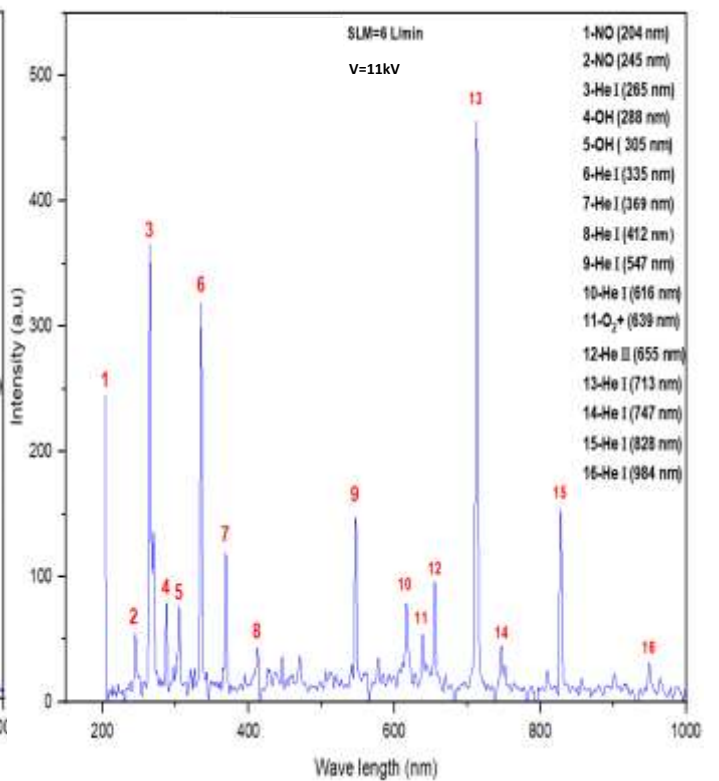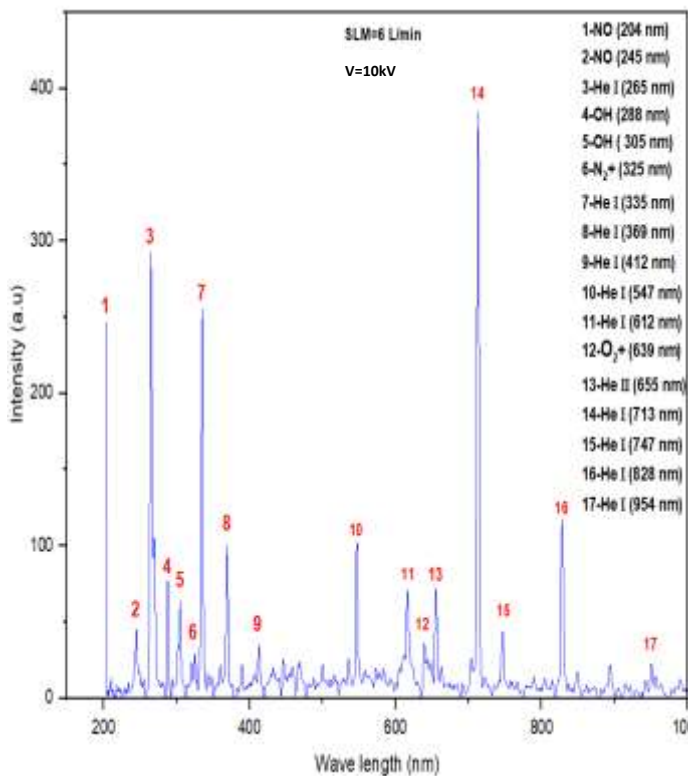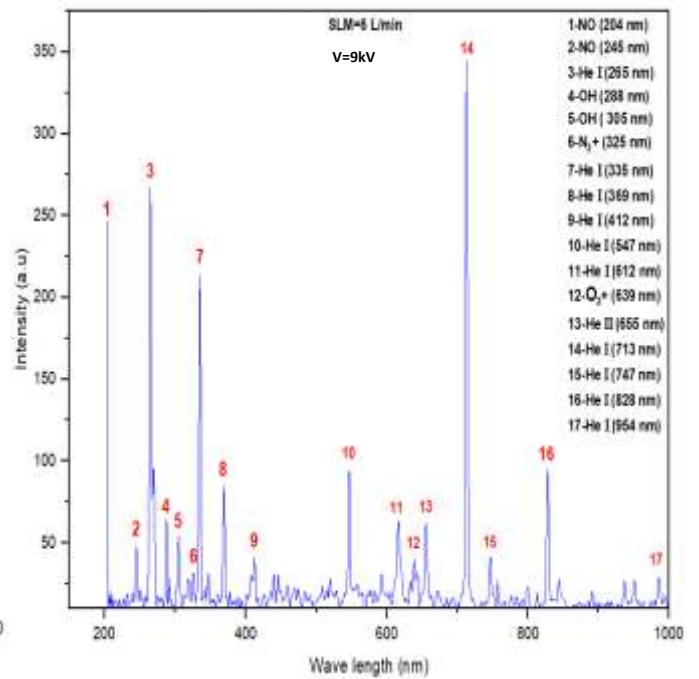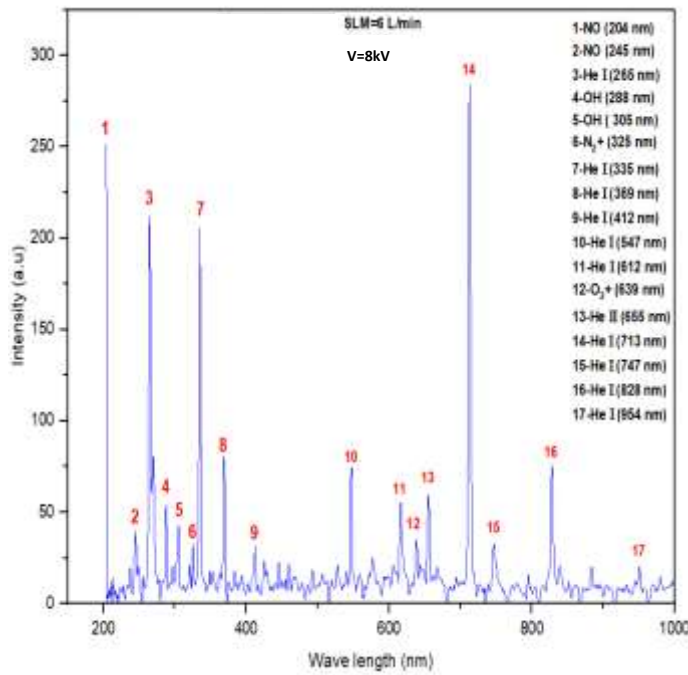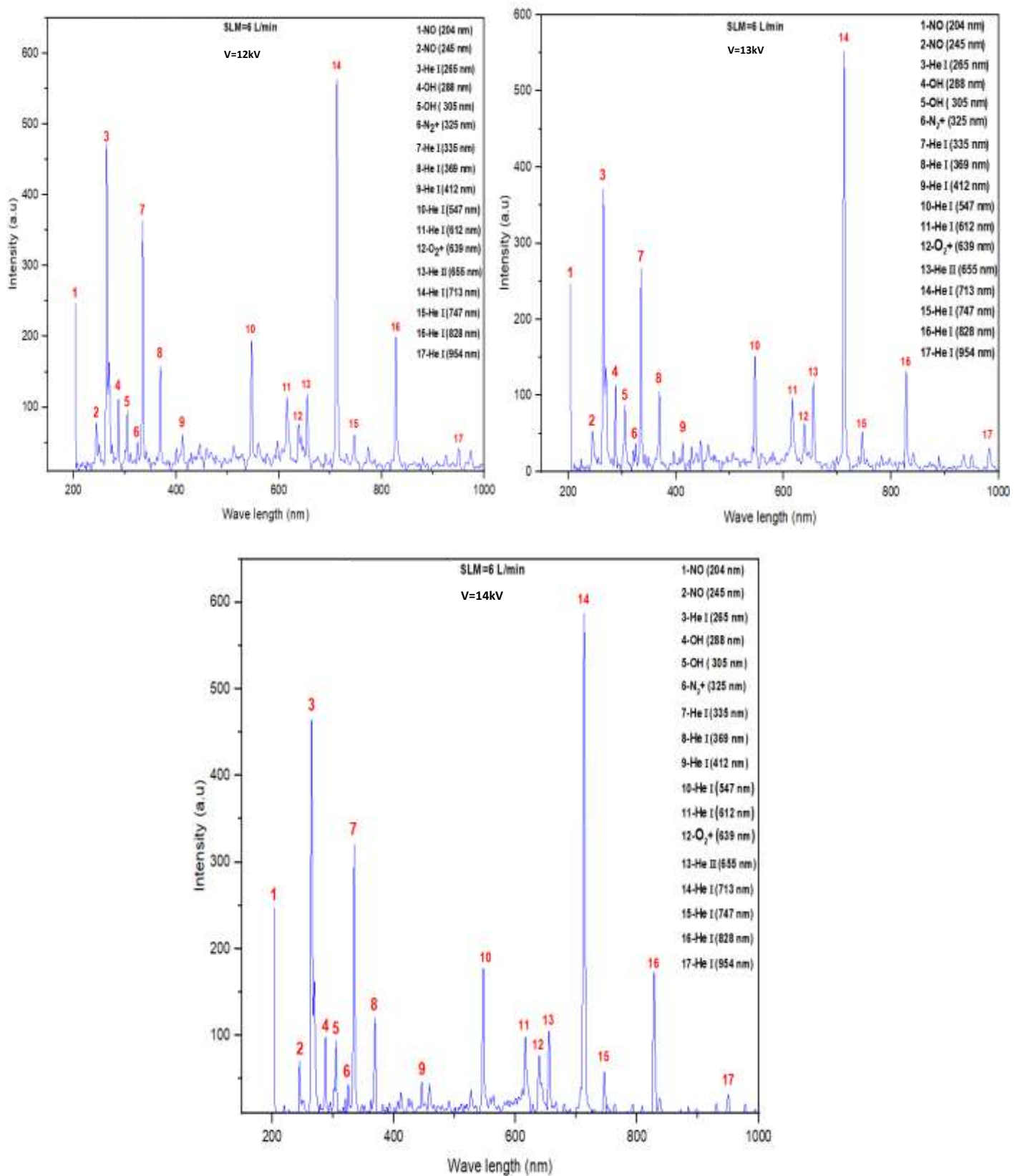
Figure (4-17): The spectrum of Helium plasma jets at atmospheric pressure for voltage (1-14) kV and a rate of flow 6L/min.

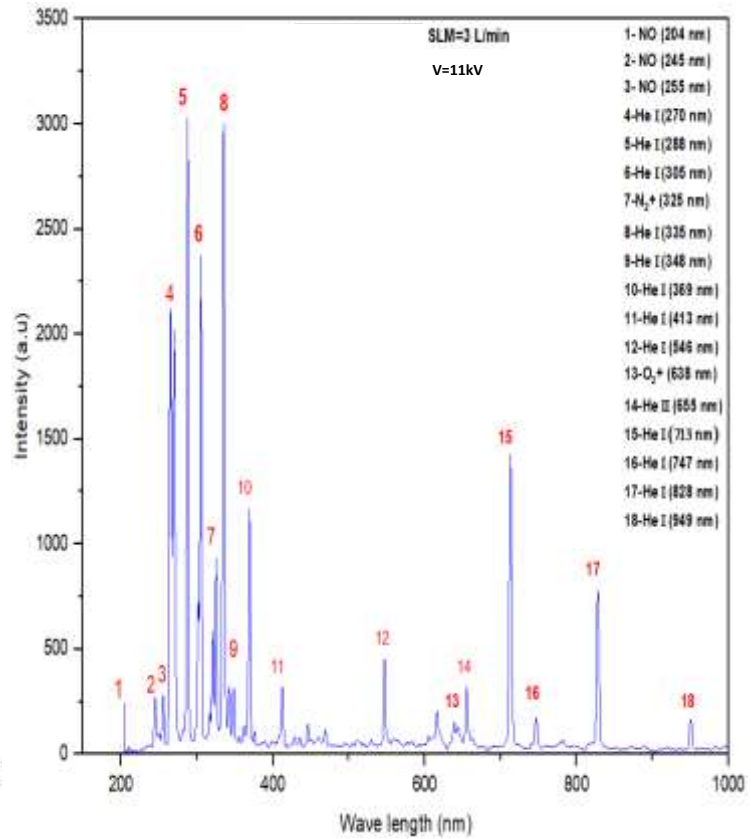Table (4-8): The intensity of reactive species for applied voltage (8-14) kV and
flow rate is 1L/min.

Ion Intensity (a.u)

Volt(kV)	HeI	HeII	NO	OH	N_2	O_2
8	204	46	245	204	54	23
9	208	47	246	201	56	25
10	242	81	247	218	70	61
11	282	64	244	279	88	46
12	356	76	240	304	102	56
13	382	92	238	351	119	60
14	378	84	240	348	119	57

Table (4-9): The intensity of reactive species for applied voltage (8-14) kV and
flow rate is 2L/min.

Ion Intensity (a.u)

Volt(kV)	HeI	HeII	NO	OH	N_2	O_2
8	462	54	235	892	254	62
9	552	71	233	1080	293	54
10	892	81	238	1766	484	51
11	1251	91	231	2442	685	47
12	820	79	237	1575	438	44
13	417	67	208	532	155	46
14	1686	108	242	3061	945	48

Table (4-10): The intensity of reactive species for applied voltage (8-14) kV and flow rate is 3L/min.

Ion Intensity (a.u)

Volt(kV)	HeI	HeII	NO	OH	N_2	O_2
8	2135	176	238	2076	602	126
9	1338	203	229	2293	651	131
10	2833	258	278	2945	883	137
11	2081	323	280	3029	933	143
12	3143	378	336	3272	1035	165
13	459	46	240	693	191	67
14	585	74	253	661	177	46

Table (4-11): The intensity of reactive species for applied voltage (8-14) kV and flow rate is 4L/min.

Ion Intensity (a.u)

Volt(kV)	HeI	HeII	NO	OH	N_2	O_2
8	2834	506	403	2476	875	357
9	3087	240	215	2464	720	126
10	3685	318	272	3070	975	151
11	3781	354	334	3435	1133	159
12	2890	299	267	2527	731	138
13	2585	372	397	938	281	173
14	2065	290	295	479	157	154

Table (4-12): The intensity of reactive species for applied voltage (8-14) kV and flow rate is 5L/min.

Ion Intensity (a.u)

Volt(kV)	HeI	HeII	NO	OH	N_2	O_2
8	1538	217	245	983	285	98
9	330	68	247	112	49	50
10	381	65	245	109	42	45
11	454	101	256	142	62	66
12	521	104	253	136	498	54
13	567	110	246	138	52	78
14	565	104	244	123	43	51

Table (4-13): The intensity of reactive species for applied voltage (8-14) kV and flow rate is 6L/min.

Ion Intensity (a.u)

Volt(kV)	HeI	HeII	NO	OH	N_2	O_2
8	283	59	251	54	32	33
9	344	62	246	64	32	40
10	384	67	246	72	28	35
11	464	96	244	77	26	53
12	503	118	246	112	50	75
13	552	117	246	107	35	63
14	586	105	246	98	43	77

The comparison between the intensity of reactive species (NO and OH) in different conditions for applied voltage range (8-14) kV and gas flow (1-6) L/min, as shown in figures (4.12-4.17) and tables (4.2-4.7). The results show that the intensity of (NO and OH) are (403 and 2476) which is the highest intensity value of the same reactive species but at other conditions, for the

working parameters (8kV) and (SLM 4L/min) gas flow rate given the high intensity of reactive species as illustrated in table (4.5). It is possible to adopt that this condition is optimized for the generation of atmospheric pressure plasm jet. The flame (6 cm) from the end of the Pyrex tube is also obtained at these working parameters in addition, it will keep us safe from spark problems if we get close. Because the plasma contains excited atoms, reactive species (e.g. O_2^+, N_2^+, OH, NO, etc.) are at an appropriate density [106].

4.6 Electron Temperature and Electron Density

Reactive species can be obtained in atmospheric pressure plasma jets by analyzing their OES, for different working parameters such as employed voltage and rate of gas flow. The diagnostic plasma depends on electron temperature Te and electron density ne parameters, which are evaluated by the equations (2.1 and 2.2) respectively.

The values of A_u g_u, E_u are considered from the database saved in the National Institute of Standards and Technology NIST for Helium gas [26]. The spectrum lines appear in the UV-Vis-NIR regions. The spectrum contains hydrogen oxide (OH) and (NO) which are recorded in the helium plasma spectrum. The Boltzmann plot is suitable for calculating T_e for helium plasma jets. Six spectral lines of wavelength (412.25, 447.75, 655.543, 716.704, 826.89, 951.33) nm were dependent to estimate T_e. and the relative intensities were considered from the OES. The electron excitation temperature [107].

The graph for different values of $ln(\lambda I)/(A_u g_{u)}$ is plotted against the upper-level energies E_u giving a straight line with slope (-1.97853) which corresponds to T_e of 6102.21 K (see figure (4-18)).

Table (4-14): The values of parameters opener's (A_u , g_u , E_u)of the helium spectrum lines depend on NIST.

Species	Wavelength λ (nm)	Intensity (a.u)	A_u (S^{-1})	g_u	E_u (eV)	$\ln\left(\frac{\lambda I}{A_u g_u}\right)$
He I	412.25	462.22	1.48E+06	1	25.8761	-4.90131
He I	447.75	346.71	1.84E+07	2	25.3062	-3.32743
He II	655.543	506.86	1.15E+07	3/2	24.4561	-2.12132
He I	716.704	1541.7	9.56E+04	0	24.3432	-1.42106
He I	826.89	717.16	1.87E+05	1	23.8486	-1.90612
He I	951.33	316.72	3.45E+04	1	23.7182	-0.42014
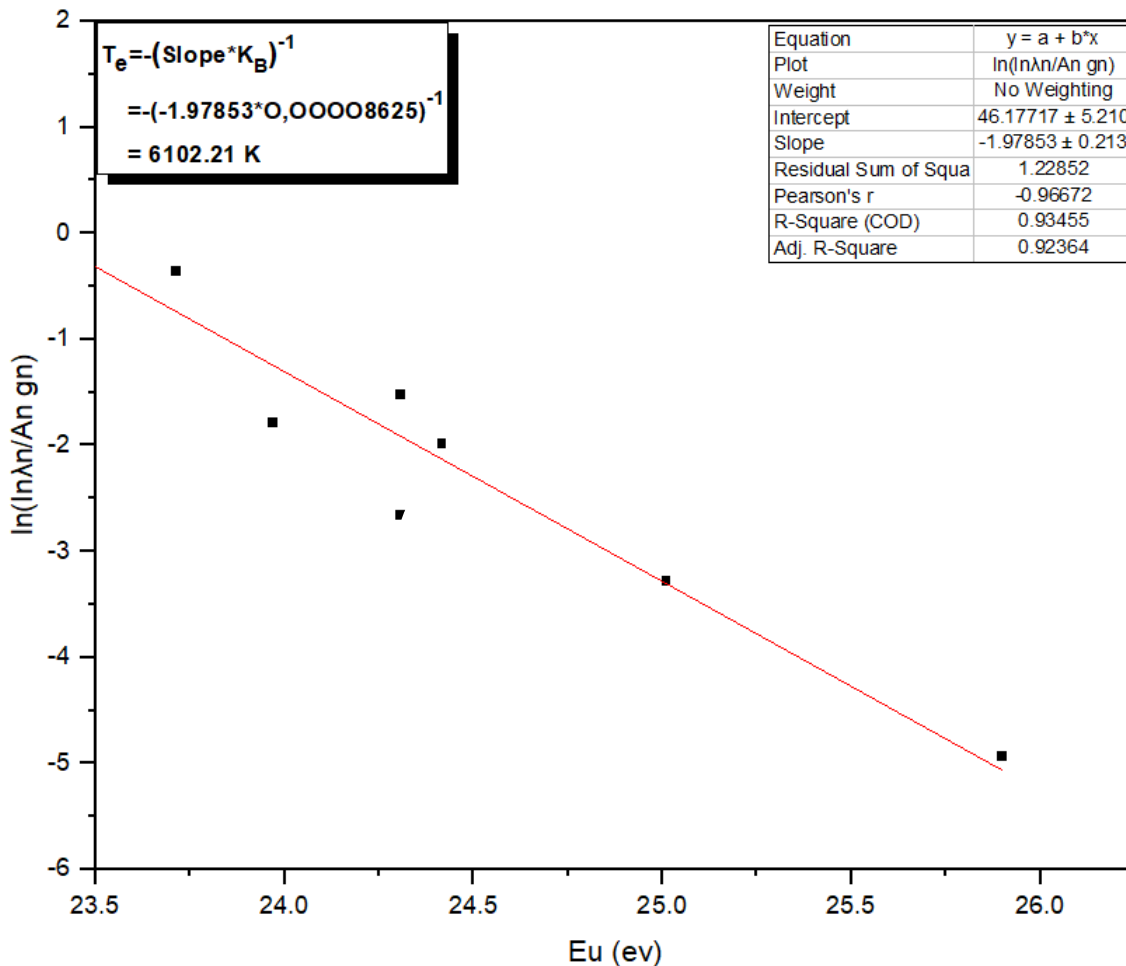
Figure (4-18): Boltzmann plot for atomic Helium spectral lines.

Electron density n_e can be estimated from the singly charged ion (ionic) and the neutral particle (atomic). The plasma spectrum explained emitted spectral lines by using the Saha-Boltzmann equation as illustrated in equation (2-1) to evaluate electron temperature.

Electron density n_e estimated by using equation (4-2) and by depending on the first wavelength of spectral lines is 696.54 nm and the last wavelength is 860.57 nm, the intensities of spectral lines for each wavelength, the produced electron density is equal to 1.57×10^{13} cm^{-3}.

4.7 Conclusions

1- The Pyrex tube thickness and the distance between the electrodes of the plasma system have a significant effect on the characteristics of atmospheric pressure helium plasma jets.

2- The temperature of the generated plasma jet was close to room temperature and is suitable for biomedical applications. The temperature decreases slightly as the gas flow rate rises, while it increases as the applied voltage increases.

3- The plume length of the generated plasma is (6 cm) which is convenient to keep us safe from electric field problems, and suitable for applications, the length of the plasma plume depends on the applied voltage and gas flow rate.

4- The Boltzmann plot method is a reliable way to determine of electron temperature and electron density of the helium plasma jet which are (6102.22 K) and (1.57×10^{13} cm^{-3}) respectively, with an applied voltage of (8 kV) and an gas flow rate is (4 L/min).

5-Recorded and analysis of helium plasma jet spectrum are suitable methods to determine the formation and intensity of reactive species, where values are 403 and 2476 of NO and OH respectively.

6- The optimal values of working parameters (applied voltage and gas flow rate) used in this plasma system are (8 kV) and (4L/min) respectively, which generated a helium plasma jet with the best characteristics.

4.8 Future work

1-Investigating on characteristics of atmospheric pressure helium plasma jet to use in wound healing.

2-Investigation on characteristics of atmospheric pressure helium plasma jet with an array of Pyrex tubes configuration system.

3- Investigating of characteristics of atmospheric Pressure helium Plasma Jet with pin-electrode configuration system.

4- Developing of atmospheric Pressure helium Plasma Jet system and its application in the de-coloration of organic wastewater.

References

References

[1] D. Frank-Kamenetskiĭ," Plasma: the fourth state of matter", Macmillan International Higher Education, Vol. 278, p. 36,1972.

[2] W. Siemens, "Ueber Die Elektrostatische Induction und Die Verz̈ogerung Des Stroms in Flaschendr̈ ahten," Annalen der Physik, Vol. 178, No. 9, pp. 66–122, 1857.

[3] J. Townsend, "Motion of Electrons in Gases," Journal of the Franklin Institute, Vol. 200, No. 5, pp. 563–590, 1925.

[4] U. Bogenschutz, "Dielectric-Barrier Discharges: Their History, Discharge Physics, and Industrial Applications," Plasma Chemistry and Plasma Processing, Vol. 23, No. 1, pp. 1–46, 2003.

[5] S. S. Block, "Disinfection, Sterilization, and Preservation, 3rd Ed." Lippincott Williams & Wilkins, Vol. 158, pp. 363–380, 2001.

[6] D. M. Manos and D. L. Flamm, "Plasma Etching: An Introduction." Elsevier, Vol. 128, pp. 163–175, 1989.

[7] W. B. Thompson, "An introduction to plasma physics", Elsevier, Vol. 188 p. 3-4,2013.

[8] S. Eliezer, Y. Eliezer, "The fourth state of matter: an introduction to plasma science ",2nd Edition, CRC Press, Vol. 148, p. 26,2001.

[9] N. Misra, O. Schl̈ user, and P. Cullen, "Cold Plasma in Food and Agriculture: Fundamentals and Applications." Academic Press, Vol. 168, p. 36, 2016

[10] H.R. Metelmann, T. V. Woedtke, and K. D. Weltmann. *"Comprehensive Clinical Plasma Medicine: Cold Physical Plasma for Medical Application",* Springer, Vol. 182, p. 44, 2018.

References

[11] I. H. Hutchinson, "Principles of Plasma Diagnostics." Plasma Physics, and Controlled Fusion. 44, no. 12,2603. p. 237,2002.

[12] K. S. Thorne, and R. D. Blandford. *"Modern Classical Physics: Optics, Fluids, Plasmas, Elasticity, Relativity, and Statistical Physics",* Princeton University Press, p. 997,2017.

[13] M. I., P. Fauchais Boulos, and E. Pfender, "Thermal plasma Fundamental and applications", Plenum Press, New York, Vol. 1(1994)

[14] A., Neyts E., Gijbels R., Bogaerts, and Mullen J. V., "Gas discharge plasma and their applications"; Spectrochemical Acta Part B, Vol. 57 (2002) PP 609-658.

[15] J. Heinlin, G. Morfill, M. Landthaler, W. Stolz, G. Isbary, J. L. Zimmermann, T. Shimizu, and S. Karrer, "Plasma Medicine: Possible Applications in Dermatology," JDDG: Journal der Deutschen Dermatologischen Gesellschaft, Vol. 8, No. 12, pp. 968–976, 2010.

[16] H., FL, Plasma Polymerization, Academic Press Inc.: Orlando, Vol. 112, No. 24, pp. 268–276 (1985).

[17] K. Yasuda, "Fundamentals of plasma physics," Choice Rev. Online, vol. 44, no. 04, pp. 44-2166-44–2166, 2006, doi 10.5860/choice.44-2166.

[18] H. A. Hyman, "Degree of ionization of a high-temperature plasma," Appl. Phys. Lett., vol. 25, no. 10, pp. 553–555, 1974, doi:10.1063/1.1655307.

[19] F. Luis and G. Moncayo, Title Low-Temperature Plasma Technology, 1st ed. London New York: 2014 by Taylor & Francis Group, LLC, Vol. 10, No. 16, pp. 768–776 2014.

[20] C. Tendero, C. Tixier, P. Tristant, J. Desmaison, and P. Leprince, "Atmospheric pressure plasmas: A review," Spectrochim. Acta - Part B At. Spectrosc., vol. 61, no. 1, pp. 2–30, 2006, doi: 10.1016/j.sab.2005.10.003.

[21] A. Sakudo, Y. Yagyu, and T. Onodera. "Disinfection and Sterilization Using Plasma Technology: Fundamentals and Future Perspectives for

References

Biological Applications." International Journal of Molecular Sciences, 20, no. 20 (2019): 5216.

[22] S. H Helgadóttir. "Cold Plasma in Medicine Combatting Bacterial Biofilms." 2016.

[23] A. Piel, "Plasma Physics: An Introduction to Laboratory, Space, and Fusion Plasmas." Springer Science & Business Media, 2010

[24] K. Wasa, S. Hayakawa, "*Handbook of Sputter Deposition Technology: Principles, Technology, and Applications*", Materials Science and Process Technology Series, 1992, William Andrew Inc., P:304.

[25] A. Sakudo, Y. Yagyu, and T. Onodera. "Disinfection and Sterilization Using Plasma Technology: Fundamentals and Future Perspectives for Biological Applications." International Journal of Molecular Sciences, 20, no. 20 (2019): 5216.

[26] P. K. Chu and X. Lu, "Low-Temperature Plasma Technology: Methods and Applications." CRC Press, 2013.

[27] T. Yokoyama, M. Kogoma, T. Moriwaki, and S. Okazaki, "The Mechanism of the Stabilisation of Glow Plasma at Atmospheric Pressure," Journal of Physics D: Applied Physics, Vol. 23, No. 8, p. 1125, 1990.

[28] S. I. Umran, M. Gołkowski, *"Principles of Plasma Physics for Engineers and Scientists*", Publ. Cambridge University Press, p.284,2011.

[29] C. Hoffmann, C. Berganza, and J. Zhang. "Cold Atmospheric Plasma: Methods of Production and Application in Dentistry and Oncology." Medical gas research, 3, no. 1 p. 1-15, (2013).

[30] D. Nicholson and D. R. Nicholson. *Introduction to Plasma Theory.* Wiley New York, p.p,3-5. 1983.

[31] A Roosmalen, , J. Baggerman, and S. Brader. *Dry Etching for Vlsi.* Springer Science & Business Media, Vol. 21, No. 12, p. 11-25, 2013.

References

[32] P.Gibbon, "Introduction to Plasma Physics." arXiv preprint arXiv:.04783. Vol. 27, No. 18, p. 1025, (2020).

[33] D. Nicholson, and D. Nicholson. *Introduction to Plasma Theory.* Wiley New York, p,9-13, 1983.

[34] k.Wiesemann,:. "A Short Introduction to Plasma Physics." arXiv preprint arXiv, Vol. 17, No. 13, p. 102-105, (2014).

[35] Y.Maron, "Experimental Determination of the Thermal, Turbulent, and Rotational Ion Motion and Magnetic Field Profiles in Imploding Plasmas." Physics of Plasmas, 27, no. 6, p. 060901, (2020).

[36] H. Conrads and M. Schmidt, "Plasma generation and plasma sources," Plasma Sources Sci. Technol., vol. 9, no. 4, pp. 441–454, 2000, doi: 10.1088/0963-0252/9/4/301

[37] M. López et al., "A review on non-thermal atmospheric plasma for food preservation: Mode of action, determinants of effectiveness, and applications," Front. Microbiol., vol. 10, no. APR, 2019, doi: 10.3389/fmicb.2019.00622.

[38] N. Misra, O. Schluuter, and P. Cullen, Eds., Cold Plasma in Food and Agriculture Fundamentals and Applications, 1st ed. London: Academic Press is an imprint of Elsevier, Vol. 14, No. 7, p. 1021-1035, 2016.

[39] H. Conrads, M. Schmidt, "Plasma generation and plasma sources". *Plasma Sources Science and Technology,* 9, 441- 454, (2000).

[40] D, Koten, Maria B., S. Dana, and A.o Subiantoko. "The Effect of Argon Pressure on Plate-Shape Electrodes Plasma Forming Behavior." International Journal of Research in Engineering and Science (IJRES), (2018).

[41] G. Komarzyniec, and M. Aftyka. "Operating Problems of Arc Plasma Reactors Powered by Ac/Dc/Ac Converters." J Applied Sciences,10, no. 9 (2020): 3295.

References

[42] N. B. Sahari . "Generation of homogeneous glow discharge using a combination of fine wire mesh and perforated Aluminum electrode", Faulty of Electrical Engineering, Universiti Teknologi Malaysia, 2013.

[43] D.A. Staack. "Characterization and Stabilization of Atmospheric Pressure Dc Microplasmas and Their Application to Thin Film Deposition." (2009).

[44] A.Bogaerts, Annemie. "The Glow Discharge: An Exciting Plasma!". Journal of Analytical Atomic Spectrometry. 14, no. 9 (1999): 1375-84.

[45] B. Eliasson and U. Kogelschatz, "Nonequilibrium Volume Plasma Chemical Processing," IEEE Transactions on Plasma Science, Vol. 19, No. 6, pp. 1063–1077, 1991.

[46] E. A. Razaq, "Design and Study of Variable Magnetic DC Sputtering System",(Ph.D.) thesis, college of Science, University of Baghdad (2012).

[47] K. A. Wahid, "Design and Construction of DC Planer Magnetron Sputtering to Prepared Se Thin Films", Thesis, College of Science, University of Baghdad, (2010).

[48] Y.Yan, J. Miao, Z.Yang, F.X. Xiao, H. B. Yang, Bin Liu, and Y. Yang. "Carbon Nanotube Catalysts: Recent Advances in Synthesis, Characterization, and Applications." Chemical Society Reviews, 44, no. 10 (2015): 3295-346.

[49] R. E Sladek. "Plasma Needle: Non-Thermal Atmospheric Plasmas in Dentistry." Abstracts International, 2006.

[50] E.L. Quiros, "Plasma Processing of Municipal Solid Waste," Brazilian Journal of Physics, Vol. 34, No. 4B, pp. 1587– 1593, 2004.

[51] A. Schutze, J. Y. Jeong, S. E. Babayan, Ja. Park, G. S. Selwyn, and R. Hicks. "The Atmospheric-Pressure Plasma Jet: A Review and Comparison to Other Plasma Sources." IEEE Transactions on plasma science, 26, no. 6 (1998): 1685-94.

References

[52] E. Ocak, H. A. Yucer, I C. Kocum, and D. Cokeliler. "Design and Implementation of Radio Frequency Glow Discharge System." Paper presented at the 2009 14th National Biomedical Engineering Meeting, 2009.

[53] F. Mehmood, T. Kamal, and U. Ashraf. "Generation and Applications of Plasma (an Academic Review)." (2018).

[54] J.Nakajima, H. Sekiguchi. "Synthesis of Ammonia Using Microwave Discharge at Atmospheric Pressure." Thin Solid Films, 516, no. 13 (2008): 4446-51.

[55] Y.A Lebedev ., "Microwave Discharges: Generation and Diagnostics." Paper presented at the Journal of Physics: conference series, 2010.

[56] Q. Shen, R. Huang, Z. Xu, and W. Hua. "Numerical 3D Modeling: Microwave Plasma Torch at Intermediate Pressure." Applied Sciences,10, no. 15 (2020): 5393.

[57] R. Brandenburg, "Dielectric Barrier Discharges: Progress on Plasma Sources and the Understanding of Regimes and Single Filaments." Plasma Sources Science, and Technology. 26, no. 5 (2017): 053001.

[58] M.M. Nasiru, E. B. Frimpong, U. Muhammad, J. Qian, A. T. Mustapha, W. Yan, H. Zhuang, J. Zhang, and Food Safety. "Dielectric Barrier Discharge Cold Atmospheric Plasma: Influence of Processing Parameters on Microbial Inactivation in Meat and Meat Products." Comprehensive Reviews in Food Science, (2021).

[59] U. Kogelschatz. "Dielectric-barrier discharges: their history, discharge physics, and industrial applications." *Plasma chemistry and plasma processing* 23.no 1, (2003): 1-46.

[60] U. Kogelschatz, and B. Eliasson. "Fundamentals and applications of dielectric barrier discharges." *HAKONE VII Int. Symp. On High-Pressure Low-Temperature Plasma Chemistry, Greifswald*. 2000.

[61] G.V. Prakash, K. Patel, N. Behera, and A. Kumar. "Characterization of Atmospheric Pressure Plasma Plume." preprint arXiv,03691 (2019).

References

[62] J. Arrieta, J Asenjo, I Vargas, and Y Solis. "Atmospheric-Pressure Non-Thermal Plasma-Jet Effects on Ps and Pe Surfaces." Paper presented at the Journal of Physics: Conference Series, 2015.

[63] M. Domonkos, P. Tichá, J. Trejbal, and Pavel %J Applied Sciences Demo. "Applications of Cold Atmospheric Pressure Plasma Technology in Medicine, Agriculture, and Food Industry." 11, no. 11 (2021): 4809.

[64] X. Lu, M. Laroussi, V. Puech, "On Atmospheric-Pressure Non-Equilibrium Plasma Jets and Plasma Bullets." Plasma Sources Science and Technology. 21, no. 3 (2012): 034005.

[65] J. Šimončicová, S.Kryštofová, V. Medvecká, K. Ďurišová, B. Kaliňáková, and biotechnology. "Technical Applications of Plasma Treatments: Current State and Perspectives." Applied Microbiology, 103, no. 13 (2019): 5117-29.

[66] D. Hassanpour, S.J. Pestehe,. "The Effects of Grounded Electrode Geometry on Rf-Driven Cold Atmospheric Pressure Plasma Micro-Jet." Journal of Theoretical and Applied Physics,14, no. 4 (2020): 387-98.

[67] J. A. Mora, A. V. Brenes, R Montiel, "Atmospheric-Pressure Non-Thermal Plasma Jet for Biomedical and Industrial Applications." Arrieta, and VI Vargas. Paper presented at the Journal of Physics: Conference Series, 2015.

[68] G. Bonnizzoni and E. Vassallo. "Plasma physics and technology; industrial applications".Vacuum, 64:327-336, (2002).

[69] H. W. Herrmann, I. Henins, J. Park and G. S. Selwyn. "Decontamination of chemical and biological warfare (CBW) agents using an atmospheric pressure plasma jet (APPJ)". Physics of Plasmas, 6: 2284-2289, (1999).

[70] I. Moon and C. Hyun Won, "Review of the Current State of Medical Plasma Technology and its Potential Applications" Med Laser; Vol,7(1), pp,1-5, 2018.

References

[71] J. Winter, R. Brandenburg, and K. Weltmann, "Atmospheric Pressure Plasma Jets: An Overview of Devices and New Directions," Plasma Sources Science and Technology, Vol. 24, No. 6, p. 064001, 2015.

[72] J. Checa and J. M. Aran, "Reactive oxygen species: Drivers of physiological and pathological processes," J. Inflamm. Res., vol. 13, pp. 1057–1073, 2020, doi: 10.2147/JIR.S275595.

[73] S. Das, V. P. Gajula, S. Mohapatra, G. Singh, and S. Kar, "Role of cold atmospheric plasma in microbial inactivation and the factors affecting its efficacy," Heal. Sci. Rev., vol. 4, no. July, p. 100037, 2022, doi 10.1016/j.hsr.2022.100037.

[74] E. G. Alves Filho, E. S. de Brito, and S. Rodrigues, Effects of cold plasma processing in food components. Elsevier Inc., 2019

[75] F. O. Borges, G. H. Cavalcanti, and A. G. Trigueiros, "Determination of plasma temperature by a semi-empirical method," Brazilian J. Phys., vol. 34, no. 4 B, pp. 1673–1676, 2004, doi: 10.1590/S0103- 97332004000800030.

[78] M. Aflori, G. Amarandei, L. M. Ivan, D. G. Dimitriu, and D. Dorohoi, "Estimating particle temperature for an argon-oxygen discharge by using Langmuir probe and optical emission spectroscopy," Acta Phys. Slovaca, vol. 55, no. 6, pp. 491–499, 2005.

[77] P. Wei, Z. Wei, G. Zhao, Y. Bai, and C. Tan, "Effect of Processing Parameters on Plasma Jet and In-flight Particles Characters in Supersonic Plasma Spraying," High Temp. Mater. Process., vol. 35, no. 8, pp. 775– 786, 2016, doi: 10.1515/htmp-2015-0077.

[78] N. OHNO, M. A. RAZZAK, H. UKAI, S. TAKAMURA, and Y. UESUGI, "Validity of Electron Temperature Measurement by Using Boltzmann Plot Method in Radio Frequency Inductive Discharge in the Atmospheric Pressure Range," Plasma Fusion Res., vol. 1, no. January, pp. 028–028, 2006, doi: 10.1585/pfr.1.028.

[79] H. H. L. A. Y. R. K. R. Ibrahim, "Analytical Methods in Plasma Diagnostic by Optical Emission Spectroscopy: A Tutorial Review," J. Sci.

References

Technol., vol. 6, no. 1 SE-Articles, Jul. 2014, [Online]. Available: https://publisher.uthm.edu.my/ojs/index.php/JST/article/view/787.

[80] C. Hoffmann, C. Berganza, and J. Zhang, "Cold Atmospheric Plasma: Methods of production and application in dentistry and oncology," Med. Gas Res., vol. 3, no. 1, pp. 1–15, 2013, doi: 10.1186/2045-9912-3-21.

[81] K. Urabe, Tadasuke Morita, author B. Ganguly Investigation of discharge mechanisms in helium plasma jet at atmospheric pressure by laser spectroscopic measurements Published 10 March 2010.

[82] Q. Nie, An Yang, authors Cheng-Yu Bao Characteristics of Atmospheric Room-Temperature Argon Plasma Streams Produced Using a Dielectric Barrier Discharge Generator With a Cylindrical Screwlike Inner Electrode Published 10 August 2012.

[83] J. Raud, I. Jõgi, author Marti Laast Temporal and spectral characteristics of atmospheric pressure argon plasma jet Published 1 February 2013.

[84] Chen Qian, Zhi Fang, Jingru Yang, Mingrui Kang Investigation on Atmospheric Pressure Plasma Jet Array in Ar (2014).

[85] Cheng Zhang, T. Shao, authors P. Yan A comparison between characteristics of atmospheric-pressure plasma jets sustained by nanosecond- and microsecond-pulse generators in helium Published 1 October 2014.

[96] W. Yan, Fucheng Liu, author Dezhen Wang Two-dimensional numerical study of an atmospheric pressure helium plasma jet with dual-power electrode, Published 10 April 2015.

[87] Rizan Rizon Elfa; Mohd Khairul Ahmad; Chin Fhong Soon; Mohd Zainizan Sahdan; Jais Lias; Mohamad Hafiz Mamat; Mohamad Rusop; Nafarizal Nayan Electrical and optical characteristics of atmospheric pressure plasma needle jet driven by a neon transformer (2017).

[88] Bo Zhang, Z. Fang, authors Ruoyu Zhou Comparison of characteristics and downstream uniformity of linear-field and cross-field atmospheric pressure plasma jet array in He Published 1 June 2018.

[89] Nima Bolouki, J. Hsieh, author Yi-Zheng Yang Emission Spectroscopic Characterization of a Helium Atmospheric Pressure Plasma Jet with Various

References

Mixtures of Argon Gas in the Presence and the Absence of De-Ionized Water as a Target Published 4 July 2019.

[90] Jõgi1 Rasmus et al Comparison of two cold atmospheric pressure plasma jet configurations in argon Indrek 2020.

[91] M. Hofmans, P. Viegas, authors A. Sobota "Characterization of a kHz atmospheric pressure plasma jet: comparison of discharge propagation parameters in experiments and simulations without target Published (2020).

[92] A. Asghar, A. Galaly The Effect of Oxygen Admixture with Argon Discharges on the Impact Parameters of Atmospheric Pressure Plasma Jet Characteristics Published 26 July 2021.

[93] H. Sakakita, T. Shimizu, S. Kiyama Electrical characteristics of a low-temperature, atmospheric-pressure helium plasma jet Published 8 January 2021.

[94] Y. Jiang, Yanhui Wang, +2 authors Dezhen Wang Numerical study on the production and transport of O and OH in helium–humid air atmospheric pressure plasma jet interacting with a substrate Published 1 October 2021.

[95] A. J. Mohamed, Mohammed K. Khalaf, Awatif Sabir Jasim The Study of the Characteristics of a Microwave Plasma Jet Operated with Ar at Atmospheric Published 29 November 2022.

[96] O. Jovanović, N. Puač, N. Škoro A comparison of power measurement techniques and electrical characterization of an atmospheric pressure plasma jet, Published 2022.

[97] J. Jia-Shiuan Tsai, Jian-Zhang Chen Influence of Oxygen Impurity on Nitrogen Atmospheric-Pressure Plasma Published 26 March 2023.

[98] R. T P, S. Kar Effect of an additional floating electrode on radio frequency cross-field atmospheric pressure plasma jet, Published 1 July 2023.

[100] H. B. Baniya, R. Shrestha, R. P. Guragain, M. B. Kshetri, B. P. Pandey, and D. P. Subedi. "Generation and Characterization of an Atmospheric-Pressure Plasma Jet (Appj) and Its Application in the Surface Modification of Polyethylene Terephthalate." International Journal of Polymer Science (2020).

References

[101] S. D. Anghel. "Generation and Electrical Diagnostic of an Atmospheric-Pressure Dielectric Barrier Discharge." IEEE Transactions on Plasma Science 39, no. 3 (2011): 871-76.

[102] Q. Li, J.Li, W.Zhu, X. Zhu, and Y. Pu. "Effects of Gas Flow Rate on the Length of Atmospheric Pressure Nonequilibrium Plasma Jets. Applied Physics Letters ," 95, no. 14 (2009): 141502.

[103] A. Basher, and A. H. Mohamed. "Laminar and Turbulent Flow Modes of Cold Atmospheric Pressure Argon Plasma Jet." Journal of Applied Physics, 123, no. 19 (2018): 193302.

[104] H. Ley, Analytical Methods in Plasma Diagnostic by Optical Emission Spectroscopy: A Tutorial Review," Journal of Science and Technology, Vol. 6, No. 1, 2014.

[105] A. Kramida, Y. Ralchenko, J. Reader, and N. Team, \NIST Atomic Spectra Database (Version 5.4). National Institute of Standards and Technology," 2017.

[106] N. Ohno, M. Razzak, H. Ukai, S. Takamura, and Y. Uesugi, Validity of Electron Temperature Measurement by Using Boltzmann Plot Method in RadioFrequency Inductive Discharge in the Atmospheric Pressure Range," Plasma and Fusion Research, Vol. 1, pp. 028, 2006.

[107] F. Sohbatzadeh, S. Mirzanejhad, H. Mahdavi, and Z. Omidi, Characterizationof Argon/air Atmospheric Pressure Capacitively Coupled Radio FrequencyDielectric Barrier Discharge Regarding Parasitic Capacitor at 13.56 MHz," Journal of Theoretical and Applied Physics, Vol. 6, No. 1, p. 32, 2012.

الخلاصة

تعتبر خصائص بلازما الهيليوم النفاث عند الضغط الجوي (APHPJs) مهمة بسبب استخدامها في تطبيقات مختلفة مثل الطب والطب الحيوي والزراعة والصناعة. في هذا العمل، تم استخدام نظام تفريغ حاجز العزل الكهربائي (DBD) لدراسة خصائص (APHPJs) في مختبر البلازما المتقدم في جامعة كربلاء، كلية العلوم، قسم الفيزياء. مكونات الجهاز عبارة عن مولد تيار متردد عالي الجهد (0-20) كيلو فولت، وأنابيب بيركس بسماكات مختلفة (0.1، 0.2، 0.5، 1) ملم، قطبين كهربائيين مصنوعين من الألمنيوم بسماكة 1 ملم موضوعين حول البايركس، والغاز العامل للتفريغ الكهربائي هو الهيليوم (He). تلعب درجة حرارة البلازما وطول عمود البلازما دورًا رئيسيًا في تطبيقات البلازما الباردة المختلفة، لذلك تم دراسة تأثير سماكات أنابيب البايركس والمسافة بين الأقطاب الكهربائية على الخصائص الكهربائية (طول العمود ودرجة حرارة البلازما) للبلازما المتولدة. يتم استخدام جهاز استشعار حراري إلكتروني بسيط من نوع (UTS) لتقدير درجة حرارة البلازما وتم قياس عمود البلازما بالمتر القياسي. تم تقدير درجة حرارة البلازما وطول اللهب لمعدلات تدفق الغاز المختلفة (1-6)لتر/دقيقة ومدى الجهد المطبق (8-14) كيلو فولت.

يتم استخدام طريقة التحليل الطيفي للانبعاث البصري (OES) لتسجيل وتحليل طيف بلازما الهيليوم النفاثة لمجموعة من الجهد المطبق (8-14) كيلو فولت ومعدل تدفق غاز الهيليوم (1-6) لتر/دقيقة. يتم حساب درجة حرارة الإلكترون (T_e) وكثافة الإلكترون (n_e) باستخدام طريقة بولتزمان ويتم أخذ الكثافة المناسبة للأنواع المتفاعلة في الاعتبار في قاعدة البيانات المسجلة في المعهد الوطني للمعايير والتكنولوجيا.

أظهرت النتائج أن طول عمود البلازما هو تباين عشوائي بسبب سمك أنبوب البايركس، ثم يتم الحصول على خاصية التحسين عندما يكون الجهد المطبق 8 كيلو فولت ومعدل تدفق الغاز (4)لتر/دقيقة, في حالة سمك أنبوب البايركس 1 ملم، يبلغ طول عمود البلازما 6 سم وتكون درجة حرارة البلازما محصورة بين (24-26) درجة مئوية، تكون قريبة من درجة حرارة الغرفة.عندما تكون المسافة بين الأقطاب الكهربائية في مدى (1-2.5) سم، والجهد المطبق (8 كيلو فولت) ومعدل تدفق الهيليوم (4)لتر/دقيقة ، تتولد البلازما ولكن طول عمودها يتناقص مع زيادة المسافة، وكذلك درجة حرارة البلازما لها نفس السلوك.

يتم تسجيل وتحليل أطياف نفاثات بلازما الهيليوم عند الضغط الجوي للجهد (8-14) كيلو فولت ومعدل التدفق (1-6)لتر/دقيقة ، وتظهر خطوط الطيف في نفاثات بلازما الهيليوم في مناطق الأشعة فوق البنفسجية والضوء المرئي ومنطقة الاشعة تحت الحمراء (NIR). تم استخدام ستة خطوط طيفية لجذور الأنواع التفاعلية للبلازما المتولدة لتقدير درجة حرارة الإلكترون (T_e) وكثافة الإلكترون (n_e). معاملات

العمل المثلى لتوليد بلازما الهيليوم ذات الخصائص الجيدة هي معدل تدفق الغاز (4) لتر/دقيقة والجهد المستخدم (8) كيلو فولت. الخاصية المثلى للبلازما المتولدة في هذا العمل هي طول العمود 6 سم، درجة حرارة البلازما (26) درجة مئوية، كثافة الأنواع المتفاعلة العالية (O$_2$,N$_2$,OH,NO) هي (403و2476و875و357) على التوالي، ودرجة حرارة الإلكترون أقل من 1 الكترون فولت (6102.21 كلفن) وكثافة الإلكترون (1,57×10^{13})سم$^{-3}$. يمكن استخدام (APHPJs) المتولدة في التطبيقات الطبية الحيوية والطبية بسبب الكثافة العالية للأنواع المتفاعلة، كما أن قيم درجة حرارة الإلكترون (T$_e$) وكثافة الإلكترون (n$_e$) تقع في نطاق البلازما الصناعية.

جامعة كربلاء

كلية العلوم

قسم الفيزياء

التحقق من خصائص بلازما الهيليوم النفاث عند الضغط الجوي

رسالة مقدمة الى

مجلس كلية العلوم-جامعة كربلاء

كجزء من استكمال متطلبات نيل درجة الماجستير في علوم الفيزياء

تقدم بها

مصطفى موسى شاكر عبد الحسين

بكالوريوس علوم فيزياء (2017)/جامعة بابل

اشراف

أ.د فاضل خدام فليفل

أ.د رجاء خضر محمد

2023م

1445ه